University College of Southeast Norway
Faculty of Technology, Natural Sciences and Maritime Sciences

Doctoral dissertation no. 30
2018

Haakon Karlsen

Smartphone-based urinary biomarker detection: an application-oriented device and algorithm

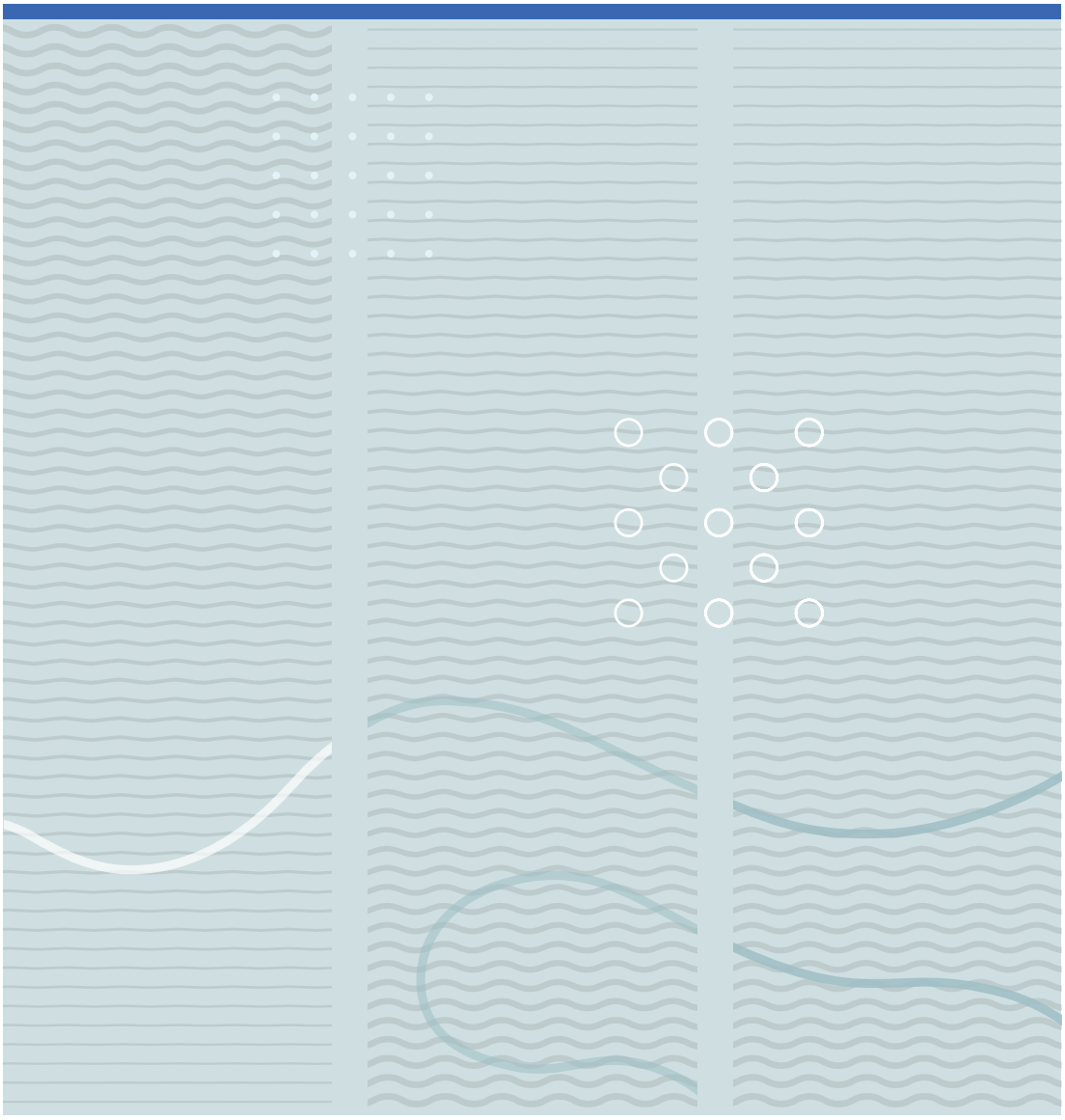

HSN

Haakon Karlsen

Smartphone-based urinary biomarker detection: an application-oriented device and algorithm

A PhD dissertation in
Applied Micro- and Nanosystems

Faculty of Technology, Natural Sciences and Maritime Sciences
University College of Southeast Norway
Borre, 2018

Doctoral dissertations at the University College of Southeast Norway no. 30

ISSN: 2464-2770 (print)
ISSN: 2464-2483 (electronic)
ISBN: 978-82-7860-314-7 (print)
ISBN: 978-82-7860-315-4 (electronic)

Print: University College of Southeast Norway

Preface

The thesis is submitted by a candidate for the degree of philosophiae doctor from the Department of Microsystems (IMS), Faculty of Technology, Natural Sciences and Maritime Sciences (TNM), University College of Southeast Norway.

The doctoral study was conducted from August 2014 to November 2017. Professor Tao Dong was the primary supervisor.

Financial support:

- KD program
- The Oslofjord fund (Project No.: 234972 and 255893)
- FORNY2020 (Project No.: 268481)

Acknowledgements

I thank my primary supervisor Professor Tao Dong for instruction, encouragement, and motivation during my time as a PhD candidate. My research achievements could not have been realized without his valuable advice, support and supervision, by which the scientific work can be achieved here. I am very grateful for his, diligent and enthusiastic assistance and support of my work.

Many thanks also to my co-supervisor, Professor Zhenhe Suo, for his discussion and guidance.

The extensive contact network of my supervisor, Professor Tao Dong, gave my PhD work acces to support from interdisciplinary cooperating partners; institutions, companies and hospitals, related to fabrication and experimental work: Chongqing Technology and Business University (CTBU, China), which I had the opportunity to visit, and Jilin Shenhua Medical Equipment Co., Ltd. (China). I am grateful for the contact with Zhou Jianyu, Pengfei Cai, Haotian Zhang, Yongheng Hu and Professor Peiyi Liu.

Furthermore, I am grateful for the cooperating partners within the Oslofjordfondet major project and the FORNY2020 commercialization project: Sensovann, Kjeller Innovation and Sandefjord Kommune.

I want to thank Nuno Miguel Matos Pires, Zhaochu Yang, Zhongyuan Shi, Linbo Lee, Francesco Dell'Anna for support, discussion and good cooperation over the period I have had the pleasure of your acquaintance. I also want to thank the master students that I have worked with Adriana Miguel Serra Silva Couto, Ana Raquel Bertão, Chen Xing, Jennifer Bergstrøm, Shilun Feng, Carlos Honrado and Cátia Barbosa.

I also appreciate my colleagues Zekija Ramic, Yngvar Berg, Kristin Skjold Granerød, Siri Tønnessen, Maaike M.B.W. Dooper and others for their support and cooperation.

Finally, I want to thank my parents, and acknowledge my 8 year old (as of writing this) son Johannes for being my primary source of motivation, and the most important person in my life.

Sammendrag

Personer i høy alder har en høyere risiko for å få urinveisinfeksjon enn resten av befolkningen. Fysiske funksjonsnedsettelser, kognitive funksjonsnedsettelser, urininkontinens og høy alder vanskeliggjør håndteringen av urinveisinfeksjon. Personer på sykehjem eller som mottar andre former for pleie, slik som hjemmesykepleietjenester, har ofte symptomer som tolkes som urininkontinens, og bruker dermed ofte voksen bleier. Funksjonsnedsettelser, inkontinens og bleiebruk kan vanskeliggjøre innsamling av urinprøver for analyse.

Et pasientnært hurtigscreening system som ikke medfører fysiske inngrep ble utviklet for å unngå unødvendig kateterisering som kan medføre utilsiktet urinveisinfeksjon, unngå overforbruk av antibiotika som kan medføre utvikling av antibiotikaresistente bakterier, og for å hjelpe sykepleiere i hjemmesykepleien. Systemet består av et papir-basert mikrofluidisk kolorimetrisk assay kompatibelt med kommersielt tilgjengelige bleier, og en smarttelefon applikasjon for analyse av kolorimetriske resultater. Enheten er i stand til automatisk urinprøveinnhenting fra en bleie ved hjelp av absorberende medium, og transporterer urinen internt ved hjelp av kapillærstrømning i porøst medium til et sett med blokker av porøst medium med kolorimetriske reaksjonskjemikalier. En ventil av superabsorberende polymer lukker inngangen etter en tilstrekkelig mengde urin har blitt absorbert, og isolerer innsiden av enheten fra ekstern miljøpåvirkning og evaporering. Enheten er spesifikt laget for å tilby automatisk prøveinnsamling og test av urin uten fysiske inngrep, hvor hjemmesykepleiere kan sette inn en enhet ved et bleieskift, og fjernes og leses av ved påfølgende bleieskift.

- Den fremstilte prototypenheten utviser konsistent og repeterbar atferd. Metning av reaksjonsblokkene og lukking av ventil inntraff i løoet av omtrent 7 minutter. Alle kolorimetriske kjemikalier var ferdig reagert innen 30 minutter, og reaksjonsfargene var stabile og ulike nivåer kunne identifiseres opp til 8 timer etter metning.

- Smarttelefon applikasjonen forsøker å tilby en objektiv måling uavhengig av lys- og maskinvareforhold, og presenterer målinger i et rapportformat eller fremstiller resultatet grafisk med historiske data for å visualisere biomarkørutvikling over tid. Lys- og maskinvareuavhengighet er avgjørende. Hvis test og kalibrering foregår under forskjellige forhold, er det ikke sikkert av kalibreringen er en representativ basis for sammenligning med test. Andre publiserte metoder i litteraturen hadde en tendens til å benytte upraktiske begrensninger, slik som å begrense tillatt fargeendring for reaksjonene. For å tilby lys- og maskinvareuavhengighet for generelle kolorimetriske reaksjoner uten å kreve tilleggsutstyr, slik som apparater festet på telefonen, tilleggslyskilder, oppsett, etc. ble et sett med trykte referansefarger laget for hver biomarkør. Når test og referanse fotograferes samtidig, vil forholdene gjelde omtrent likt for begge og dermed minimalisere påvikningen som lys- og maskinvareforhold har på fargene. For et antall biomarkører og referanser for hver biomarkør, kreves det datauthenting fra flere punkter på enhetens overflate. For å oppnå brukervennlighet og enkelhet ble en mønstergjenkjenningsalgoritme inkludert for å finne enhetens hjørner, og en homografisk transformasjonsalgoritme for å etablere en transformasjon mellom kjente datauthentingspunkter i designet og ukjente posisjoner i det fotograferte bildet. Algoritmen var i stand til å klassifisere korrekt under forskjellige lysforhold og på forskjellige smarttelefoner.

Abstract

Persons of advanced age have a higher risk of contracting urinary tract infection than the general population. Functional impairments, cognitive impairments, urine incontinence and advanced age encumbers the management of urinary tract infection. Persons in nursing homes or who receive other types of care, such as home care services often present with symptoms interpreted as urinary incontinence, and hence a large portion often use adult diapers. Impairments, incontinence and diaper usage can make collection of urine samples for analysis difficult.

A non-invasive rapid screening point-of-care system was developed to avoid unnecessary catheterization that may inadvertently cause infections, avoid overuse of antibiotics that may increase antibiotic resistance of bacteria, and to help nurses in the home care service. The system consists of a paper-based microfluidic colorimetric assay compatible with commercially available diapers, and a smartphone application for analysis of colorimetric results. The device is capable of automatic urine sampling from a diaper by utilizing absorbent media, and transports the urine internally with capillary flow in porous media to a set of colorimetric reaction pads. A superabsorbent polymer-swelling valve closes the inlet after a sufficient amount of urine have been absorbed and isolates the inside of the device from environmental influence and evaporation. The device is specifically made to provide a non-invasive solution for automatic sampling and testing of a urine sample, where, in the case of home care nurses, a device can be inserted during one diaper change, then removed and read during a consecutive diaper change.

- The fabricated prototype devices exhibited consistent and repeatable behaviour. Saturation of reaction pads, and valve swelling occurred in approximately 7 minutes. All colorimetric reactions had run to completion within 30 minutes, and reaction colors were preserved and distinguishable for 8 hours after saturation.
- The smartphone application attempts to provide an objective measurement independent of illumination and device conditions, and presents measurements in a report format or as a historical plot that includes previous tests to visualize

biomarker variation over time. Illumination and device independence is crucial. If test and calibration is performed under different conditions, the calibration may not be a representative basis of comparison for the test. Other published methods in the scientific literature tended to have impractical constraints, such as putting limitations on the permissible color change. To provide Illumination and device independence for general colorimetric reactions without requiring additional equipment such as smartphone attachments, illumination sources, setups etc. a set of printed reference colors were provided for each biomarker. When photographing test and reference simultaneously, the variation in conditions apply approximately equally to both, thereby minimizing the impact of illumination and device conditions. Multiple references for multiple biomarkers require data extraction from multiple locations on the device surface. For the purpose of user-friendliness and simplicity, a pattern detection algorithm was included to detect device corners, and a homographic transform algorithm was implemented to establish a map between the known data extraction locations in the design and the photographed image. The algorithm was capable of correct classification for different illuminations on different smartphone models.

Keywords: Capillary flow, Microfluidics, Rapid Screening, Urinary Tract Infection

List of papers

Article 1 [IEEE conference publication]

Karlsen, H. and T. Dong, A smart phone-based robust correction algorithm for the colorimetric detection of Urinary Tract Infection. 37th Annual International Conference of the IEEE Engineering in Medicine and Biology Society (EMBC), publisher: IEEE, 2015: p. 1251-1254. DOI: 10.1109/EMBC.2015.7318594

Article 2 [IEEE conference publication]

Karlsen, H. and T. Dong, Illumination and device independence for colorimetric detection of urinary biomarkers with smartphone. 38th Annual International Conference of the IEEE Engineering in Medicine and Biology Society (EMBC), publisher: IEEE, 2016: p. 5184-5187. DOI: 10.1109/EMBC.2016.7591895.

Article 3 [IEEE international journal publication, Nivå 2]

Karlsen, H. and T. Dong, Smartphone-Based Rapid Screening of Urinary Biomarkers. IEEE Transactions on Biomedical Circuits and Systems, publisher: IEEE, 2017. 11(2): p. 455-463. DOI: 10.1109/TBCAS.2016.2633508

Article 4 [RSC international journal publication]

Karlsen, H. and T. Dong, Biomarkers of urinary tract infections: state of the art, and promising applications for rapid strip-based chemical sensors. Analytical Methods, publisher: Royal Society of Chemistry, 2015. 7(19): p. 7961-7975. DOI:10.1039/C5AY01678A

Article 5 [Springer conferance publication]

Karlsen, H. and T. Dong, A Compact Device for Urine Collection and Transport in Porous Media. Mechatronics 2017: Recent Technological and Scientific Advances, publisher Springer, 2017. 644: p. 3. DOI: 10.1007/978-3-319-65960-2_1

Article 6 [Springer international journal publication]

Karlsen, H. and T. Dong, A diaper pad for diaper-based urine collection and colorimetric screening of urinary biomarkers. Accepted. Annals of Biomedical Engineering, publisher: Springer

Abbreviations

CAGR – Compound Annual Growth Rate

CAUTI – Catheter-Associated Urinary Tract Infection

CDC - Centers for Disease Control and Prevention

CPCI – Clopper-Pearson Confidence Interval

IVD – In-Vitro Diagnostics

KS – Kolmogorov-Smirnov (test)

LTCF – Long Term Care Facility

MPO – Myeloperoxidase

OAB – Overactive Bladder

POC – Point-Of-Care

PVR – Post void Retention

SAP – Superabsorbent polymer

TMA – Trimethylamine

UI – Urinary Incontinence

UTI – Urinary Tract Infection

WCI – Wilcoxon Confidence Interval

WHO – World Health Organization

XO – Xanthine Oxidase

Table of contents

Articles omitted due to publisher's restrictions

1 Background on Urinary Tract Infection

Urinary tract infection (UTI) is a common infection, caused by microorganisms entering the urethra and infecting a section of the urinary tract. UTIs are often classified according to the confinement of infection [1]:

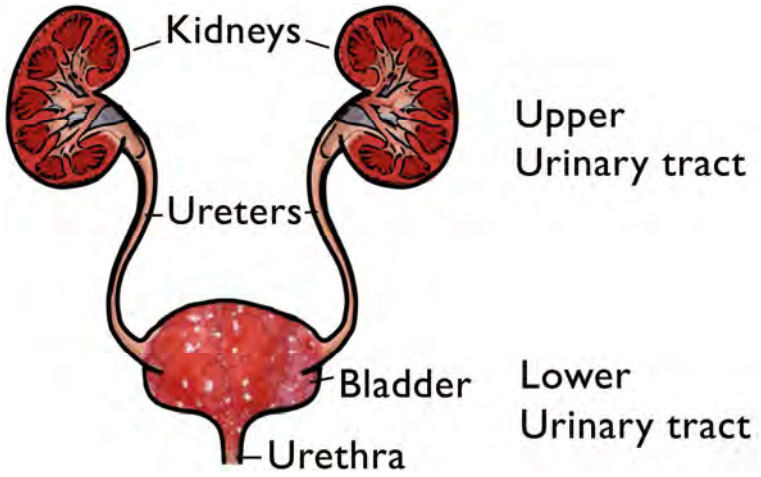

Figure 1 Illustration of urinary tract

UTIs are also classified as *uncomplicated* for normal hosts with absence of structural/functional abnormalities, pregnancy, catheterization or other instrumentation, while all other UTIs are considered *complicated* [1]. UTIs are often distinguished according to patient category such as Hospital acquired (nosocomial) infections and Community acquired infections, which displays a difference in etiology and antibiotic resistance patterns [2].

UTI accounts for a large portion of infections, with *Escherichia coli* being the predominant uropathogen in both community acquired and hospital acquired infections [2-13]. Other (less) common infectious agents are *Klebsiella* spp., *Enterococcus* spp., *Citrobacter* spp., *Enterobacter* spp., *Staphylococcus* spp., *Pseudomonas* spp. [9, 14]. The prevalence of UTI and frequency of isolation of infectious agents other than *E*. coli appear to vary between institutions and studies, which can be caused by demographics, variations in protocols, or infection criteria, etc.

Bacteria are the predominant cause of UTI, but viral, fungal and parasitic infections can also occur. Infection by viruses such as BK Virus, JC Virus, adenovirus and cytomegalovirus is increasingly being recognized as a cause of haemorrhagic cystitis in immunocompromised patients, especially in transplantation recipients [15]. However, identifiable inflammatory symptomatic viral organisms is uncommon in immunocompetent patients [16].

Fungal pathogens is a common occurrence predominantly as a nosocomial infection by *Candida spp.* [6, 10, 17, 18]. Significant risk factors for nosocomial UTI include transurethral and intermittent catheterization [19], which is also considered a predisposing factor for Candiduria or symptomatic *Candida spp.* infections UTI [20], and *Candida spp.* is frequently isolated from Catheter-associated UTI (CAUTI), see Table 1. Platt et al. [21] reported *Candida spp.* in 26.5% of CAUTI, but did not distinguish between colonization (asymptomatic) and infection (symptomatic) [20]. The data in Table 1 follows the NHSN (the CDC's National Healthcare Service Networks) standard definition of CAUTI [22], which excludes asymptomatic bacteriuria/funguria and is no longer reported as of 2009 [11]. Many patients who test positive for *Candida spp.* does not experience symptoms in which case Candiduria can be a benign event without need for antifungal treatment, but in symptomatic *Candida* infection, the symptoms can be difficult to distinguish from bacterial infections [23, 24]. *Candida spp.* infections, primarily by *C. albicans* is frequently a cause of infection, but mostly in the hospital setting for catheterized patients. In community settings the occurrence of yeast infections is much less common [17]. Because of the infrequent occurrence in the community settings and the predisposition to instrumentation, fungal UTI was not a focus for the target population group.

Parasitic infections such as Schistosomiasis most commonly occur in or near tropical regions, such as in parts of Africa, and is therefore not considered relevant [25-27].

Viral, fungal and parasitic infections occur commonly under specific and mostly irrelevant predisposing factors or geographical locations. Since bacteria are the most common cause of infections, they are the focus.

Table 1 Catheter-Associated Urinary Tract Infection 1997-2014

Pathogen	1997-1998 % [13]	2006-2007 n (%) [10]	2009-2010 n (%) [11]	2011-2014 n (%) [12]
Staphylococcus aureus	3.0	208 (2.2)	442 (2.1)	2,515 (1.6)
CoNS	2.4	234 (2.5)	467 (2.2)	3,696 (2.4)
Enterococcus faecalis	10.2	335 (3.6)	1,519 (7.2)	10,728 (7.0)
Enterococcus faecium	-	562 (6.0)	654 (3.1)	4,212 (2.7)
Enterococcus spp.	-	496 (5.3)	1,010 (4.8)	6,291 (4.1)
Candida albicans	-	**1,361 (14.5)**	**1,887 (8.9)**	**17,926 (11.7)**
Candida glabrata	-	-	-	**4,121 (2.7)**
Yeast NOS	-	-	-	**9,443 (6.1)**
***Candida spp.* or NOS**	**6.6**	**613 (6.5)**	**811 (3.8)**	**5,178 (3.4)**
Escherichia coli	32.5	2,009 (21.4)	5,660 (26.8)	36,806 (23.9)
Pseudomonas aeruginosa	10.8	938 (10.0)	2,381 (11.3)	15,848 (10.3)
Klebsiella (*pneumoniae/oxytoca*)	10.2	807 (8.6)	2,365 (11.2)	15,471 (10.1)
Enterobacter spp.	4.8	384 (4.1)	880 (4.2)	5,689 (3.7)
Acinetobacter baumannii	1.8**	109 (1.2)	185 (0.9)	-
Serratia spp.	-	-	204 (1.0)	-
Proteus spp.	4.7	-	1,013 (4.8)	6,108 (4.0)
Bacteroides spp.	-	-	-	2 (<0.1)
Other pathogen	13	1,321 (14.1)	1,633 (7.7)	9,771 (6.4)
Total	100	9,377 (100)	21,111 (100)	153,805 (100)

-, not reported; NOS, not otherwise specified
"other"-groups may group different sets of pathogens between years
** presumably *Acinetobacter baumannii*

1.1 Prevalence and definition of the 'elderly'

Bacteria can more easily colonize the bladder of females due to the length of urethra and proximity of urethra to vaginal cavity and rectum [1]. Bacteria can colonize the urethra of both males and females without causing colonization in the bladder because the bacteria can be washed away by urination. The shorter female urethra makes it easier for bacteria to reach the bladder. Women throughout their life are significantly more likely to get infections compared to men (except for in early childhood [28]) and almost half of all women will be infected in their lifetime [29, 30]. UTI is uncommon for adult-to-middle age males, until prostatic hypertrophy or prostatitis becomes a relevant issue [31].

The conventional definition of elderly/old has mainly been a chronological one, where a person becomes elderly/old when they reach an arbitrary age, such as 65. Ryder [32]

proposed an age range based on what age the life expectancy falls below an arbitrary length of time such as 10 years. This type of index is more useful in that it allows the start of old age to change based on the variation of life expectancy in the population [33]. A range more accurately models reality since, as noted by Hamilton-Miller [34]; some individuals show signs of what would be considered "old" at the age of 60, while others seem "young" even when they are 90, and therefore a definition based on functional status has a more useful meaning. The incidence of UTI is high for both sexes after the age of 65 [31, 35], but there are distinct differences between groups depending of the degree of independence and need for care. Whether the difference in incidence comes as a result of their conditions of care or whether it originates from the underlying pathology that sets the requirement for the particular type of care is unclear. Hamilton-Miller [34] proposes, in ascending order of dependence and need for care, people that live:

- independently
- in supervised communities
- institutions
- hospitalized

This group distinction appears to form an appropriate image for the prevalence of bacteriuria and UTI in older patients, where the independent and ambulatory group has a lower prevalence while the institutionalized has a higher prevalence [31, 35].

In this thesis the relevant group of patients are not specifically the hospitalized or institutionalized patients, since institutions and hospitals may have more available resources and equipment compared to what is available for the patients that live at home or in supervised communities, who receive care in the form of home care services.

For the purposes of clarity, the use of the word elderly in this thesis is not strictly based on age, but is more based on the type of functional ability. Persons of advanced age living at home or in supervised communities and who receive home care services (or similar) because of age-related health decline is considered "elderly" in the context of this work.

This is not meant as a definition that encompasses the entire demographic that experience UTI-related problems. It does not exclude patients in institutions or hospitals, but does exclude people of advanced age living independently without need for care because of problems related to advanced age.

1.2 Predisposing factors and comorbid factors

There are many factors that are relevant for the relevant population group, and a set of risk and complicating factors are associated with either age, UTI or both. Following is a set of some relevant factors.

1.2.1 Urinary incontinence and diaper use

Urinary incontinence is a term that describes involuntary leakage of urine [36], and is prevalent among the general population and increases with age [37-39]. Prevalence of urinary incontinence in general appear to be higher for women than men [37]. A brief review of available data in the literature of UI also revealed a similar trend of increasing prevalence of UI with age, see Figure 2 (total prevalence across included age groups in table 2).

Table 2 overall prevalence

	Age range	Men	Women	Total
Aggazzotti et al. [40]	33-102	39.2	59.8	54.5
Thomas et al. [39]	5-85	8.7	25.1	17.1
Malmsten et al. [38]	45-90+	9.2		
Irwin et al. [37]	18-70+	5.4	13.1	
Ouslander et al. [41]	65-85+			49.7

Whether UI increases the odds of UTI or vice versa appear to deviate between studies. However, a systematic review of five studies found a consistent increased odds of UI among men with UTI of 3.6 (2.17-6.0) [42]. Other data not included in the systematic review is presented in Table 3.

Table 3 UI in patients with and without UTI

	UTI	Non-UTI	Total	OR (95% CI)*	p-value**
Elderly hospitalized [43]	42/150	36/115	78/265	0.85 (0.50- 1.45)	0.56
Community dwelling elderly women [44]	6/99	30/499	36/598	1.03 (0.37-2.39)	0.95
Institutionalized [40]	64/79	393/760	457/839	3.94 (2.26-7.32)	<0.001
Post-menopausal women [45]				5.79 (2.05-16.45)	0.0009***
Elderly nursing home [41]	29/491				

*Crude OR estimate with mid-p exact CI, ** mid-p exact without continuity correction, ***multivariate

There can be various underlying causes of UI. Still, diagnostic/therapeutic approaches to the real problem is often overlooked, and the problem is superficially solved with absorbent material-based products and various catheters [46].

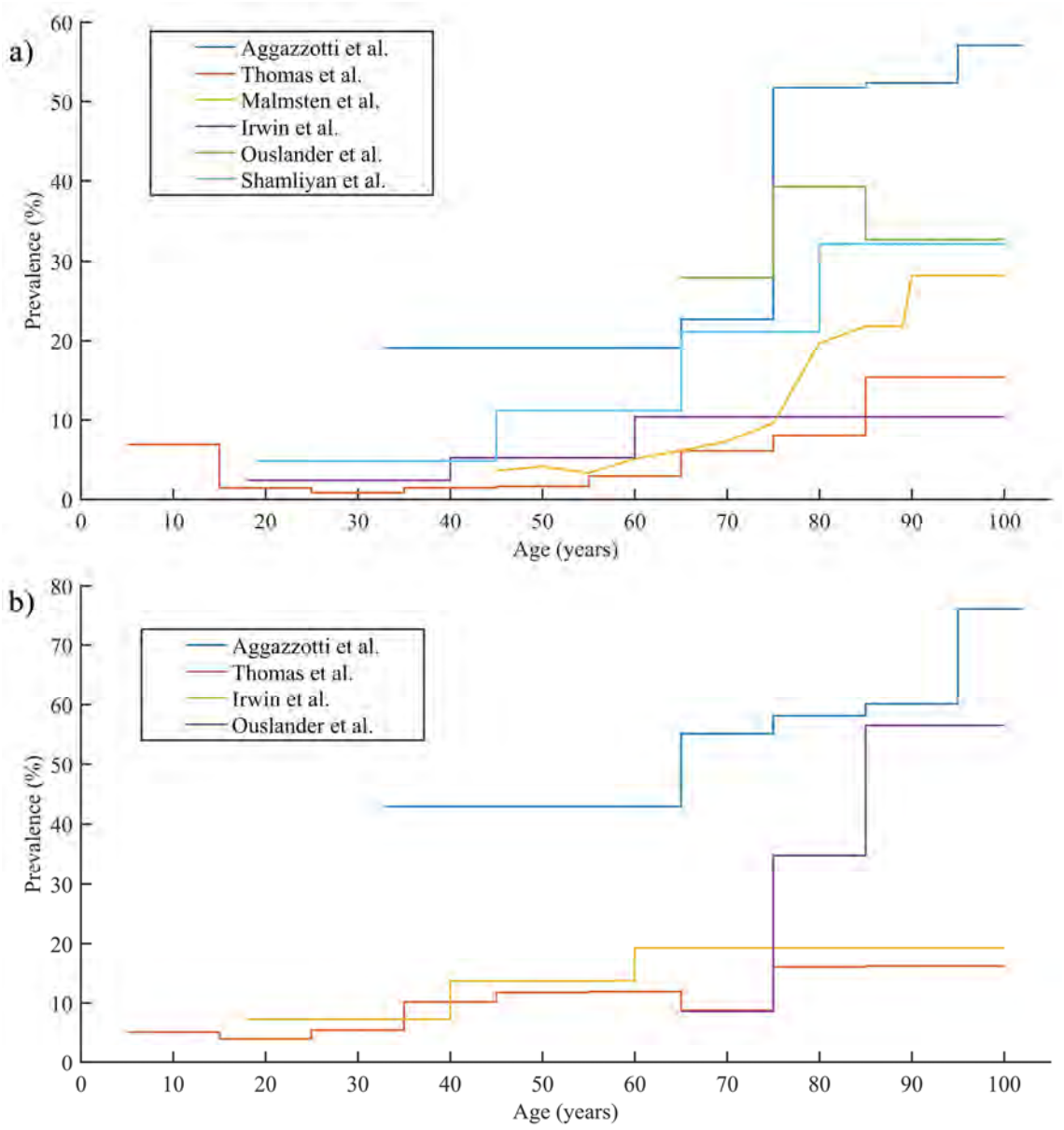

Figure 2 Urinary Incontinence prevalence of a) Males and b) Females. Data from Aggazzotti et al. [40]: overall prevalence in residential or nursing homes. Thomas et al. [39]: Regular incontinence of people in care of various health and social service agencies as well as postal survey of people on general practicioners list. Malmsten et al. [38]: Postal survey of men born in specific years to obtain cohorts of 5 year intervals. Irwin et al. [37]: weighted prevalence, Ouslander et al. [41]: Frequent and occasional UI prevalence in nursing homes, Shamliyan et al. [42]: Total UI prevalence, pooled analysis from 69 studies.

A disposable diaper solution to alleviate the challenges of UI has advantages and disadvantages [46]. From the perspective of the service provider/nurse, diapers are easy to handle and prevent excessive cleaning of clothes, bed sheets etc., which may be both time and cost effective compared to doing nothing to manage UI, although long term use of diapers does introduces a cost. From the patient/resident perspective, they gain an increased level of mobility without being constrained by catheterization, urine smell and urine stained clothes. On the other hand, the use of diapers is not a dignifying solution, and neither does it cure incontinence. Diapers may actually encourage a lack of urinary control due to the "safety net" that is in place, and because a person who would like to urinate normally in a toilet may have difficulties removing a diaper. The aforementioned advantages and disadvantages are practical in nature; there may however be more serious side effects from long term use of diapers such as irritation of the skin. It has also been suggested that the use of absorbent products in itself plays a role in the pathogenesis of UTI in patients with UI. Omli et al. [47] observed higher risk for UTI during follow-up for patients using absorbent products compared to those that did not.

The proportion of Institutionalized elderly that wear diapers tend to be high, 66%-83% [40, 46-48], although there may be variation from institution to institution depending on the education opportunities for nurses, financial stability of the institution, availability of human resources and general working conditions.

1.2.2 Overactive bladder

Overactive bladder (OAB) have been shown to be more prevalent than all UI types combined and prevalence increases with age, with an overall prevalence of 11.8% [37]. UTI is a comorbidity associated with OAB and is known to increase the cost of OAB. After diagnosis of OAB, the claims and cost of comorbid UTI have been shown to decrease [49-51]. The prevalence of UTI is also higher among patients with OAB compared to control subjects 28.0% to 8.4% respectively [52].

1.2.3 Catheterization

Reasons to use catheters are typically: surgery, urine output measurement, urine retention and urinary incontinence [53]. CAUTI (along with central-line associated bloodstream infections) are the most common nosocomial infections [10-12, 54]. The majority of uropathogens that cause catheter-acquired bacteriuria ascend along the interface of mucosa and catheter [55]. Biofilms form on the inner and outer surfaces of the urinary catheters and migrate to the bladder within 3 days [56-58]. Daily Incidence of bacteriuria for patients with indwelling catheters are in the range of 3%-8% [55]. This is mainly for extended catheterization longer than 7 days [54]. However, both transurethral indwelling catheter and repeated intermittent catheterization were both found by Nguyen-Van-Tam [19] to be significant independent risk factors for hospital acquired UTI with odds ratios of 4.62 (95% CI 2.75-7.75) and 3.73 (95% CI 1.74-8.01) respectively in one hospital.

1.2.4 Postvoid Residual Volume

Postvoid Residual Volume (PVR) is a measurement of residual urine volume present in the bladder after voluntary voiding [59]. PVR is considered to be related to UTI and other lower urinary tract symptoms, and in one study was found to be significantly different between positive and negative urine cultures [60]. However these results of PVR alone fail to be replicated in other studies [61-64], although it has been suggested that low functional level and significant PVR are risk factors for UTI [62]. High PVR is common in nursing home patients, and appears to increase with age [61, 65-68]. Another study found no significant association with age of men, but with prostate volume [69]. Prostate volume on the other hand is associated with increasing age [70, 71]. Conflicting results between studies could be due to the differences between patient groups.

1.2.5 Dementia

Dementia is common in nursing homes [72]. Advanced dementia can exacerbate the problems surrounding diagnosis and treatment of UTI. Due to limited communication abilities, cognitive deficits and high prevalence of urinary incontinence it is difficult to

detect UTI symptoms, and necessary signs and symptoms often does not satisfy minimum criteria for initiation of antibiotic treatment [43, 73, 74]. This has implications for the level of provided care, and the risk of antibiotic resistance development and emergence of multidrug-resistant organisms [75, 76]. Advanced dementia in Long-term care facilities is a significant risk factor for multidrug-resistant gram-negative infections [77].

1.2.6 Nurse staffing and burnout

In hospitals, studies have revealed that higher nurse staffing can be associated with a lower incidence of urinary tract infections [78, 79]. Nurses experience work stress and a high patient-to-nurse ratio can lead to burnout, which is often characterized by feelings of ineffectiveness, emotional depletion and distancing from patients, which may lead to reduced quality of care [80-82]. Burnout has been significantly associated with UTIs, although burnout and quality of care may both be associated through the underlying working conditions [80, 83, 84].

1.2.7 Potential consequences of UTI for older adults

There are several clinical features associated with UTI. From less serious symptoms such as increased urinary frequency, which is a need to urinate frequently (e.g. once every hour) and urgency, which is a strong feeling of the need to urinate, and cloudy urine. More uncomfortable symptoms such as dysuria, which is a collective term that describes painful urination (either during or after urination), fever, chills, flank pain, suprapubic pain, nausea, vomiting, gross haematuria (urine discoloured by blood or blood clots) [29, 85]. However, old age tends to obscure the picture of common symptoms and often majorly exhibit gastrointestinal or respiratory clinical features [86].

More serious scenarios occur when the infection leads to bacteremia i.e. presence of bacteria in blood [35], and UTIs are considered the most common cause of bacteremia in elderly [85-87]. Bacteremia can lead to sepsis which recently have been defined by Singer et al. [88] (Sepsis-3) as "life-threatening organ dysfunction caused by a dysregulated host response to infection", whereas a subset of sepsis with considerably increased mortality

due to underlying circulatory and cellular/metabolic abnormalities is called septic shock. Definitions related to sepsis, severe sepsis, septic shock etc. have been somewhat unclear and have changed over time, which can make comparison of studies challenging. Studies have reported a wide range of mortality related to sepsis, septic shock or bacteremia in elderly from 9 % up to 50% [87, 89-95].

1.3 Typical diagnostic procedures and the associated problems

Typical diagnostic procedures for UTI may differ between countries, but it is usually based on a clinical part with observation and recording of signs and symptoms, and a test part with laboratory proceduress such as urine culturing and possibly some form of pre-screening such as urine dipsticks on mid-stream urine samples.

The Center for Disease Control (CDC) have established a set of definitions for UTI, and according to the CDC [22] a general Symptomatic Non-Catheter-Associated UTI must meet the following three points:

(1) One of the following is true:
    a. Indwelling urinary catheter has not been in place more than two days on the day of event
    OR
    b. No catheter on the day of event or the day before
(2) At least one of the following symptoms
    a. Fever (>38^{o}C) in a patient ≤ 65 years of age
    b. Suprapubic tenderness
    c. Costovertebral angle pain or tenderness
    d. Urinary frequency
    e. Urinary urgency
    f. Dysuria (painful urination)
(3) A urine culture with no more than two species of organisms identified, where at least one is a bacterium of ≥10^5 CFU/mL (Colony forming units/mL)

According to the CDC, a UTI event in a long term care facility (LTCF) is only registered as an LTCF UTI event 2 days after admission. LTCF UTI Criteria for LTCF patient with admission and last use of indwelling catheter >2 days [96]:

(1) Either of the following points are true:
    a. Acute dysuria
    b. Acute pain, swelling, or tenderness of testes, epididymis or prostate
(2) Either of the following points are true:
    a. Fever:
        i. single temperature ≥ 37.8^{o}C
        ii. repeated temperature ≥ 37.2^{o}C
        iii. baseline increase ≥ 1.1^{o}C
    b. Leukocytosis: > 14,000 cells/mm^{3}

    And, one or more of the following points are true:
    a. Costovertebral angle pain/tenderness
    b. Suprapubic tenderness
    c. Visible hematuria
    d. New or increased incontinence
    e. New or increased urgency
    f. New or increased frequency
(3) *Two* or more of the following points are true:
    a. Costovertebral angle pain/tenderness
    b. Suprapubic tenderness
    c. Visible hematuria
    d. New or increased incontinence
    e. New or increased urgency
    f. New or increased frequency
(4) And, either of the following points are true:
    a. Positive culture with equal or less than 2 microorganism species (of which at least one is a bacterium ≥10^{5} CFU/mL) in clean catch voided urine sample.

b. Positive culture for any number of microorganism (of which at least one is a bacterium $\geq 10^2$ CFU/mL) from sample collected with in/out straight catheter.

If either (1),(2) or (3) is true, and (4) is also true, A diagnosis of symptomatic UTI is appropriate according to the CDC definition for LTCF events.

Other symptomatic UTI criteria are the McGeer Criteria which was established for surveillance of infection in LTCFs [97]. The criteria for patients/residents without indwelling catheter:

At least three of the following signs and symptoms

a. Fever ($\geq 38^{o}$C), or chills
b. New or increased
    i. Burning pain on urination
    ii. Frequency
    iii. Urgency
c. New flank or suprapubic pain or tenderness
d. Change in character of urine
e. Worsening of mental or functional status (may be new or increased incontinence)

Loeb et al. [98] reports results from a consensus conference, and describes an attempt at developing minimum criteria for initiation of antibiotics in LTCF-residents. The criteria for patients/residents without indwelling catheter:

Acute dysuria alone or fever (>37.9ºC or 1.5ºC increase above baseline temperature)

and at least one of the following, new or worsening:

a. urgency
b. Frequency
c. Suprapubic pain
d. Gross hematuria
e. Costovertebral angle tenderness

f. Urinary incontinence

According to the CDC criteria, it is likely not sufficient with either signs/symptoms or test on its own, because it is an important point to separate between infections worth treating (symptomatic) and asymptomatic infections that often resolves themselves.

Urine dipsticks use colorimetric reactions to detect nitrite, a metabolite from bacteria, and Leukocyte Esterase (LE), enzymes from white blood cells, as an indication of bacterial infection of the bladder [99]. The reliability and accuracy of nitrite and leukocyte esterase reactions and whether they can/should be used to diagnose UTI have been debated, and studies have reported large variations in the diagnostic sensitivity [100], especially on the nitrite test, reported from as low as 10% [101], and up to 93% [102]. A meta-analysis by Devillé et al. [103] reached a conclusion that the high post-test probability of negative nitrite and leukocyte esterase tests makes the strip useful to exclude infection.

Rapid screening cannot reach the level (or will likely never be accepted on the level) of urine culturing and a solution will therefore only attempt to satisfy the purpose of rapid screening as described by Pezzlo [6], which is to provide accurate information rapidly and to eliminate negative samples.

The Regional research project the work of this thesis is associated with attempts to alleviate challenges in a particular aspect of elderly care. According to municipal medical service providers (nursing homes and home care services) in Sandefjord municipality (previously Stokke) in Vestfold county, Norway, management and treatment of UTI is challenging for patients in nursing homes and receivers of home care services. A large portion of nursing home residents and home care receivers wear diapers. Either according to necessity due to the previously described high prevalence of urinary incontinence, or (unfortunately) for simplicity due to insufficient staff despite the possible disadvantages of unnecessary diaper use [47, 104]. The high prevalence of UTI in these populations makes UTI an important condition to monitor.

The challenge lies in the difficulty of collecting urine samples from diaper-wearing incontinent patients. In the case of home care services, nurses visit the residence of

patients and have limited time per residence. The patients may not be able to deliver a urine sample voluntarily in the available time, either from lack of cooperation due to reduced cognitive abilities from dementia, delirium or other conditions, or from genitourinary conditions making them incapable of controlling urination, which makes collection of uncontaminated mid-stream urine samples difficult. This was described as a cause of frustration for the nurses.

Available options to collect a urine sample are: (1) Clean the genital region of the patient and wait for urination, (2) Catheterization (e.g. indwelling, intermittent, suprapubic or external), (3) Collect sample from incontinence product (e.g. diaper):

- Waiting for a urine sample is inefficient, as it may take several visits to collect a sample, which puts a strain on the human resources as well as introducing unwanted delays in the diagnostic process.
- Invasive catheterization is efficient, but uncomfortable, and increases the risk of infection.
- Sample extraction from an incontinence product such as a diaper or external catheter (such as a condom catheter) bag. Belmin et al. [105] found good agreement between analysis of urine extracted from diapers worn for 3 hours and urine collected by invasive catheterization from elderly women with severe incontinence. Although agreement in this particular study was found to be good, it is likely only applicable in ideal cases since urine extracted from a diaper is very likely to come in contact with contamination sources such as fecal matter, skin, anus, or vaginal opening. The degree to which a urine sample is representative of the conditions in the urinary tract may be compromised after a period of exposure to these potential contamination sources. Or simply due to the fact that the collected urine sample will be aged.

The degree to which the urine sample is representative of the conditions in the bladder – which is what is tested – is highly important for the interpretation of test results. Without proper care for representativeness, test results will likely exhibit high false positive rates, since what is measured is the contamination not the actual presence of

infectious microorganisms. The sampling methods ranked in descending order of representativeness are

- Invasive catheterized urine sample
- Voluntary mid-stream urine sample
- Clean patient and wait for collection of urine sample
- External catheterized (aged) urine sample
- Diaper extracted urine sample

For a sampling method – not included in the list above – to retain a high degree of representativeness it is necessary to collect freshly voided urine, isolate the sample from contact with patient-related or external contamination sources, and test the sample within a relatively short time.

A rapid screening solution to the problem was requested from the home care service provider, but is also relevant for nursing homes, and for others with functional impairments, multiple sclerosis, mental disorders, infants or in general patients who are incapable of removing bodily waste on their own due to any reason.

Nursing homes does not have the same limitations as home care services, as they may be better equipped with access to e.g. dipstick readers, and depending on nurse-to-patient ratio for individual nursing homes may not be subject to the same level of efficiency requirement and time restrictions. However, they still have difficulties with collection of urine samples from functionally impaired and incontinent patients. Whereas access to a dipstick reader does not provide a solution to the problem.

To sum up the problem:

(1) UTI is prevalent in the elderly population and is increasingly so for deteriorating health conditions and increased level of dependence
(2) UTI may have severe consequences
(3) Sample collection is challenging
(4) Invasive catheterization is a risk factor for UTI

(5) "Gold standard" tests are time consuming and costly if many samples (that turn out negative) that could be excluded with other methods are included

(6) Overuse of antibiotics

2 Paper-based microfluidic devices and solutions

2.1 Reviewing possible solutions to the problem

Initially the problem was analysed from the perspective of considering simply: what are the observable/measurable variables for the relevant patient group that might indicate UTI?

- *Observable symptoms* are already part of the diagnostic process (see diagnostic procedures in chapter 1). A technical solution would mostly be limited to decision-making software, and does not really solve the problem in particular because, many of the typical clinical features may not present themselves in elderly, and therefore does not qualify as a standalone solution.
- *Urine* is affected typically affected by the cause (organism) of the UTI either through metabolism of the organism, immune response or functional changes in the urinary tract, and thus is likely the best way to approach UTI.
- *Blood* may show markers related to general infections, but is likely not selective or specific.

In the second turn, the problem was analysed by introducing the context of the user (nurses). A solution must be portable, low-cost, time-saving (compared to existing methods), simple to use (not require extensive training or re-education).

- *Urine culture* is commonly used in diagnosis, but requires a urine sample, transport and time for laboratory analysis [106].
- *Flow cytometry* equipment such as the UF1000i (Sysmex) has shown great potential for excluding negative urine samples [107], but is still mostly benchtop equipment. There has been attempts at making technology that is wearable [108].
- *Biomarkers and analytes* in urine can be analysed with different methods such as:
    - Nuclear magnetic resonance and liquid chromatography mass spectrometry
    - Electrochemical sensor probes

- Colorimetric reactions
- Voltammetric analysis
- Spectrophotometric analysis
- Titration
- Capacitance based sensor
- Surface acoustic wave based sensor
- Etc.

All the presented methods need access to a urine sample and since sampling is a challenge, the only method of accessing the sample here is through either invasive means such as catheterization, or automatic external means such as collection from incontinence products. A catheter with an integrated sensor is possible with miniaturized sensors, and have been developed [109]. This would likely retain the highest degree of representativeness of the conditions in the bladder. However, if the patient quality of care is taken into account, when catheterization is a known risk factor for infection, it only leaves the sampling from incontinence products as a viable solution within the confinements of the problem and the research project this work was performed under. Diapers are very common in the relevant patient group and was therefore selected as the target source of urine sample collection.

Initially the choice of chemical analysis method was intended to be capacitance based sensors, but after problems with calibration due to the variability in concentration of urine constituents, this was abandoned. Electrochemical sensors was attempted, but required extraction of urine from the diaper which introduced unwanted steps in the procedure, involving cutting a piece of the absorbent diaper material, and mixing the cut-out material with a solution that expels urine from the superabsorbent material.

The potential cost (development cost and final unit cost) of a technical solution was considered along with the accuracy and known risk of contamination. This made it reasonable to go ahead with a solution that is based on relatively mature technology. Therefore, a solution based on colorimetric reactions with transport in porous media,

hereby described as paper-based microfluidics, was chosen. It is also an advantage that a battery is not necessary.

This matches with the main goal of the "Touchsensor for enklere og raskere urinprøvetaking og analyse" proj. no. 234972 (translated: Touchsensor for simple and faster urine sampling and analysis):

English translation of primary goal:

"Develop a portable and user-friendly Touchsensor prototype for simple, safe and fast urine sample collection and analysis from ordinary disposable diapers and urine samples"

Detection through colorimetric reactions is the same sensing method that is employed in urine dipsticks, and transport by capillary flow in porous media is similar to the transport method that is employed in lateral flow assays such as pregnancy tests. This approach leaves one issue as a problem. A survey carried out within the related research project (Touchsensor) found that assistant nurses and registered nurses were uncertain about the reading of results from colorimetric reactions on urine dipsticks [110]. Hence, the selected method alone may suffer from uncertainty due to subjective interpretation by the user. For this issue, it was decided that the selected method were to be accompanied by an application (app) for smartphones (with camera), where the smartphone camera can provide an objective record of colors and classify them. Recent smartphone models have relatively large computational capabilities that makes a smartphone more suitable, more affordable and more practical compared to making a stand-alone readout device.

2.2 Paper-based microfluidics Introduction

In recent years paper-based microfluidics have become an increasingly popular research topic, although it has been actively used for a long time, considering Litmus paper was reportedly used in the early 1800s [111]. There are several advantages of paper based microfluidic devices that make them attractive compared to microfluidic devices fabricated with more traditional materials such as glass, silicon and polymers, albeit these traditional materials have the advantage of mechanical robustness and reusability:

Cellulose paper (or other porous materials such as woven and non-woven fabrics) is hydrophilic and can transport liquids through capillary action without active pumping action from complex integrated microfluidic pumps (see Figure 3) or external pumps, and without the need for external power supply to said pumps.

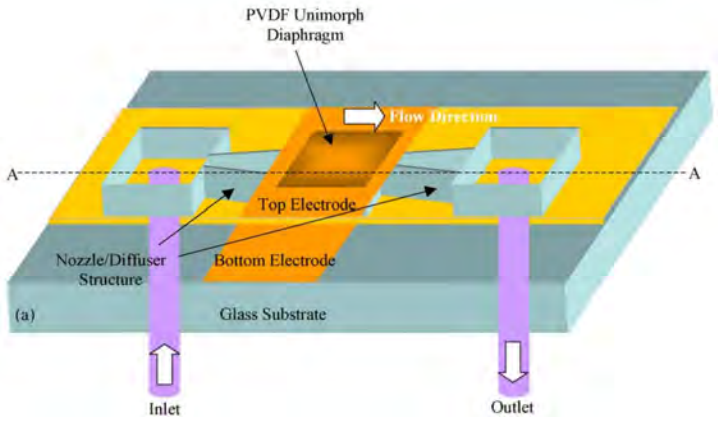

Figure 3 A planar, valveless, microfluidic pump using electrostrictive poly(vinylidene fluoride-trifluoroethylene), reprinted from Xia et al [112], Copyright 2006, with permission from Elsevier.

(1) Capillary action is relatively robust towards effects of gravity.

(2) There are several available techniques for fabrication of well-defined channels. Hydrophobic patterns that constrain or direct liquids can be made by e.g. photolithography, wax printing, screen printing and plasma treating. Alternatively cutting and lamination/encapsulation can be utilized to form a network of channels.

(3) Cellulose materials are inexpensive, and with simple inexpensive methods for forming channels, the paper-based substrate facilitates fabrication of low-cost disposable devices.

(4) A high surface area to volume ratio improves detection limits for colorimetric methods.

(5) Fibre networks in paper or related porous materials can store reagents in active form.

Although paper-based microfluidic devices can be fabricated with well-defined channels, fabrication of small dimensions is more problematic due to the fibrous nature of the

substrate compared to fabrication on e.g. silicon, but paper-based devices can process small sample volumes in the µL range, which facilitates low reagent consumption and chemical waste. On the other hand, transport in porous material is facilitated and restricted by the material properties of the material. It does not require an external power source, but the level of control in terms of flow speed and direction is limited, making, for example multistep operations and tuning difficult [113].

Many "Traditional" lab on chip devices and intricate microfluidic devices have been designed and created, but the success of bringing it from lab to commercialized product is still fairly limited [114]. This could be because of lack of communication between researchers and industry, development of modules that alone are not commercially viable or easily integrable in more complex systems, or that an ideal application for these system has yet to be discovered (an application in which microfluidic systems outperform more traditional disciplines both in terms of performance and cost efficiency), or that developed devices are still not simple and robust enough for practical commercial use. Despite the success of urine dipsticks and pregnancy tests, and the promising nature of paper-based microfluidic diagnostic platforms, it has similar problems of realization into successful commercial products. Its simplicity in terms of relatively low cost materials and the absence of intricate external control mechanisms, translates well into feasibility of mass produced disposable devices, but does apparently not translate well into commercial success for new devices [115]. It is instead stuck in lab in the traditional two-dimensional form of hydrophilic paper with hydrophobic barriers either printed, stamped, cut, deposited, patterned, etc. with wax, polymers, photoresist [113], see Figure 4.

There has also been advances from 2D to 3D stacked/folded devices that facilitates packaging and multiplexing (see Figure 5) and advances in form of added functionality and enhanced control capability out-of-plane in terms of: Timing by including a tunable shunt to delay capillary flow [116], or by using a dissolvable bridge that functions as a timed off-switch (Figure 6) [117]. Timing can also be tuned in-plane by changing

dimensions of the channel such as with varying width of the channel cross-section, but this is an “expensive” tuning procedure as it requires major changes to design.

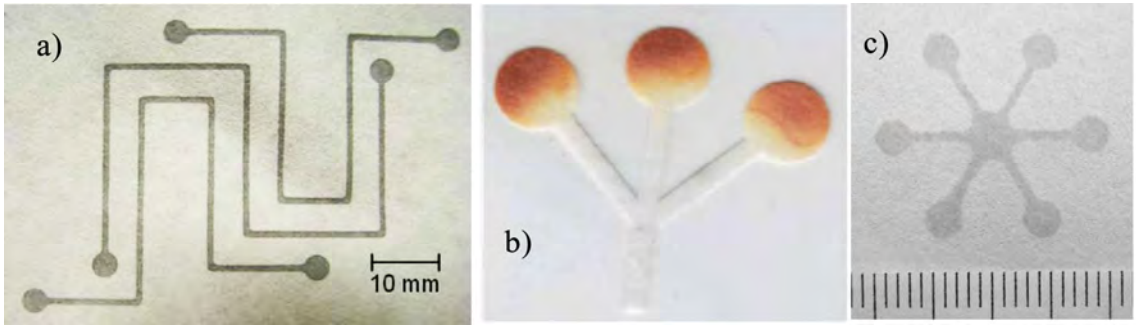

Figure 4 examples of paper-based microfluidic 2D devices: a) ink jet printed hydrophilic-hydrophobic contrast patterns reprinted from Li et al. [118], Copyright 2010, with permission from Elsevier, b) Filter paper cut with CO_2 laser, adapted from Evans et al. [119] with permission of The Royal Society of Chemistry, c) Plasma treatment generation of microfluidic patterns, reprinted from Li et al. [120]

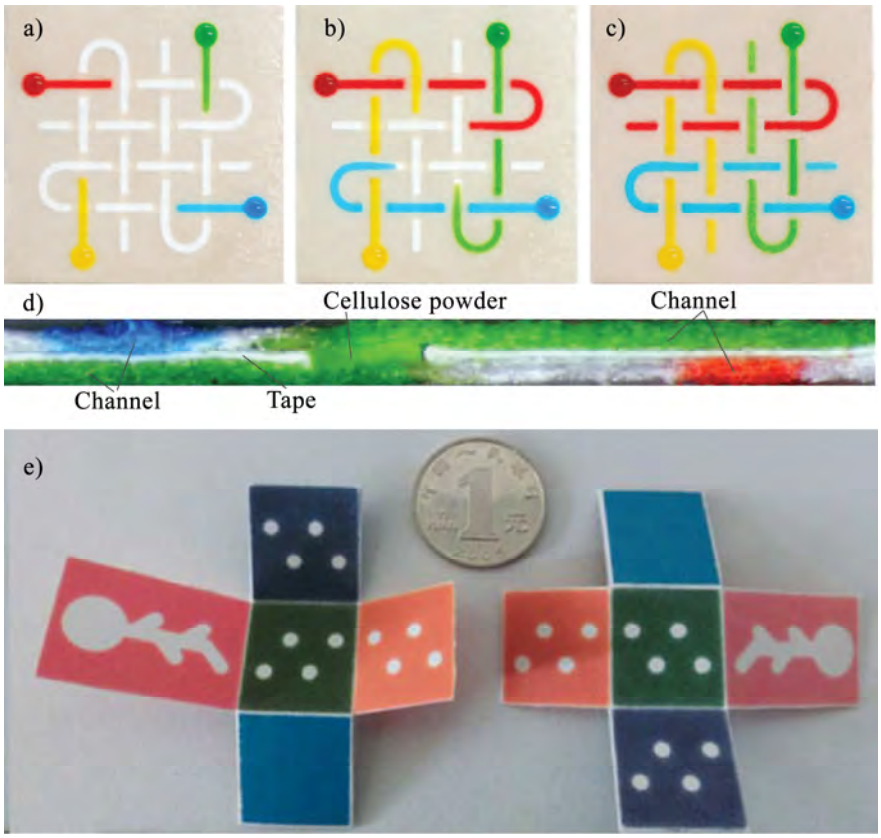

Figure 5 Three dimensional stacked or folded paper-based microfluidic device: a-d) layered paper-based microfluidic device with crossing paths, reprinted from Martinez et al. [121] Copyright 2008 National Academy of Sciences, e) Foldable paper-based microfluidic device for multiplexed sandwich chemiluminescence, adapted from Ge et al. [122] with permission of The Royal Society of Chemistry.

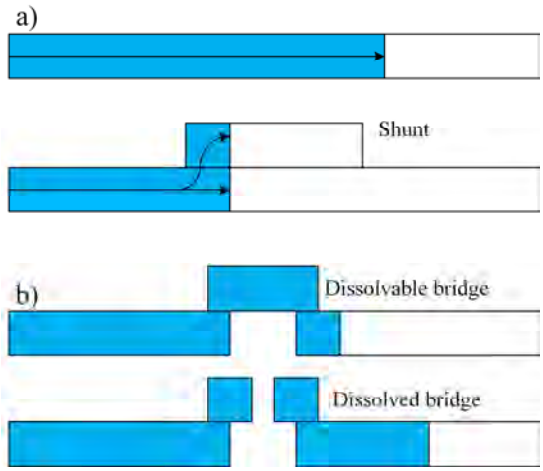

Figure 6 Sideview of modified porous media channel: a) Shunt for tuning of capillary flow speed, adapted with permission from Toley et al. [116], Copyright 2013 American Chemical Society, b) dissolvable bridge, adapted with permission from Houghtaling et al. [117], Copyright 2013 American Chemical Society.

2.3 Applications

Possible useful areas of application for rapid diagnostics with paperbased microfluidics:

2.3.1 Urinalysis

Urinalysis is relevant due to the normally simple access to samples, inexpensive materials and the need for POC analysis in ambulatory and resource-poor environments, where extensive and expensive diagnostic infrastructure is not accessible.

2.3.2 Immunoassays

Immunoassays are a widely used diagnostic procedure for detection of a particular disease based on the interaction between an antigen and a known antibody. Conventional procedures requires multiple steps carried out by trained personnel in laboratory environment, which is not available in ambulatory environment [123]. Paper-based methods can facilitate the use of simple, affordable and portable solutions that can be used in POC situations and at least provide rapid screening functionality and make it more available to e.g. unknowing carriers of disease [124], although accurate quantitative estimation is more challenging. Examples of paper-based immunoassays:

- Paper-based enzyme-free immunoassay for rapid detection of influenza A H1N1 and H3N2 viruses [125]
- Paper-based assay for determination of HPV vaccination status [126]
- Paper-based label-free immunoassay of biotin-avidin binding reaction [123]
- Multiplex paper-based immunoassay for diagnosis of Hepatitis C infection [124]

2.3.3 Environmental monitoring

Water sources intended for human consumption and water distribution networks is a path of exposure to large populations. Sudden outbreaks of waterborne illnesses or toxicants can therefore cause considerable harm to large groups of humans (as well as aquatic ecosystems). An important step to limiting the impact of severe contamination threats is the time necessary to detect contamination and the response time to act and implement corrective measures. Traditional monitoring often requires discrete (spot) sampling on-site and transportation – which may compromise samples – to laboratory facilities for determination of sample characteristics [127]. Rapid spatiotemporal variation means that results from traditional methods may not be an accurate/precise representation of the relevant water characteristics. Inexpensive rapid paper-based microfluidic solutions can provide rapid information of a selection of relevant characteristics, which can complement the traditional laboratory methods.

- Paper-based microfluidic detection of metal pollutants [128-130], non-metals, organic molecules, pesticides, bacteria, etc. [131]

2.3.4 Terrorism

Where environmental monitoring can be considered monitoring of unintentional contamination in water sources and distribution networks, terrorism prevention would be monitoring of intentional contamination. Water distribution networks are considered more vulnerable to locally injected contamination, since it bypasses the protection barriers set in place by the water distributor and due to the difficulties of monitoring the entire network. In addition, a local injection will not be diluted to the same degree as it

would be in the in a water reservoir [132]. In case of terrorism attempts, rapid solutions to detect presence of harmful substances is critical. Terrorism is of course not limited to water sources and distribution networks, other rapid screening applications includes detection of chemical warfare agents [133] and explosives [134].

2.3.5 Food safety

Contamination will generally affect food in an undesired way, either the quality of food may be reduced, or cause the food to be harmful to human health. In either way, it is preferable to know before consumption. Contamination can originate from e.g. improper storage refrigeration, poor hygiene during preparation, or from animals ingesting infectious organisms or heavy metals. In cases of microbial contamination, foodborne infections can occur by the infectious organisms in food infecting the consumer, or by microorganisms in food producing toxins [135]. Common foodborne pathogens are pathogenic strains of *E.coli*, *Salmonella* spp., *Listeria monocytogenes*. Paper-based microfluidic devices has a potential to be used as low cost and rapid screening before the much slower, but more selective culture methods [136]. Examples of paper-based microfluidic devices for food safety monitoring:

- Pesticides and foodborne pathogens [136, 137]
- Heavy metals and antibiotics [138]

2.4 Features

The World Health Organization (WHO) have established a set of criteria that is necessary for point-of-care (POC) diagnostic tests (in resource poor environments). The criteria are called ASSURED [139], which is an abbreviation for:

- Affordable
- Sensitive
- Specific
- User-friendly
- Rapid & robust

- Equipment-free
- Delivered (as in accessible)

Existing paper-based microfluidic tests such as dipsticks and lateral flow assays can satisfy the criterias: affordable, user-friendly, rapid & robust, equipment-free (although generally require some form of readout equipment for objective readings). The sensitivity and specificity is more problematic for dipsticks, such as false positives and false negatives from contamination and interference, although it is possible to reduce this impact by increasing the number of measured parameters and make a decision informed by a multivariable assessment of how the parameters affect sensitivity and specificity. E.g. Leukocyte Esterase in Bayer multistix dipsticks [99] is affected by elevated glucose levels, while glucose sensitivity is reduced by high ketone levels. Nitrite is affected by how long the urine have been in the bladder, which can be estimated qualitatively with a creatinine reaction.

Of the ASSURED criteria, the Affordable, User-friendly, Rapid & robust, Delivered are the easiest to satisfy. By allowing devices to be read by naked eye or with smartphones – which are available to most people, in particular in the developed world – the Equipment-free criteria is partially sacrificed to implement objective measurement and the opportunity for multivariable analysis to improve sensitivity and specificity.

One of the major challenges in the paper-based microfluidics is how to design devices that are capable of providing the desired functionality while being compatible with the requirements and restriction posed by the application to a degree that makes it possible to realize a robust device. The desired functionality in this work requires features, which can be provided by a set of modules.

- *Sampling module:* Automatic sampling is achieved by having an open inlet that is ready to collect the relevant sample once the event that produces the sample triggers. The purpose of the sampling module is to put the sample into contact with the porous media of the transport module

- *Transport module:* once the sample is absorbed, the transport module transports the sample to following modules.
- *Valve module:* To protect the sample after it has been absorbed, the valve module takes a portion of the absorbed sample and swells to seal off the inlet.
- *Test module:* Analyse sample provided by the transport module with a detection principle, such as colorimetric reactions.
- *Observation module:* make results from the test module available for observation, by either naked eye or equipment.

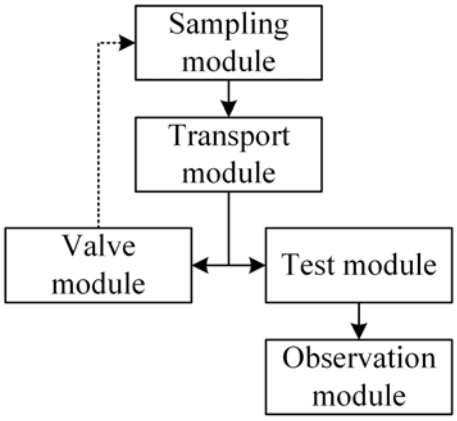

Figure 7 device modules

Comparing this modular scheme with a dipstick, the dipstick does not require automatic operation and therefore only requires the test and observation module, whereas the inlet, transport and valve is replaced with human interaction, through the process of manually collecting a urine sample and dipping the dipstick in the sample. A lateral flow assay such as a pregnancy test does not require automatic sampling, but utilizes a transport, test and observation module.

2.5 Market and commercialization.

Based on the work presented in this thesis, performed within the Touchsensor project, the candidate prepared a majority of a commercialization project proposal to the FORNY2020 program of the Research Council of Norway, which was granted and started in 2017, with a total budget of 8235 kNOK. The purpose of this project is to attempt to

commercialize the research done by the candidate within the Touchsensor project. As a part of the project proposal writing process an introductory investigation of issues related to commercialization potential was conducted, which is included here. Research presented in this thesis is applied, in the sense that it is a response to a direct request for a solution to a problem, and without commercialization potential, the research and development achievements will "die in the lab", and no real attempt at solving the problem can ever occur. Therefore, it is worth to continue the research and development towards a commercial product.

2.5.1 Market potential

Life expectancy has been steadily increasing in the 20th century (Figure 8a), and the global population is estimated to grow to around 11 billion by 2100 (Figure 8b). The increased life expectancy causes the proportion of the people over 65 to increase considerably moving forwards to 2100 (Figure 8c). This increase is going to make medical technology for elderly care important in the 21st century.

The global industry for medical technology have been estimated to grow at a Compound Annual Growth Rate (CAGR) of 5.1%, with global sales of 522 billion $ in 2022 [140]. "In Vitro Diagnostics" (IVDs) describe tests that can be used to detect diseases, conditions, or infections. IVDs are both for laboratory and other professional settings as well as for normal consumer use. IVDs are estimated to be one of the largest sectors in terms of market share and CAGR, see Figure 9. If the population growth and age distribution trend continues as estimated, the market value of IVDs will likely continue to grow.

An increased quality of care and healthcare spending may increase life expectancy. The dependency ratio increases after the age of 75, and therefore increased life expectancy – when it is over 75 – can produce a larger number of dependent people, which will require more spending on long term care, unless increased healthcare spending at birth provides more healthy years in old age [141]. However, the ratio of (age ≥ 70)/(20 ≤ age < 70) in Norway have been estimated to increase to 0.39 in the year 2100 compared to 0.17 in 2016 [142]

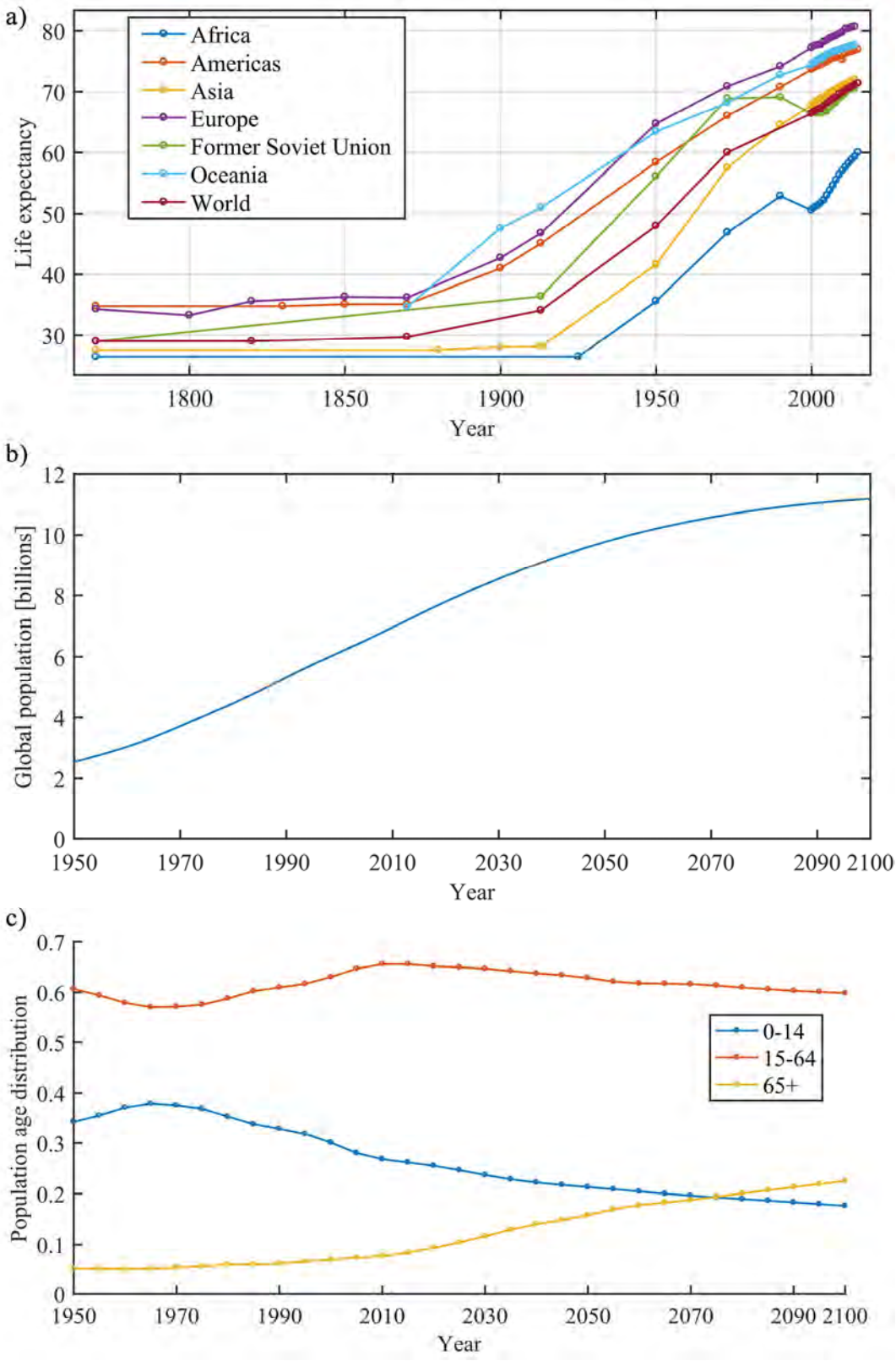

Figure 8 Population data: a) Global and regional life expectancy [143], b) Global population projection towards 2100 [144], c) Broad age group distribution trend towards 2100 [144]

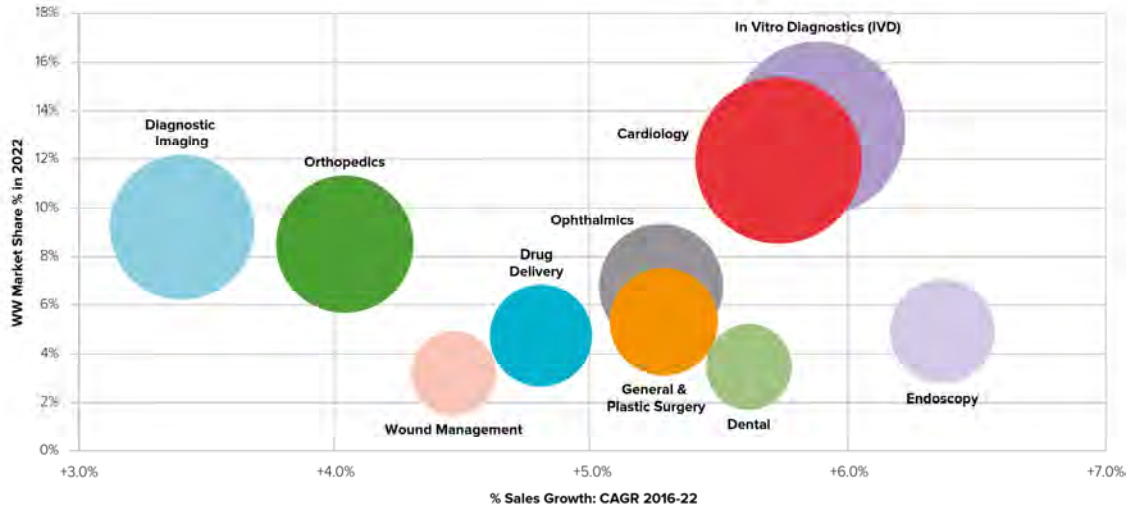

Figure 9 Analysis on top device areas with market share and CAGR estimates 2016-2022 [140]. Size of bubbles is the expected worldwide sales in 2022.

An investigation (unpublished) was carried out to assess the global demand (The national demand is considered to be settled since the research was requested by nurses in various municipalities): The following were contacted:

- 20 nursing homes (9 responded) in Canada,
- 20 nursing homes (11 responded) and 13 home care nurses (2 responded) in UK,
- 40 nursing homes (19 responded), 15 home care nurses (6 responded), 3 laboratories (3 responded), 8 support networks (4 responded), 2 adult diaper wholesalers (1 responded) in USA

They were asked about their current approach to the problem, if they used dipstick, whether the proposed solution would be helpful, and brands of products currently used. There are two relevant market categories: tests for professional usage and consumer home usage. The solution in this project is mostly oriented towards the professional usage, and the investigation revealed that the North American market is not ideal, mostly because market entry in the professional category in USA is impeded by health insurance programs, whereas the European market entry is less difficult due to widespread universal health care [145].

Based on numbers provided by partner municipalities in the touchsensor project (Stokke (now a part of Sandefjord municipality), Bærum, Grimstad. Nøtterøy, Larvik, Drammen), a solution to the presented problem (sample and analyze urine samples) can save 13 minutes per patient. Based on numbers from KOSTRA (Municipality-state-reporting, Statistics Norway) the total saved time on a national scale was 97 full time equivalent positions in the municipal nursing and care sector in Norway.

2.5.2 Risk overview

There are risks associated with the potential for commercialization, both related to the actual performance and utility of the device (mainly the ASSURed criteria), as well as market, competition, certification and regulation related risks. A brief summary of risks, consequences and possible actions to reduce risk is summarized below:

Table 4 Risk table

Description	Consequence	Action
Low cost efficiency	Not Affordable (**A**), higher production cost than expected	Ensure use of low cost and easily obtained materials. Reduce the number of suppliers and increase volume
Unsatisfactory performance (**SSR**)	Barrier to market entry; Reduced market share	Involve users; more tests and development
Insufficient User-friendliness (**U**)	Reduced demand and sales	Involve users early in the commercialization process; involve subcontractors for design and user-friendliness
Production risk	Low product quality; high defect rate.	Promote good practice and international standards for quality control; select partners that implement such standards
Competition	Slow and reduced sales; reduced profit; loss of market share	Rapid improvement of technology; enhance product portefolio; reduce sales price
Insufficient IPR-protection	Similar product concepts distributed in target markets	Patent for product technology and methods granted in priority countries before introduction to market
Lack of certification	Cannot enter market	Involve regulatory consultant
National changes to health and safety guidelines	Reduced market share and sales	Stay updated on guidelines; dialog with relevant government bodies; Flexible design that can be tailored towards different guidelines

In the research and development portion of the process, the largest risk is the competitive solution. The only available commercial product is Tena U-test, which entered the market after the solutions in this thesis was selected. The Tena U-test is a diaper pad with nitrite and LE biomarkers, and is compatible with commercial diapers. The sales price is high (259 NOK/ 2 units). Compared to the solution presented in this thesis, the U-test is not a scalable/flexible design, and the development in this work has focused more on adding functionality as well as strong focus on contamination prevention. Other competitors are Pixie Scientific (New, York, USA) and Diaper detective (student project at UC Riverside, USA, no recent activity as of 2017). A comparison of the features from the different competitors follows:

Table 5 Comparison of competitive technologies

	Dipsticks	Diaper detective	Pixie scientific	Tena U-test	This work
Retain results ≥ 8 h	No	Unknown	No	Yes	Yes
Effective sampling	Manual	Unknown	No	No	Yes
Contamination control	No	Unknown	No	No	Yes
Universal diaper compatibility	No	Yes	Yes	Yes	Yes
High TRL	Yes	No	Yes	Yes	Yes
Target adult users	Yes	No	Yes	Yes	Yes
> 2 biomarkers	Yes	No	Yes	No	Yes
Available analysis software	Only lab	No	yes	No	Yes

2.5.3 Classification for certification

Based on the investigation of international commercial potential, the EU area was found to be the most promising. To realize a commercial potential it is necessary to obtain CE marking. The system developed in this work is intended to be a medical device, which is a piece of equipment and software to be used in vitro for examination of specimens derived from the human body for the purpose of providing information concerning a pathological process, which falls under the definition of 'in vitro diagnostic medical devices' as paraphrased from the REGULATION (EU) 2017/746 [146].

The target market is the professional market, and a non-invasive device intended for use outside of laboratory environment by health professional near a patient is a 'device for

near-patient testing' according to the regulation. A 'device for near-patient testings' for the purpose described in this work falls under class B, which requires a quality management system and a review of technical documentation by a notified body designated by a EU country to assess a product before being introduced to the market (in contrast to class A which can self-certify) [146, 147].

3 Smartphone app method for colorimetric analysis

A description of considered methods, challenges and solutions to realize a colorimetric measurement algorithm that can operate with sufficient robustness under the constraints posed by the intended application, which is to photograph the results of a colorimetric test irrespective of device and illumination conditions and assign a label to the test colors that represents a biomarker quantity.

3.1 Color dependencies

At some point in the process of assigning a label to a test color, it is necessary to compare an obtained result with a calibration curve or a reference of some sort. However, if the conditions that applies to the construction of a calibration curve are not representative of the conditions that apply for extracted test data, then the calibration curve will not be able to accurately link a test to the corresponding calibrated quantity. In addition, if the only information available is an image, then information about what those conditions are is not explicitly known, and neither is the relationship between the significant condition-related parameters and variation in perceived colors. Color perception depends on a several variables, such as: illumination type, color and intensity, device model, image sensor spectral sensitivity, camera settings, internal camera processing. Therefore, a set of problems must be addressed to ensure robust operation. Figure 10 displays a set of factors related to camera and illumination that affect the perception of colors. The most obvious factors are illumination spectrum and intensity, while other parameter such as software or hardware settings e.g. ISO, shutter speed, aperture or white balancing may have an equivalent or even more significant effect on the perceived color.

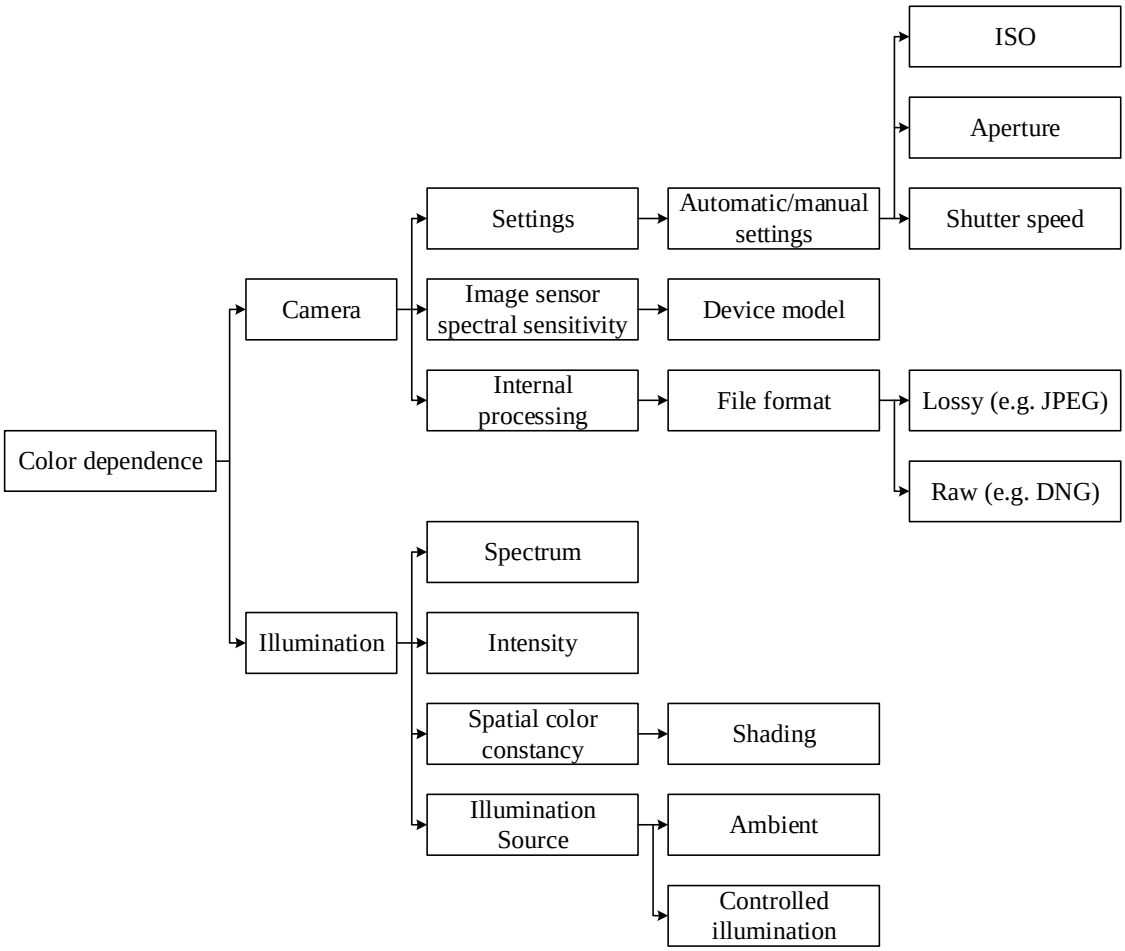

Figure 10 Relevant color dependencies

3.2 Color correction or standardization procedures

Initially, consider a case where two images are obtained from one camera with fixed device conditions. To overcome the challenge of difference in illumination conditions, a correction procedure based on information present in the image can be used to estimate the difference in illumination conditions and attempt to transform a set of test data to the conditions of the reference data or vice versa, thereby providing color constancy between the two cases. This relies on the assumption that information regarding the illumination source is present in the data and can be extracted either from the image as a whole or from designated reference locations. It has been proposed that in the case of 3 photoreceptor classes, surface reflectance can be recovered from a surface reflection

fixed model with no more than two degrees of freedom, and in general, reflectance recovery is an ill-posed problem [148, 149]. The sensor response can be described as:

$$\rho_k = \int R_k(\lambda)S(\lambda)E(\lambda)d\lambda$$

Where index *k* is sensor channel, *R* is image sensor sensitivity, *S* is surface reflectance, and *E* is ambient light spectral power distribution. Given an image, only the processed sensor response is provided, while the individual contributions of either image sensor sensitivity, surface reflectance properties or illumination spectrum cannot easily be decoupled, and is assumed unknown. If the case is expanded to include variation in device conditions as well, the problem is complicated further. Examples of color constancy algorithms can be found in Barnard et al. [150, 151]. Attempts at determining any of the functions could simplify the decoupling of the remaining functions, and could be done by introducing standardization equipment or methods, such as isolating the scene from ambient illumination and/or providing a standardized known illumination source, characterizing the illuminant, or characterising the camera image sensor. None of these methods are practical. Hence the following constraints are posed for simplicity and generalization purposes:

- No physical attachment
  - A smartphone physical attachment may require device specific design.
- No external standardization equipment
  - Equipment such as a box to avoid ambient light and a lamp makes the procedure more laborious and cumbersome for a user.
- Hardware specifications or characteristics are unknown
  - If the app depends on model specific data, the app would require adjustments for every smartphone model
- A minimum of user interaction
  - If excessive user interaction is required, it will reduce user-friendliness of the app.

3.3 Calibration

Instead of generating a global calibration curve, it is possible to generate calibration curves relative to a reference. Published literature appeared to lack potential to generalize to other reactions. Examples with ascending degree of generalization potential:

- *Reaction color and image sensor channel matching:* McGeough et al. [152] published a method that requires a colorimetric reaction to vary in intensity in a wavelength compatible with a color filter in the image sensor (in their case blue), and fitting a nonlinear function to data extracted from a single color channel.
- *Constant hue procedure*: Summriddetchkajorn et al. [153] measured color as a reference weighted greyscale (similar to intensity). This approach allows colorimetric reactions that change color according to color intensity as long as the hue is approximately constant, e.g. light-yellow to yellow or light-purple to purple.
- *xy-chromaticity interpolation*: Yetisen et al. [154] prepared a set of colorimetric reaction colors from known concentrations and recorded each color individually as a calibration procedure before a test. Calibration data was transformed from RGB color space to xy-chromaticity data, and then first order interpolated. This procedure opens up for all colorimetric reactions that produce significant difference in xy-chromaticity space, but is impractical as it requires manual calibration of one reference color at a time with individual images. This approach provides illumination independence assuming that the illumination is constant over the entire calibration procedure, and provides image sensor independence assuming that the same camera is used over the entire calibration procedure. However, it does not provide independence from internal camera processing.

The raw data from smartphone cameras typically come in .DNG format as a color filter array where every square pattern of 4 pixels consist of one red, one blue and two green pixels [155]. The internal processing of the smartphone converts the color filter array into three (RGB) color channels with interpolation of missing values, and performs various

processes such as white balancing, sharpening and gamma correction. The raw image file is stored in sRGB format, which can be transformed with linear and nonlinear transformations to RGB, rg-chromaticity, XYZ, xy-chromaticity, HSI, LMS and L*a*b* etc. [149].

The advantage of various color space transformations is that they may remove some of the inherent nonlinearities stemming from the continuous visible light spectrum being reduced to a representation of color in terms of 3 selected wavelengths typically red, green and blue. Color space transformations can make the representation of colors more in line with how humans perceive color. An example of this is the L*a*b* color space, which unlike RGB is designed to approximate human vision. It consists of the color lightness L*, red-green a* and yellow-blue b* [156]. This is more intuitive from a human perception perspective because a mixture of red and green or yellow and blue forms a color that is dissimilar to either of the mixed colors, whereas a mixture of e.g. yellow and red (orange) looks similar to both yellow and red. The L*a*b* color space has thereby transformed the data into a coordinate system where the a* and b* axis have opposites that cannot mix according to the human perception. Imitating human perception might be useful in certain situations, but when it comes to measurements of colors for comparison with a calibration curve the app does not have to consider the human perception. Unless the transformations increases between-group scatter relative to within-group scatter or improves homoscedasticity of sampled colors, there is little to gain from introducing several turns of fixed linear and nonlinear transformations.

Work of other researchers appeared to present the color space transformations or reaction specific transformations as a major part of their method for colorimetric detection [153, 154, 157-166], while the only apparent advantage was a dimension reduction to facilitate graphical representation. RGB space has three variables, while rg-chromaticity, xy-chromaticity, HS (from HSI) and a*b* (from L*a*b*) all contain the color information in two variables. This is a very simplistic way of approaching dimension reduction with a fixed transform without considering the image data. Methods in the cited articles also rely on multivariable statistical assumptions that are not explicitly

stated, especially related to the distribution of the recorded colors. Data was often treated as if it was homoscedastic and normally distributed without within-group correlation, skewness or kurtosis. Dimension reduction by multivariable statistical methods is more likely going to produce good results compared to a fixed transform.

3.4 Proposed method

Some of the previously described methods of other researchers appeared to be dependent on selecting appropriate colorimetric reactions. The proposed method focused on designing an appropriate algorithm compatible with relevant urinary biomarkers without specifically being designed for a colorimetric reaction, so that they are more generally applicable. This was done by making two assumptions:

Assumption 1:

Individual reference color groups are distributed in color space in agreement with their class order (Figure 11) or stated in a different way: The finite set of reference colors is assumed to be a subset of observations sampled from a colorimetric curve in color space from a continuously changing biomarker quantity, and this curve is an open non-intersecting curve.

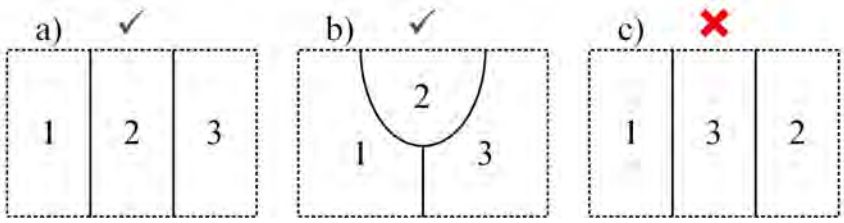

Figure 11 Data groups and class order (a) Adjacent groups correspond to adjacent ordinal classes, no shared boundaries between non-adjacent groups in the relevant region in feature space. (b) Adjacent groups still correspond to adjacent ordinal classes, but non-adjacent classes share boundaries. (c) Groups do not follow class order.

Assumption 2:

The reference groups are sufficiently well separated so that they can be distinguished by the 'naked-eye' or a smartphone camera, without significantly overlapping color distributions.

In a hypothetical self-intersecting colorimetric reaction curve in color space, the intersecting points would not be distinguishable from each other, albeit they correspond to different biomarker quantities, and therefore not be suitable for colorimetric analysis. Similarily, if the application is taken into account, that is, as a complementary objective measurement tool to support naked-eye observation of colors; if the color reference levels are indistinguishable to the naked eye, the reaction would likely not be appropriate for colorimetric analysis. Hence, these assumptions are considered reasonable.

Semi-quantitative estimates was chosen over continuous estimates since the additional information that could be gathered by making continuous estimates is unnecessary when taking into account the context of the application, which is as an objective rapid screening tool to aid nurses in management of UTI. The additional information that can be obtained from continuous estimates is not important in this context. By making the two assumptions the method in a way tries to make up for the discrete levels by taking advantage of the preservation of class order in the data. If reference data is ordinal, a misclassified test assigned to a class adjacent to the true class is “less wrong” than a misclassified sample assigned to a class two or more classes away from the true class. For biomarkers with superior dichotomous classes (positive/negative), a misclassification such as a false positive or a false negative is a complete failure, but by defining sets of ordinal sub groups within the dichotomous main groups, misclassifications between ordinal subgroups are still essentially correct.

Since variation in recorded color is affected by many variable factors (Figure 10), instead of trying to predict how the variables affect the colors, a more “holistic” approach is used. Consider the variation in recorded images from a hypothetical true (objective) color as an error term that depend on the affecting variables. Assume that the true color and thereby the error is unknown. If two colors in different locations within one image appear equal, the error and true value of the two colors are assumed equal, on the condition that affecting variables apply equally to the error of both colors (spatial uniformity). By simultaneously recording (in one image) the test and a set of provided reference colors, the color error can be neglected. In this way the issue switches from an illumination and

device dependency challenge to a reference color fabrication and colorimetric reaction stability challenge, that may make the problem more manageable.

Printed reference colors provide an opportunity for users to perform subjective readings by 'naked-eye' or use the references for objective readings on a smartphone, by classification of colors on the basis of their similarity with a reference. This approach does however introduce additional error sources, such as material reflective properties, which is likely different for the material on which the reference is printed and the biomarker reaction pad, as well as non-uniformity of illumination on the photographed surface.

3.5 Spatial uniformity

The conditions imposed by the method regarding spatial uniformity on the surface of the photographed object present two main obstacles:

- Shadows cast by user, or camera held by user
- Uniformly reflected light from the surface

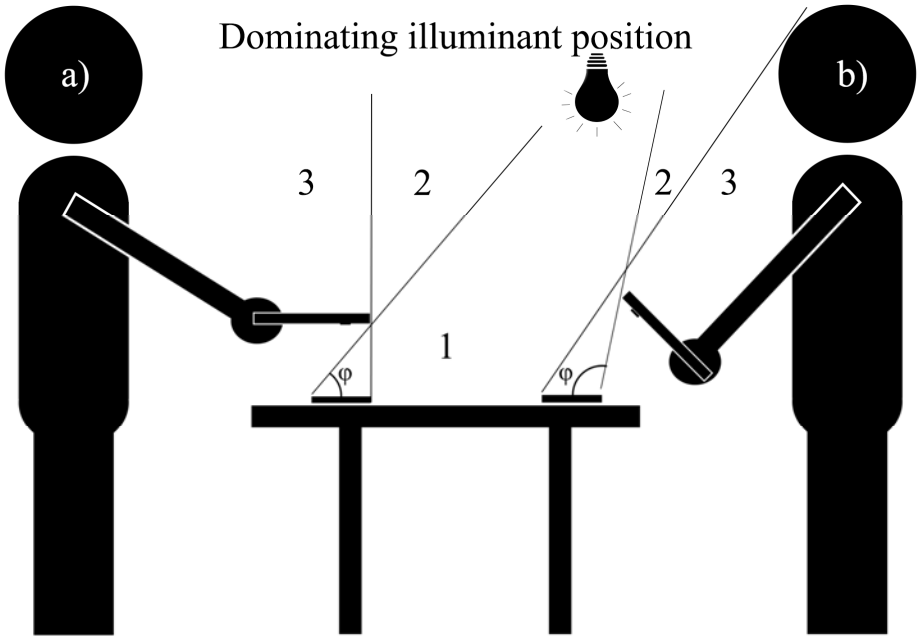

Figure 12 illustration of illuminant positions for smartphone. (a) Parallel to diaper assay. (b) Tilted. Numbered dominating illuminant positions for (a) and (b) are: (1) Acceptable angle, fully illuminated. (2) Partial shadow coverage. (3) Full shadow coverage.

The dominating illumination source in the environment (dominating here means an illumination source capable of illuminating shadows cast by other sources) dictates the possible positions of a user and the smartphone to obtain an image without shadows. A naïve initial assumption was that holding the smartphone parallel with the surface of the device would be ideal as it avoids introducing perspective in the image. This required the dominant illumination source in the location to have a very large incidence angle with respect to the surface of the device so that it illuminate the surface without casting shadows, see Figure 12a). In a ceiling-lit location, it may be near impossible to find a dominating illumination source with an acceptable angle of incidence on a horizontal flat surface without casting shadows. Three cases can occur:

- No shadow is ideal.
- Full shadow coverage is manageable because reflected light may be uniformly reflected, but is still undesirable because the range of the data is limited, increasing the risk of overlapping color distributions.
- The worst case scenario is partial shadow coverage, which can be bad in two ways
    - Shadows cover only a subset of reference colors for a biomarker. Here illumination conditions change within the reference data, making comparison invalid
    - Shadows cover a reaction/reference pad partially. This corrupts the color data, by contaminating recorded data with a mixture of no-shadow, full-shadow, and shadow gradient distributions. Figure 13 shows histograms of a partial shadow-covered surface

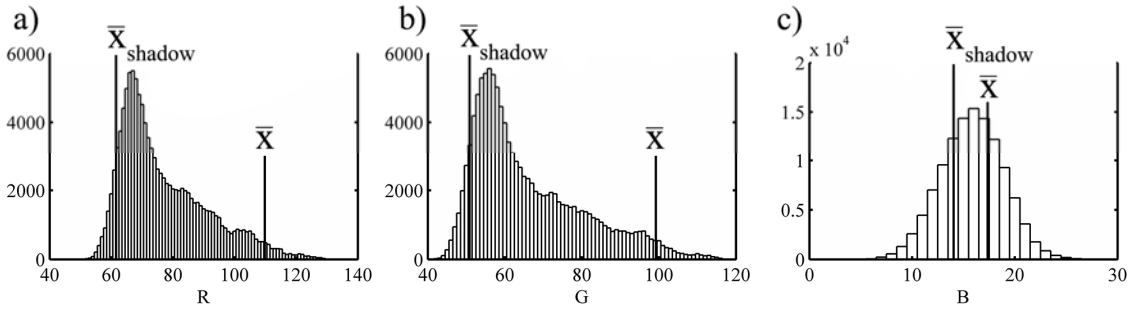

Figure 13 Partial shadow-covered surface histograms, where $\overline{X}_{shadow}$ is the mean of a region fully covered, while $\overline{X}$ is the mean of an uncovered region

A variable observation direction of the camera allows for much more freedom to avoid shadows, by positioning the camera more favourably with respect to the illumination sources available.

A rectangular surface photographed in perspective is perceived as a convex quadrilateral. The corner with the minimum angle with respect to adjacent corners forms a triangle with the two vanishing points. In case of two parallel opposing sides the rectangular surface is perceived as a trapezoid and there is only one finite vanishing points. The corners with the smallest and second smallest angle form a triangle with what is defined here as the first vanishing point, while the corners with the smallest and the third smallest angle form a triangle with the second vanishing point. The point that forms a right triangle with the two vanishing points is defined as a new origin, see Figure14

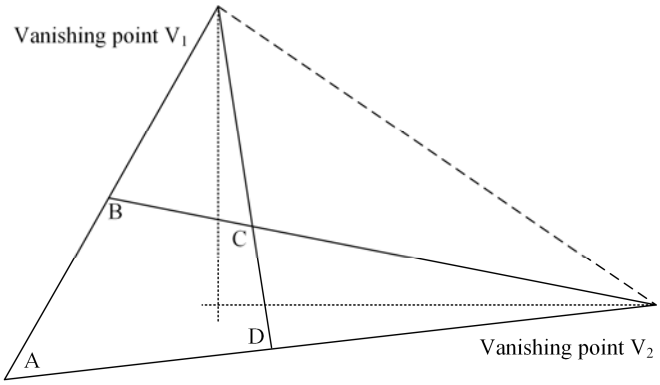

Figure 14 Perspective convex quadrilateral

The least computationally intensive method of transforming the quadrilateral to a rectangle only requires the position of vanishing points [167]. Coordinates on the rectangle (x, y) and in perspective (x', y') are given with respect to the new origin.

$$\begin{bmatrix} X \\ Y \\ Z \end{bmatrix} = \begin{bmatrix} 1 & 0 & 0 \\ 0 & 1 & 0 \\ h_{31} & h_{32} & 1 \end{bmatrix} \begin{bmatrix} x \\ y \\ 1 \end{bmatrix}$$

$$x' = \frac{X}{Z} = \frac{x}{h_{31}x + h_{32}y + 1}, \qquad y' = \frac{Y}{Z} = \frac{y}{h_{31}x + h_{32}y + 1}$$

$$x = \frac{x'}{-h_{31}x' - h_{32}y' + 1}, \qquad y = \frac{y'}{-h_{31}x' - h_{32}y' - 1}$$

where $h_{31} = \frac{1}{x'_{V_1}}, h_{32} = \frac{1}{y'_{V_2}}$ (the inverse distance between new origin and vanishing points).

The alternative method is to estimate the full homographic mapping (9 parameters) [168]:

$$\begin{bmatrix} X \\ Y \\ Z \end{bmatrix} = \begin{bmatrix} h_{11} & h_{12} & h_{13} \\ h_{21} & h_{22} & h_{23} \\ h_{31} & h_{32} & h_{33} \end{bmatrix} \begin{bmatrix} x \\ y \\ 1 \end{bmatrix}$$

$$x' = \frac{X}{Z} = \frac{h_{11}x + h_{12}y + h_{13}}{h_{31}x + h_{32}y + h_{33}}$$

$$y' = \frac{Y}{Z} = \frac{h_{21}x + h_{22}y + h_{23}}{h_{31}x + h_{32}y + h_{33}}$$

On the condition that: $\sum_{i,j} h_{ij}^2 = 1,$ the following homogenous system of equations can be formed:

$$Ah = 0$$

$$\begin{bmatrix} x_1 & y_1 & 1 & 0 & 0 & 0 & -x_1x'_1 & -y_1x'_1 & -x'_1 \\ 0 & 0 & 0 & x_1 & y_1 & 1 & -x_1y'_1 & -y_1y'_1 & -y'_1 \\ x_2 & y_2 & 1 & 0 & 0 & 0 & -x_2x'_2 & -y_2x'_2 & -x'_2 \\ 0 & 0 & 0 & x_2 & y_2 & 1 & -x_2y'_2 & -y_2y'_2 & -y'_2 \\ x_3 & y_3 & 1 & 0 & 0 & 0 & -x_3x'_3 & -y_3x'_3 & -x'_3 \\ 0 & 0 & 0 & x_3 & y_3 & 1 & -x_3y'_3 & -y_3y'_3 & -y'_3 \\ x_4 & y_4 & 1 & 0 & 0 & 0 & -x_4x'_4 & -y_3x'_3 & -x'_4 \\ 0 & 0 & 0 & x_4 & y_4 & 1 & -x_4y'_4 & -y_4y'_4 & -y'_4 \end{bmatrix} \begin{bmatrix} h_{11} \\ h_{12} \\ h_{13} \\ h_{21} \\ h_{22} \\ h_{23} \\ h_{31} \\ h_{32} \\ h_{33} \end{bmatrix} = \begin{bmatrix} 0 \\ 0 \\ 0 \\ 0 \\ 0 \\ 0 \\ 0 \\ 0 \\ 0 \end{bmatrix}$$

And solved by singular-value decomposition

$$A = USV^T$$

$$A^TA = VS^2V^T$$

h is set to be the column of *V* corresponding to the smallest eigenvalue in *S*. An example of a homographic map is shown in Figure 15. In a photograph where a rectangle is perceived as a convex quadrilateral, the homographic coefficients can be used to map

known positions on a reference surface to the corresponding positions on the photographed surface.

Since the perspective is caused by a difference in distance from points in the object plane to the camera image plane, and the resolution of a camera is finite, the resolution limits the distance and angle of incidence between the camera and surface, to allow a sufficient amount of information to be extracted.

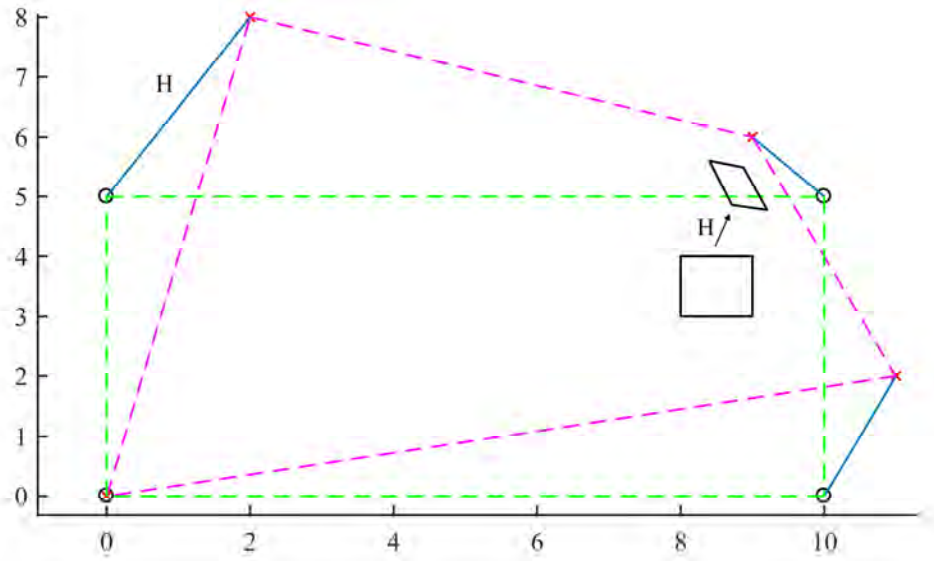

Figure 15 homographic transform. (0,0),(2 8), (9 6), (11,2) mapped to (0,0), (0,5), (10,5), (10,0). Exaggerated perspective

The number of pixels contained in a convex quadrilateral can be estimated by

$$A_{Total} = \frac{1}{2}|\det[d_1, d_2]|,$$

Where $[d_1, d_2]$ are diagonal vectors of pixel coordinates of a quadrilateral in a 2x2 matrix. The corner with the largest angle is the corner furthest from the camera, and references near this corner will contain the least amount of pixels. There are two alternatives for selection of pixels for extraction:

(1) Estimate the pixel content from the reference near the farthest corner with a margin, as absolute maximum pixels that can be extracted. Extract the maximum

pixels around the center point of all the reference and test colors, for a balanced sample size across all test and reference colors

(2) Estimate the pixel content of all reference and test colors individually based on the homographic transform and extract estimated pixels with a margin, for an unbalanced sample size

The area of reference and test positions vary depending on the perspective with respect to position on the surface. The difference in size at any point can be estimated by defining a differential square in the rectangular space (Figure 16), and calculating the ratio between the area in the homographic transformed space and the area in the rectangular space.

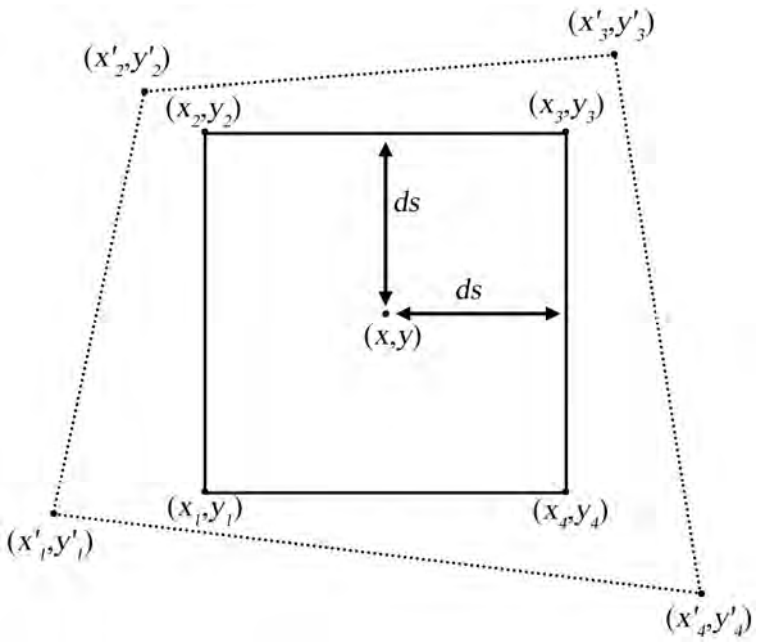

Figure 16 Differential area

$$F = \lim_{ds \to 0} \frac{dA'(x,y,ds)}{dA(ds)} = \left| \frac{1}{Z^2} det \left(\begin{bmatrix} h_{11} & h_{12} & x' \\ h_{21} & h_{22} & y' \\ h_{31} & h_{32} & 1 \end{bmatrix} \right) \right|$$

The homographic area ratio for the example of Figure 15 is shown in Figure 17.

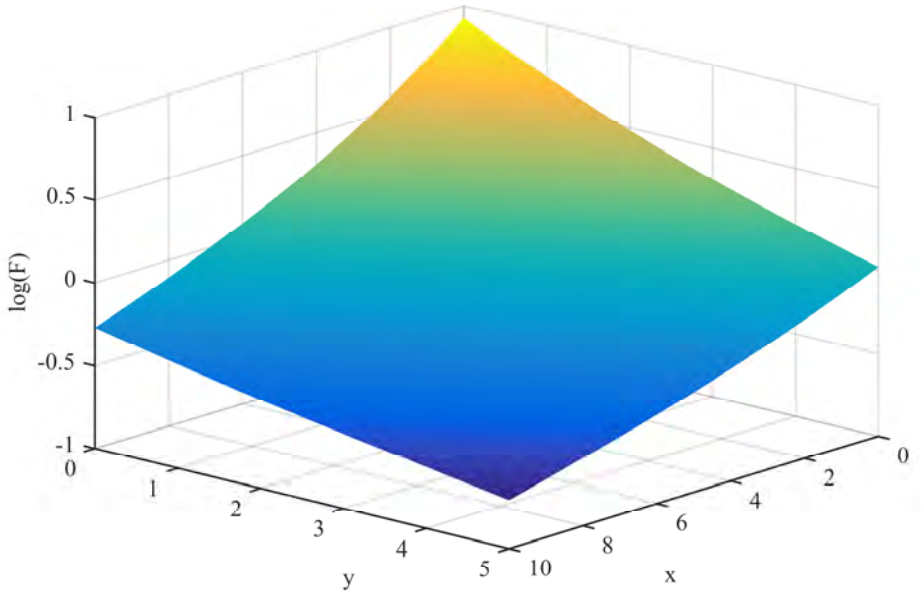

Figure 17 logarithmic homographic transform area ratio for the example in Figure 15

3.6 Illumination sources

One could imagine that a camera flash can provide controlled illumination conditions and prevent shadows. This was found to not be a viable approach due to how the reflected intensity depends on the angle of incidence. If the surface is assumed to be a diffuse reflecting (Lambertian) surface [169], the reflected intensity is independent of observation vector, but depends on the angle of incidence with respect to the surface normal. In Figure 18a) the illumination provides a stable and relatively uniform color distribution, while in Figure 18b) the shading from proximity of the flash generates large spatial non-uniformity.

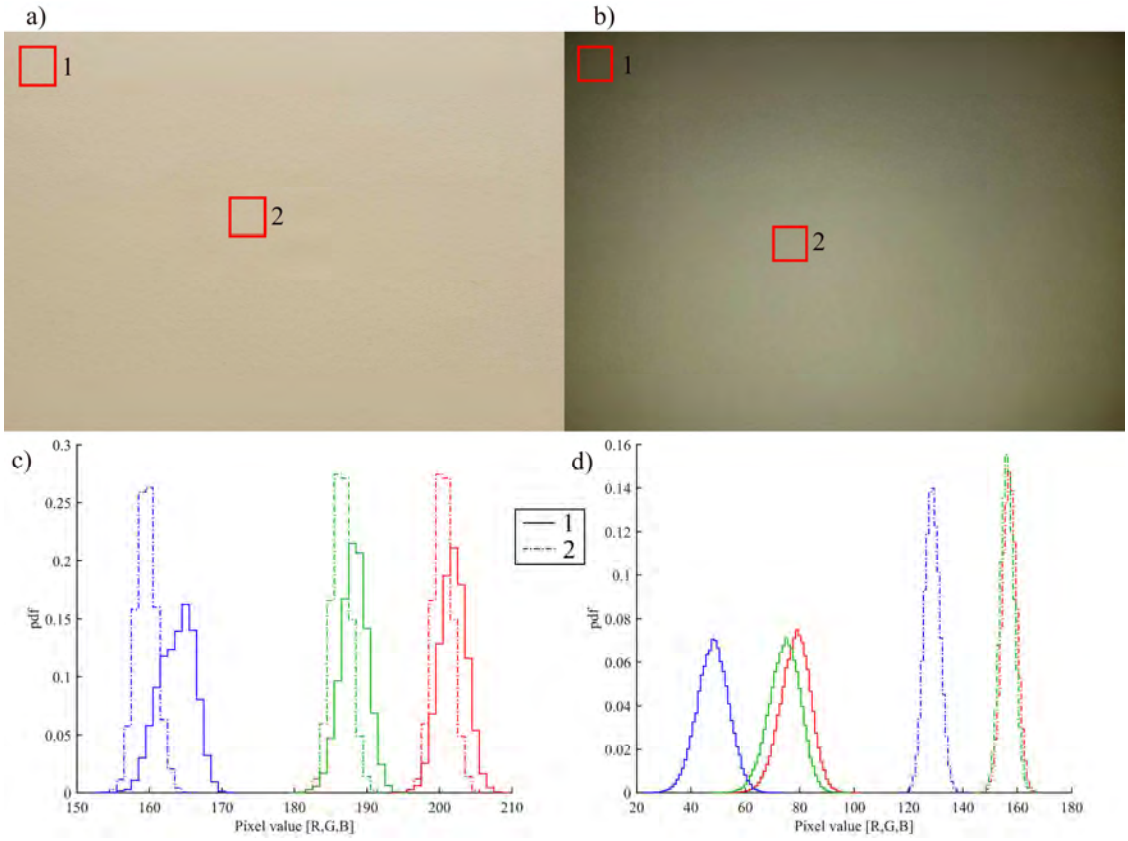

Figure 18 a) photograph of a slightly yellow surface in ambient light, b) photograph of the same surface with flash, c) histogram of position 1 and 2 without flash, Euclidean RGB distance 4.7 d) histogram of position 1 and 2 with flash, Euclidean distance 139.3

A similar effect can be seen in the work of Sumriddetchkajorn et al. [159] who use white LEDs as a reference near the sample in a closed box. The LEDs causes easily observable spatial variation in color due to shading, see Figure 19.

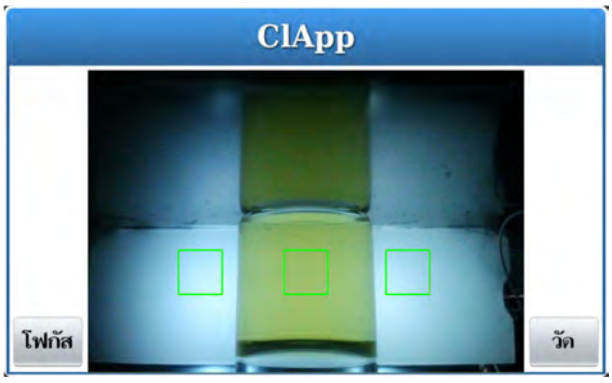

Figure 19 Reprinted from Sumriddetchkajorn et al. [159], Copyright 2014, with permission from Elsevier. The color of the liquid sample is compared with a white reference. In this example there is no ideal location to extract a white reference since the majority of the white regions are shaded.

The shading can occur due to the proximity of the illumination source to the observed surface causing a non-uniform angle of incidence over the surface, see Figure 20a. A considerable variation in angles of incidence could be modelled wiith a reflection model such as Lambertian, Blinn-Phong or Oren-Nayar reflection [169], but would introduce additional parameters to estimate.

To avoid the problem of shading, a solution was considered in context of the intended user environment. Without posing an overly restrictive requirement, it is assumed that a user performs a test in illumination conditions typically encountered in everyday life, such as can be expected from sunlight or indoor illumination. In this case the angle spanned by the extremes of the surface tends to zero for large ratios of source distance to surface width (Figure 20b).

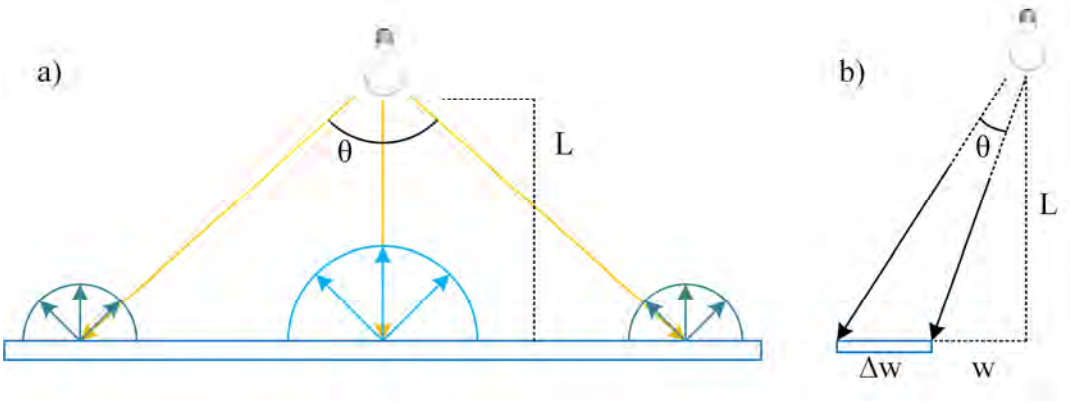

Figure 20 illustration of illumination source distance effect on reflected light: a) illumination source close to surface, b) illumination source far from surface

If L is vertical distance from source to object, w is horizontal distance (>0) from source surface normal to object, Δw is the width of the object, $(\Delta w/w) = k, (L/\Delta w) = x$, then the difference in incidence angles from the source between the extremes of the object is given by

$$\theta = \arctan\left(\frac{x}{x^2 + \left(\frac{1+k}{k^2}\right)}\right)$$

$$\lim_{x\to\infty} \theta = 0$$

If the surface is assumed to be lambertian (diffusive reflectance), the diffusely reflected light intensity is proportional to the cosine of the illumination source angle of incidence. The ratio of the lambertian reflected minimum to maximum intensity for a point source is:

$$i = \frac{I_{min}}{I_{max}} = \sqrt{\frac{(kx)^2 + 1}{(kx)^2 + (1+k)^2}}$$

Example calculation: A room with an illumination source 2.5m (L) vertical distance over a 15cm (Δw) device, with a 1.5m (w) horizontal distance, gives a k = 1/10 and x = 50/3. This results in a θ = 2.4° and i = 0.973 (-2.7%), as an absolute maximum, whereas the distance between a test color and the reference furthest away is approximately 5 cm (Δw), which results in a θ = 0.8° and i = 0.991 (-0.9%),

3.7 Classification

In this work, the reaction color is determined based on similarity to the set of provided references. There are many available classification procedures, but 5 variants where chosen here.

- k-nearest neighbours (knn): classifies unlabelled data according to the majority label among the k-nearest neighbours [170].
- Pooled discriminant score: classifies unlabelled data as the most probable group assuming homoscedastic and normally distributed data.

$$d_i = -\frac{1}{2}(x - m_i)S_W^{-1}(x - m_i)^T + \ln p_i$$

- Quadratic discriminant score: classifies unlabelled data as the most probable group assuming normally distributed data, but allows heteroscedasticity.

$$d_i = -\frac{1}{2}\ln|S_i| - \frac{1}{2}(x - m_i)S_i^{-1}(x - m_i)^T + \ln p_i$$

- Chernoff map , Linear Bayes normal classifier

- Chernoff map, Quadratic Bayes normal classifier

The Chernoff mapping is found by maximizing the Chernoff criterion [171], through eigenvalue decomposition of the matrix:

$$\sum_{i=1}^{K-1}\sum_{j=i+1}^{K} p_i p_j S_W^{-1} S_W^{-\frac{1}{2}} \Bigg(\left(S_W^{-\frac{1}{2}} S_{ij} S_W^{-\frac{1}{2}} \right)^{-\frac{1}{2}} S_W^{-\frac{1}{2}} (m_i - m_j)(m_i - m_j)^T S_W^{-\frac{1}{2}} \left(S_W^{-\frac{1}{2}} S_{ij} S_W^{-\frac{1}{2}} \right)^{-\frac{1}{2}} + \frac{1}{\pi_i \pi_j} \Bigg(log\left(S_W^{-\frac{1}{2}} S_{ij} S_W^{-\frac{1}{2}} \right) - \pi_i \, log\left(S_W^{-\frac{1}{2}} S_i S_W^{-\frac{1}{2}} \right) - \pi_j \, log\left(S_W^{-\frac{1}{2}} S_j S_W^{-\frac{1}{2}} \right) \Bigg) \Bigg) S_W^{-\frac{1}{2}}$$

For K groups Where $\pi_i = \frac{p_i}{p_i + p_j}, \pi_j = \frac{p_j}{p_i + p_j}, S_{ij} = \pi_i S_i + \pi_j S_j$, $S_W = \sum_{i=1}^{K} p_i S_i$, as a heteroscedastic extension of Linear Discriminant Analysis, to reduce the dimensions of the color data from 3 to 2, for presentation purposes and for potentially reducing the magnitude of the condition numbers. Transformations in the internal processing of cameras may aggressively sharpen the data, which makes the condition numbers large $(\kappa = \|A\|\|A^{-1}\|)$. The chernoff reduction can reduce the condition numbers if the spherical variance of the primary eigenvectors is small (i.e. oriented in the same direction)[172]. To investigate the orientation of the reference groups, the normalized eigenvector corresponding to the largest eigenvalue for each group is given a common origin and is mapped onto a unit sphere. The sample mean vector, resultant and spherical variance is calculated by

$$\overline{v} = \frac{1}{K}\sum_{i=1}^{K} v_i$$

$$\overline{R} = |\overline{v}|$$

$$\overline{Var} = 1 - \overline{R}.$$

Since the eigenvectors can be either of two directions, it is necessary to find the directions that minimizes the variance; this can be done by exploring all 2^{K-1} permutations of directions. The Chernoff mapping features from the eigenvectors corresponding to the 2 largest eigenvalues can be considered normal vectors (n_1 and n_2) to the feature planes (not required to be perpendicular to each other). The perpendicular vector to the two feature planes is the plane onto which the data are projected after feature reduction. The normal vector to this plane can be calculated by:

$$n_p = \frac{n_1 \times n_2}{|n_1 \times n_2|}$$

The angle between the projection direction and the mean normalized eigenvector direction can describe to what extent the feature reduction is tasked with reducing the condition numbers

$$cos\,\vartheta = \frac{\overline{v} \cdot n_p}{|\overline{v}||n_p|}$$

A suggested procedure for selection of classification algorithm is presented in Figure 21

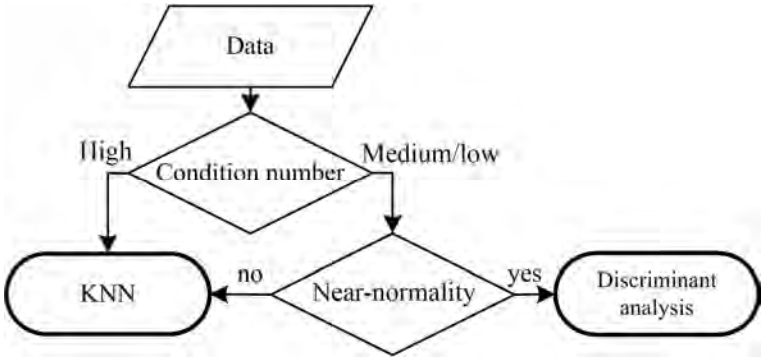

Figure 21 Classification algorithm selection

Multivariable normality can be assessed by comparing the distribution of Mahalanobis distances $D_{ij}^2 = \left(x_{ij} - \overline{x}_j\right)S_j^{-1}\left(x_{ij} - \overline{x}_j\right)^T$ where index *i* refer to observation and *j* to group, to a beta distribution, $D^2\, n/(n-1)^2 \sim Beta(p/2\,,(n-p-1)/2)$ [173, 174]. The linear classifiers are more robust to deviations from normality compared to the quadratic classifiers, whereas the quadratic classifiers take into account the difference in

covariance matrices between groups. However, for non-normal distributions or ill-conditioned covariance matrices, KNN can be used.

3.8 Smartphone app

A smartphone app can be designed taking into account the abovementioned consideration, and can be summed up in the flowchart of Figure 22.

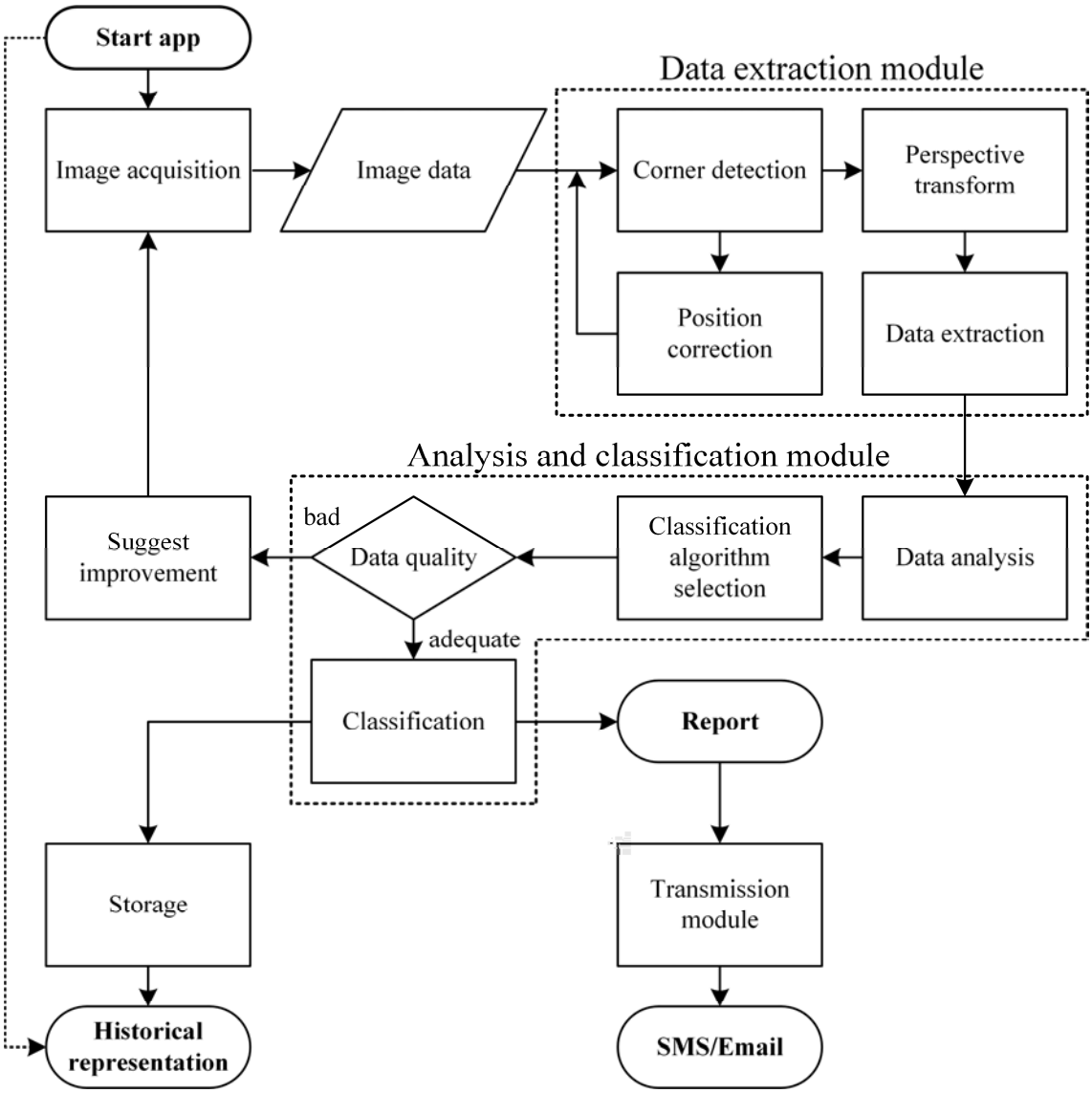

Figure 22 App algorithm flowchart

A selection of actual screenshots of a version of the app is shown in Figure 23

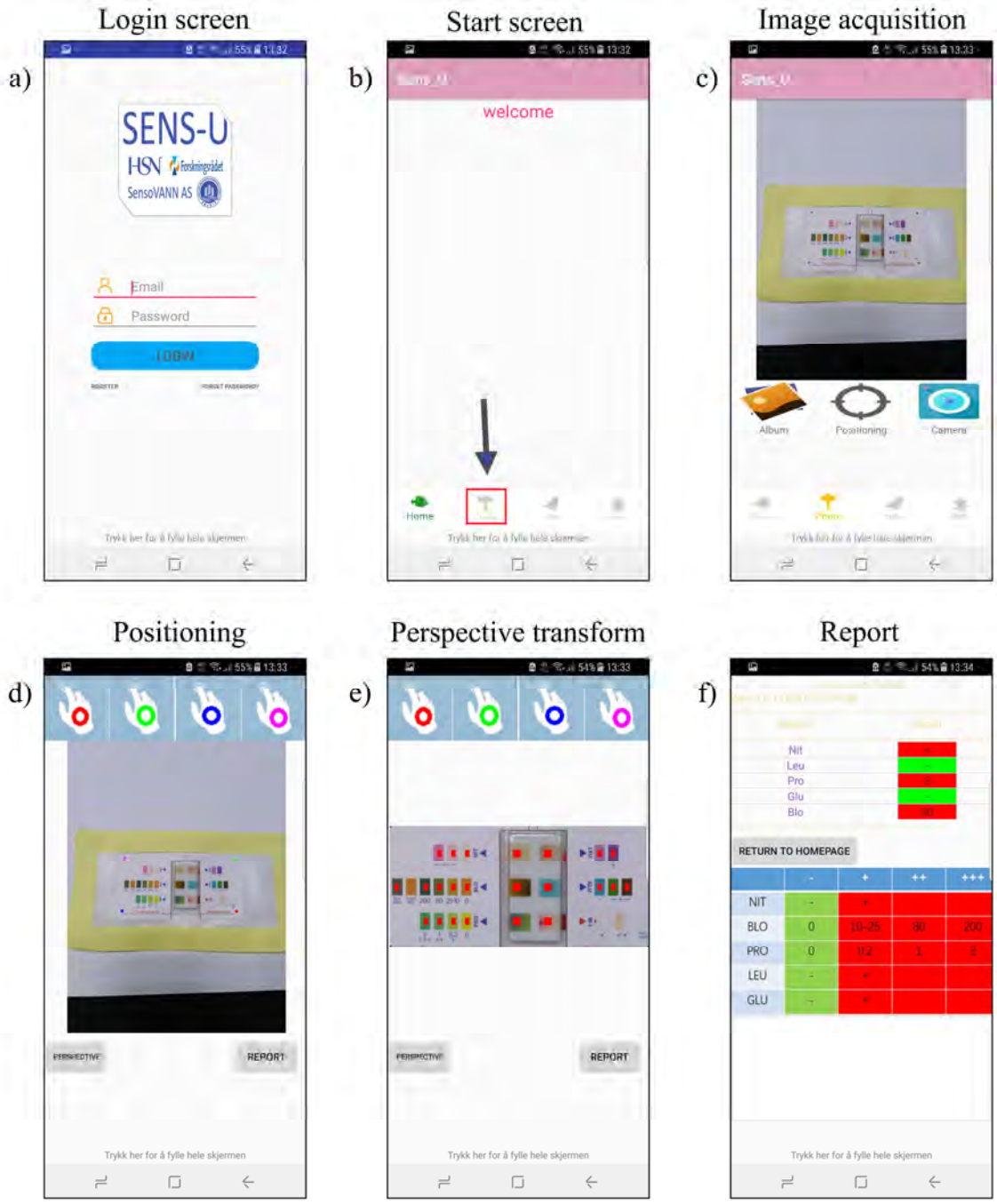

Figure 23 App, a) login screen with username and password, b) Start screen with access to different functions (not all implemented in this picture), c) Image acquisition screen, either for loading a stored image file, or start camera and acquire a new image, d) After image has been acquired, click the positioning for automatic corner detection, with opportunity for correction in cases of recognition errors, e) After positioning, the perspective can be removed and the image can be transformed into a rectangle, f) report of the results

4 Objectives and Tasks

In this thesis, the researcher aims to solve a specific problem mainly for the narrow population group; incontinent, diaper wearing elderly, in particular receivers of home care services, but also in nursing homes, which have a high prevalence for UTI. The main objectives and tasks can be briefly summarized as follows:

- *Objective 1:* Method selection for detection of UTI without invasive methods.
  - *Task 1:* Identify necessary features of a solution to the problem.
  - *Task 2:* Select an approach and establish a set of device design parameters.
- *Objective 2:* Realize a prototype with features that satisfy the requirements posed by the problem. Core requirements being non-invasive sample collection and compatibility with commercial diapers.
  - *Task 1:* Select low-cost materials.
  - *Task 2:* Design and fabricate prototypes. Perform an iterative design process.
    - *Task 2.1:* Develop a method for automatic sample collection from diapers.
    - *Task 2.2:* Develop an isolation mechanism.
  - *Task 3:* Develop point-of-care sensor method for analysis of results. A smartphone-based solution for automatic data extraction and analysis.
- *Objective 3:* Verify the technical solution in terms of individual parts/modules as well as full device performance.
  - *Task 1:* Establish a set of experimental protocols for the design process and optimization. One set that can be used in the iterative design process, and one set that can be used to assess improvement between functional device generations.
  - *Task 2:* Carry out technical tests.
- *Objective 4:* Establish a foundation for further development and potential commercialization.

- *Task 1:* Prepare the necessary background material for developing the technology further and increasing the Technology Readiness Level.
- *Task 2:* Search for potential research or commercialization project funding, potential commercialization partners or investors.

5 Contribution of the thesis

The research tasks have been fulfilled in association with the primary supervisor, who developed an initial foundation of ideas to solve the problems that was reported from discussion with representatives of municipal nurses. The device design, initial prototype fabrication, smartphone app algorithms and smartphone app design was primarily carried out by the candidate under guidance of the primary supervisor. The functional device fabrication was carried out in Jilin Shenhua Medical Equipment Co., Ltd. Experimental validation was performed by the candidate, partially with the laboratory resources of University College of Southeast Norway and Chongqing Technology and Business University. The candidate conducted the work of design, fabrication of core prototype devices, data acquisition and analysis, supervised by the primary supervisor.

The scientific contributions of this doctoral work are as follows:

(1) Development of urine test device capable of automatically sampling, isolating and analysing urine, as well as preserving the results.
(2) Development of an illumination and device independent smartphone algorithm, for colorimetric analysis and classification of biomarker reaction colors.
(3) Foundation for a commercializable product.

6 Summary and elaboration of articles

This chapter presents 6 articles that captures the research contribution of the doctoral thesis. The work involved two primary directions: 1) development of a method suitable for smartphone based measurements of colorimetric reactions reported in Article I, II, III; and 2) Paperbased rapid screening or urinary biomarkers compatible with diapers in IV, V, VI. The research in each article is application oriented, with similar backgrounds, but with a goal to solve different parts of the overall problem. The articles were written to be relatively independent by attempting to make the methods in the articles generally useful in a wider context, than to the specific problem at hand.

6.1 Smartphone based colorimetric analysis

Develop an appropriate smartphone based analysis tool for colorimetric reactions

6.1.1 A Smart Phone-Based Robust Correction Algorithm for the Colorimetric Detection of Urinary Tract Infection

6.1.1.1 Background

In the nursing home and home care sector they typically have limited resources to effectively monitor urinary tract infection in elderly, and in particular the incontinent diaper wearing elderly, because of:

a) Time constraints.
b) Sample collection difficulties.
c) High UTI prevalence among the relevant population.
d) Advanced age obfuscating typical clinical features.

The initial approach to assist the management of urinary tract infection was to develop simple, practical and low-cost tools that could simplify the interpretation of colorimetric test results. The survey presented for municipal nurses [110] revealed that they felt unsure about the interpretation of colorimetric reactions on urine dipsticks. A smartphone application was considered the most accessible platform for making a tool to alleviate the insecurity. Other alternatives would be designing and fabricating a measurement tool or using lab equipment, but these alternatives are neither accessible, practical nor affordable.

6.1.1.2 Objectives

- Identify potential challenges related to color data extraction on smartphones.
- Investigate methods for color correction that is sufficiently robust with respect to variation in illumination to achieve a satisfactory level of correction on images captured with a smartphone, so that differences between two recorded pictures allows a calibration image with colors corresponding to known biomarker

quantities to be compared to a test image with colors resulting from an unknown biomarker quantity.

6.1.1.3 Challenges

The perception of color depends on a several variables, such as: illumination type, color and intensity, device model, image sensor spectral sensitivity, camera settings, internal camera processing.

6.1.1.4 Method

A set of problems quickly emerged for the use of a smartphone as a colorimetric measurement device, and Article I attempt at dealing with the first, namely the illumination, since the perceived object color varies significantly on the illumination conditions. The initial assumption was to create a colorimetric measurement tool, it is necessary to compare a result with a calibration curve, but if the calibration curve is constructed under a different set of illumination conditions than the test is performed under, the calibration curve will not be able to accurately link a test color to a calibrated measurement quantity. To solve this problem, (while ignoring for the moment the additional color constancy challenges related to smartphones), the approach was to find a way to express measured colors independently of the illumination source and transform either the calibration curve or the test data to the other, or both to a separate set of conditions, to facilitate comparison with a calibration curve. In the scientific literature regarding color constancy, there are many methods to deal with the color constancy issue [149-151, 175-177]. Many were impractical, incompatible with smartphone usage or not suited for the purpose, at least within the context of the application.

The simplest method that gave the best result was a comprehensive normalization procedure that takes into account all the information in an image and through an iterated procedure of alternating normalization of pixel values and normalization of color channels tries to remove the effects of illumination [178]. Another method, which is a simple shift and scale procedure based on a black and a white color reference was

included as a comparison because it had been used for a similar purpose and application in the work of Hong and Chang [161].

The methods were tested on multiple photos of an X-rite Colorchecker passport as a color reference, captured under different illumination conditions.

By calculating the the root-mean-squared (RMS) Euclidean distances among the color pairs for each illumination condition. The uncorrected RMS distance error was 32.4% of the full color range. The black/white reference method was able to reduce the error to 56.5% of the uncorrected error (18.4% of full color range), and the Comprehensive normalization was able to reduce the RMS distance to 19.2% of the uncorrected distance (6.1% of full color range). For a scale limited by 8 bit resolution, this is good but not optimal, and was therefore only considered a minor step forward. However, based on the results, the comprehensive normalization appeared to perform better than the Black/white reference method. The Black/white reference method also had a tendency to transform certain colors outside the color range.

The comprehensive normalization method was quite robust and consistent towards the variation in color caused by different illumination conditions, but not as much as was needed for reliability, especially due to the reliance on information in the whole image, and therefore displaying too strong dependence on the background of the image.

As this initial step was mainly an attempt at solving the illumination problem, the other problems were ignored, it was therefore impossible to identify the source of the error. I.e. is the problem the method, or nonlinearities introduced by the other processes?

The problem was likely a combination of both since a search for a method that could solve all problems while only focusing on one, most likely made the choice of method suboptimal. However, it was based on other published material within similar topics, and the same assumptions was made. Thus, the value of this initial work is that it revealed many of the flaws present in other published works especially regarding the assumptions that was made, which helped focus the way forward.

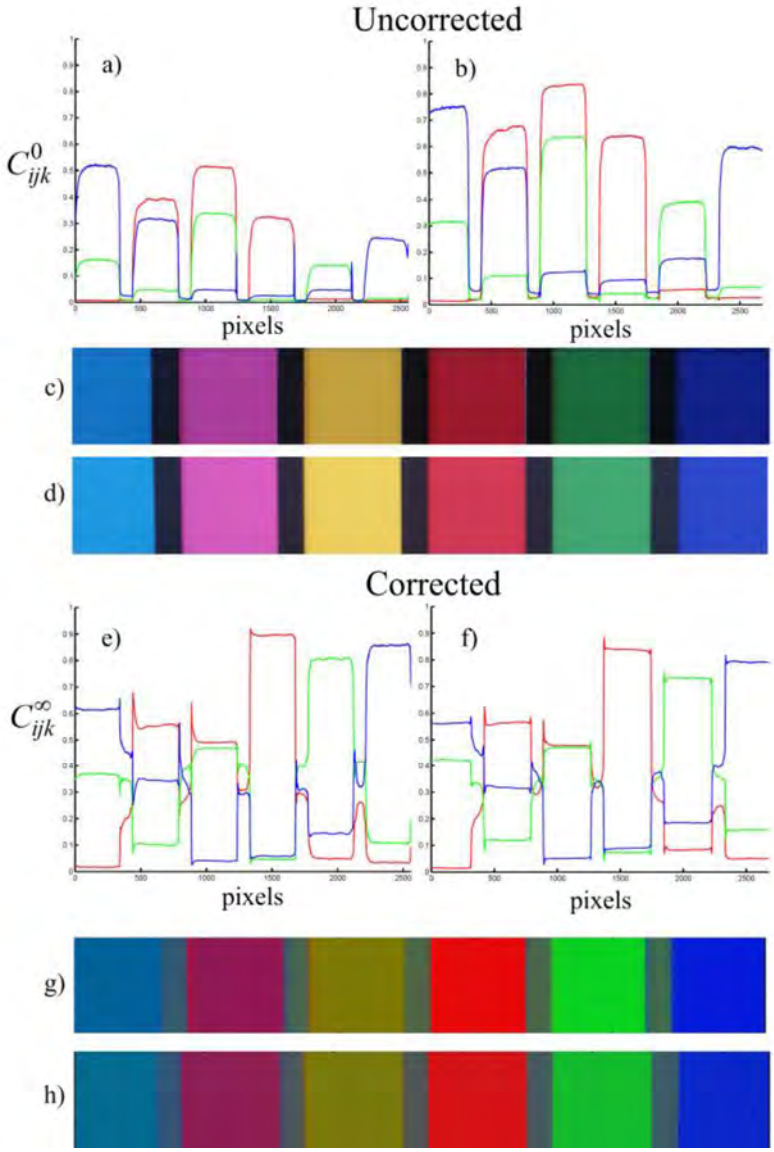

Figure 24 Colors for r,g,b channels (corresponds to the color of the lines along the cyan, magenta, yellow, red, green, blue colors. a)-d) is uncorrected, e)-h) is corrected. a), c), e) and g) corresponds to Figure 3a). b), d), f) and g) corresponds to Figure 3b)

6.1.2 Illumination and Device Independence for Colorimetric Detection of Urinary Biomarkers with Smartphone

6.1.2.1 Background

After the work with article 1, it became clear that it was important to account for the most relevant sources of variation more so than what other researchers had previously done and what was done in article 1. This was done by implementing a heavier focus on data integrity and use of multivariable statistics. Other work tended to have reliance upon color space transformation or other transformations, without clear purpose, and a lack of ability to generalize to other colorimetric reactions [153, 154, 157-166]. The raw data from smartphone cameras typically come in .DNG format as a color filter array where every square pattern of 4 pixels consist of one red, one blue and two green pixels [155]. The internal processing of the smartphone converts the color filter array into three (RGB) color channels with interpolation of missing values, and performs varies processes such as white balancing, sharpening and gamma.

A decision to avoid continuous estimates was made as the additional information that could be gathered by making continuous estimates is unnecessary when taking into account the application, which is for nurses who needs tools that are able to aid in the decision-making process.

6.1.2.2 Objectives

Devise a method that is both illumination and device independent, as well as allows generalization to a wider range of colorimetric reaction, without strong restrictions that limits the choice of colorimetric reactions

6.1.2.3 Challenge

- No external equipment or standardization is permitted
- No device hardware specification is permitted
- No color correction is permitted

6.1.2.4 Method

Universal indicator paper (pH 1-10, Merck) and Urinalysis reagent strips (pH 5-9, Suzshou Hongyi Bio-technology Co., Ltd.), both with accompanying reference colors were used together with buffers (pH, 4,7,10, Radiometer Analytical) to prepare test colors. Test colors were photographed together with the accompanying reference colors. 2601 pixels were extracted from each test and reference color and the test colors were classified by maximizing the log-likelihood of multivariate normal distributions (discriminant scores) [173]

$$d_i = -\frac{1}{2} ln|S_i| - \frac{1}{2}(x - m_i)S_i^{-1}(x - m_i)^T + ln\, p_i$$

where *d* is the discriminant score, S_i is the covariance matrix of reference *i, x* is the matrix of test data, *m* is the reference group means, and *p* is the prior probabilities (here assumed to be equal). Each pixel of the test color was labelled according to the larges discriminant score, and the test color was classified as the reference with the most frequently labelled pixels. Conditions were chosen arbitrarily as:

(1) Noon daylight indoors near window and fluorescent light,
(2) Noon daylight indoor, away from window, near table lamp,
(3) Noon daylight outdoors (partially cloudy),
(4) Fluorescent light no window,
(5) Same as 4, with exposure setting +1,
(6) Same as 4, with autocontrast setting,

With 4 smartphone models: Samsung Galaxy S6 Edge, Samsung Galaxy S3, ZTE V7 mini and Iphone 6. Results are presented in Table 6. The method was able to assign the correct label independently of smartphone model, settings and illumination.

Table 6 Classification on different model smartphones and different illumination conditions

	Device (illumination condition)	Assigned label
1	Samsung Galaxy S6 edge (Illumination 1)	4,7,10
2	Samsung Galaxy S6 edge (Illumination 2)	4,7,10
3	Samsung Galaxy S6 edge (Illumination 3)	4,7,10
4	Samsung Galaxy S3 (Illumination 1)	4,7,10
5	ZTE V7 mini (Illumination 5)	4,7,10
6	Iphone 6 (Illumination 6)	4,7,10
7	Samsung Galaxy S6 edge (Urinalysis strip) (Ill. 1)	5,7,9 *

*strip test ranges from pH 5-9, hence pH 4 and pH 10 was assigned to the nearest available reference group

6.1.3 Smartphone-Based Rapid Screening of Urinary Biomarkers

6.1.3.1 Background

The previous articles (3.1.1 and 3.1.2) established the foundation for this article.

6.1.3.2 Objectives

The approach under the conditions posed by the application was identified in the previous articles. Therefore, the objective was to properly define all assumptions and address challenges of the solution.

6.1.3.3 Challenges

Defining an appropriate set of assumptions and conditions under which the system can operate without being majorly restricted by the assumptions and conditions. An example of assumptions and conditions that are restrictive: Iqbal and Eriksson [179] attempted to provide ambient illumination independence by using controlled illumination from a smartphone screen, and record colors with the frontside camera. However, this makes the screen unavailable and leaves the user unable to align the camera properly and therefore needs an alignment setup, which is not practical.

6.1.3.4 Method

The previously described methods of other researchers appeared to be dependent on selecting colorimetric reactions that their method was suitable for. This work focused on making a method that is appropriate for the relevant urinary biomarkers without being specifically designed for a specific colorimetric reaction, so that they are more generally applicable.

A set of references for 12 colorimetric reactions (micro albumin, nitrite, bilirubin, creatinine, glucose, leukocyte esterase, urobilinogen, protein, ketones, blood, pH and standard gravity) were photographed under one illumination condition with default camera settings to observe whether the reactions satisfy the assumptions as described

in Article III and Chapter 3, related to ordering of groups and whether they are distinguishable for the camera.

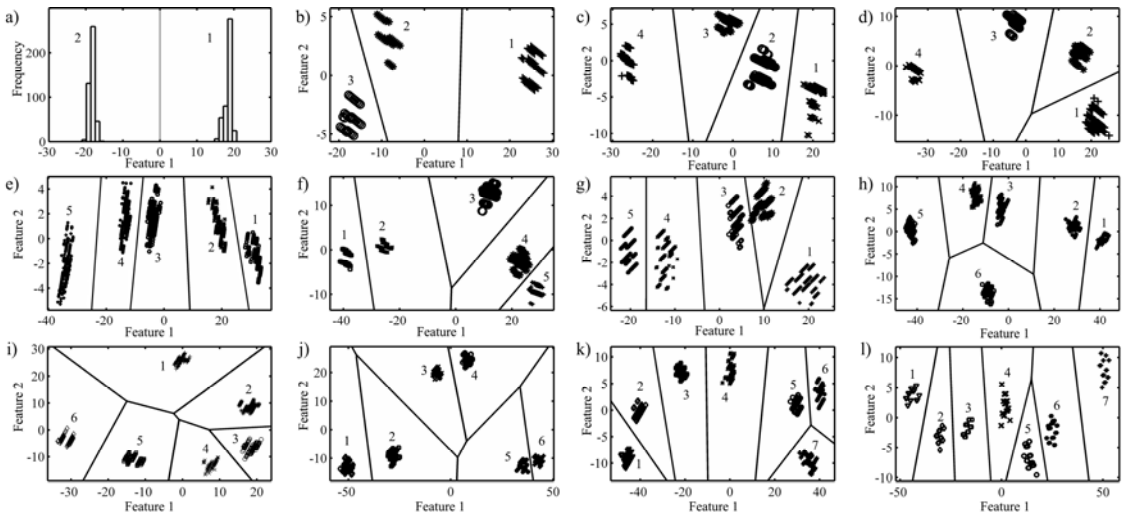

Figure 25 Scatter plots of: a) Micro albumin, b) Nitrite, c) Bilirubin, d) Creatinine, e) Glucose, f) Leukocyte esterase, g) Urobilinogen, h) Proteins, i) Ketones, j) Blood, k) pH, i) Standard Gravity. Feature 1 and 2 are the eigenvectors corresponding to the two largest eigenvalues of the maximized Chernoff criteria [171]. Reference groups are numbered in ascending order according to concentration.

In all explored cases, the reference colors were clearly distinguishable to both the 'naked eye' and the camera, and the groups were ordered according to the Figure 11a) and b), thus satisfying the 2 assumptions.

The classification procedure described in Chapter 3 was first applied to the well-known Fisher's Iris data set [180].

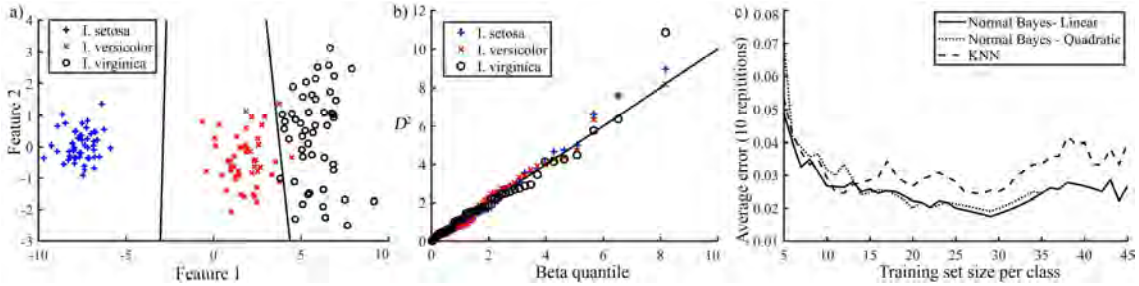

Figure 26 Validation with Fisher's Iris data set (4 variables, 3 groups, 50 samples per group). a) Chernoff-mapping with linear normal Bayes classifiers. b) D2 –Beta quantile-quantile plot. c) Averaged learning curve error for 10 repetitions with Linear/Quadratic Normal Bayes and KNN classifiers

The groups could be discriminated and classified well, and the data was distributed approximately according to the scaled Beta distribution.

Test colors were prepared using buffers (pH, 4,7,10, Radiometer Analytical) with Universal indicator paper (pH 1-10, Merck) and Urinalysis reagent strips (pH 5-9, Suzshou Hongyi Bio-technology Co., Ltd.), together with accompanying reference colors. The three test colors were classified according to five methods, KNN, pooled/quadratic discriminant analysis, and chernoff mapped linear/quadratic Bayes normal classifier.

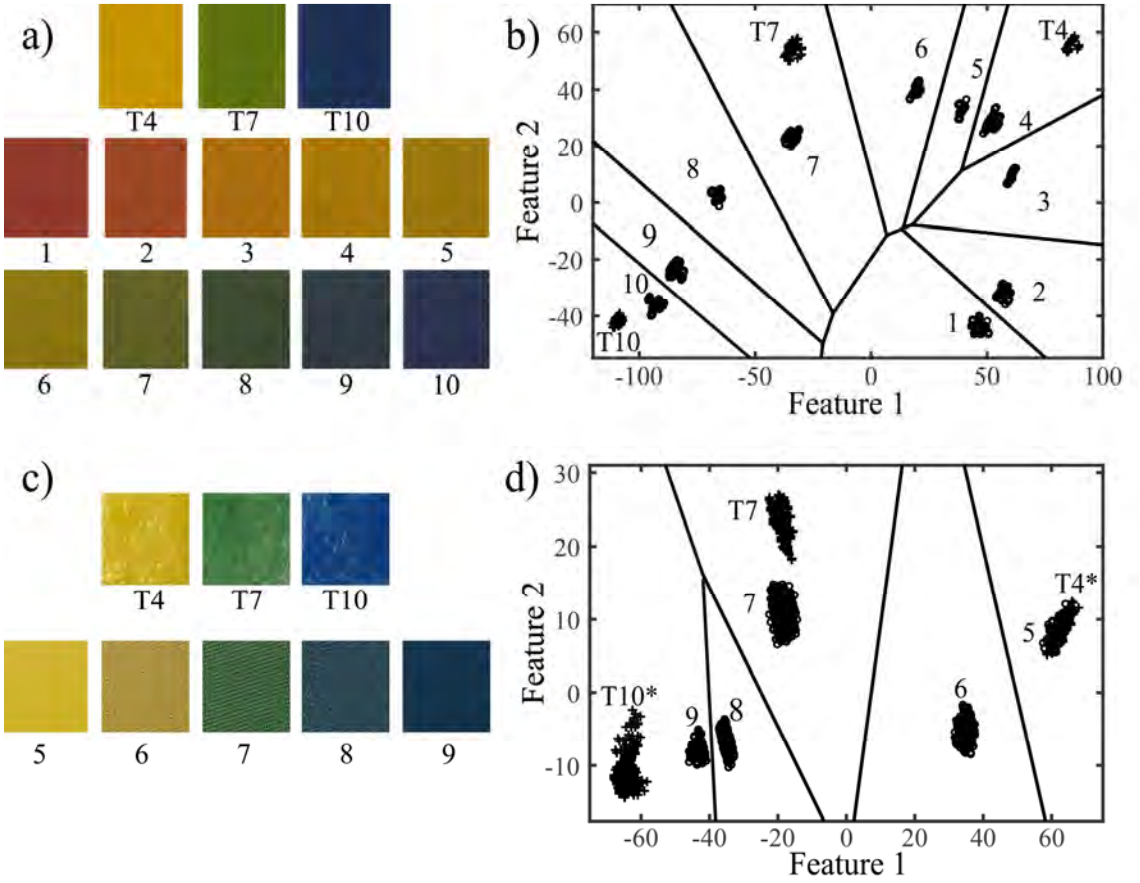

Figure 27 Recorded test/reference colors, a) Merck Universal indicator paper, b) Chernoff mapped data with linear classification boundaries from a). c) Suzhou Hongyi Bio-technology Co. Ltd. Urinalysis Teagent Strips, d) Chernoff mapped data with linear classification boundaries from c)

Table 7 Classification results of pH test data

Cases		Condition number (min-max)	KNN	Pooled Discriminant score	Quadratic Discriminant score	Chernoff map Linear Bayes Normal Classifier	Chernoff map Quadratic Bayes Normal Classifier
S6 Edge	AutoISO[a)]	15.5-∞	100	100	0,100,100	-	-
	ISO200[b)]	*20.4-1082*	*100*	*100*	*100*	*100*	*100*
	DNG[b)]	*1.6-4.7*	*97,92,80*	*99,94,94*	*95,94,95*	*99,95,94*	*96,94,95*
	ISO100[a)]	19.4-∞	100	100	0,100,100	-	-
	ISO200	28.0-127.7	100	100	0,100,100	100	0,100,100
	ISO400	21.6-312.4	100	100	0,100,100	100	0,100,100
	ISO800	32.1-308.6	88,99,100	100	0,100,100	100	0,100,100
	Strips[c)]	102.5-1002	100,100,87	100	100	100	100
S7 Edge	AutoISO	17.6-149.9	100	100	100	100	100
S3	n=2601	16.4-61.3	100	100	0,100,100	100	0,100,100
	n=100[d)]	19.0-99.1	100	99,100,100	0,100,100	99,100,100	0,100,100
ZTE	AutoISO	9.3-88.4	0,99,100	100,98,100	100,57,100	100,98,100	100,57,100
Iphone 6	AutoISO	12.5-47.3	1,100,100	87,100,100	100	87,100,100	100

Entries in percentage of correctly classified pixels for colors prepared with pH 4,7 and 10 respectively (replaced with one number if all equal).

[a)] Generalized matrix inverse used for singular covariance matrices

[b)] Same image stored in different formats

[c)] Colorimetric strip reference ranges from 5-9, hence the class of pH 5 and pH 9 where defined as pH ≤ 5 and pH ≥ 9

[d)] Randomly sampled subset of extracted pixels

As an example of orientation based on Chapter 3.7 in Table 7: The primary eigenvectors from the JPEG image (ISO 200) had a spherical variance of 0.0002, and an angle ϑ=1.4° between mean orientation and projection, whereas the same image stored as DNG, had a spherical variance of 0.2035 and an angle ϑ=72.6°. Before Chernoff mapping, the JPEG image had a condition number range from 20-1082, after Chernoff mapping, the condition number range was reduced to 1.3-40. In the case of a group with infinite condition number (a singular covariance matrix) the Chernoff mapping fails.

The classification success rate is obviously dependent on the similarity between reference colors and reaction colors. For the tested commercial colorimetric reactions, the reaction colors often appeared different from the corresponding reference color (see Figure 27ab), even with accurate buffer solutions. This was not a problem due to the linear classification regions covering a range of similar colors, but it made the quadratic classification rules fail more often. Since commercially available colorimetric reactions and references must be used as they come (assuming no prior knowledge regarding reference/test color dissimilarity), a tolerance for lower degrees of similarity is necessary for successful classification. With less strict requirements allowing prior knowledge, a

possible initialization step could include a multivariable regression procedure on a particular product to counter a known dissimilarity. The main reasoning behind the choice not to pursue continuous quantitative estimates was to retain compatibility with colorimetric tests, where control over reference color similarity is not feasible. For custom-made printed reference colors, this is less of a problem as similarity can be tuned in the printing process using process optimization with gradient descent to ensure that the similarity is acceptable [181].

6.2 Biomarkers and device design fabrication and verification

6.2.1 Biomarkers of urinary tract infections: state of the art, and promising applications for rapid strip-based chemical sensors

6.2.1.1 Background

Colorimetric tests of biomarkers in urinalysis has been in use for a long time. Examples of common markers are Glucose, Ketones, Proteins, pH, Standard gravity, Blood Nitrite, Leukocyte esterase. Despite having been in use for a long time, the only markers typically in use for UTI are Nitrite and Leukocyte esterase, which both have some merits and drawbacks. The dipstick tests are rapid and simple to use, although false negative nitrite results are known to occur for abnormal urobilinogen levels, pH < 6 and Gram-positive infections, while proteins may interfere with leukocyte esterase results [106]. Studies have reported large variations in the diagnostic sensitivity especially on the nitrite test, reported from as low as 10% up to 93%. However, the meta-analysis by Devillé et al. [103] reached a conclusion that the high post-test probability of negative nitrite and leukocyte esterase dipstick tests appears to be useful for ruling out infections, which matches well with the purpose of rapid screening as presented by Pezzlo: Improve efficiency and cost-effectiveness by (1) rapid provision of accurate information and (2) ruling out negative samples [106].

6.2.1.2 Objectives

Review the literature for reported biomarkers that have a potential for complementing the NIT and LEU markers, with respect to UTI.

6.2.1.3 Challenge

The challenge is to find potential biomarkers that are both capable of identifying bacterial infections in the urinary tract, while also being appropriate for detection using a strip test.

6.2.1.4 Results

By expanding the set of measured variables, it may be possible to improve the accuracy of test strips and the ability to rule in/out infections, which can help to reduce delays in treatment, inaccurate or rushed empirical treatment and avoid misuse of antibiotics. Inclusion of new markers with performance enhancing properties may be an advantageous solution. Performance enhancing properties can include higher infection sensitivity, reliability towards contamination and interfering substances, stability under protocol or diet variation, etc.

The search for UTI biomarkers focused on markers in urine for detection of bacteria, available colorimetric reactions in databases (PubMed, Science Direct, BRENDA) for combinations of “urinary tract infections”, “markers”, and “biomarkers”. Further searches were conducted for relevant results connected to background of markers, relevant species of bacteria, pathways of formation and ‘naked eye’ detectable colorimetric methods. The search revealed four markers of interest; The metabolomics-related markers trimethylamine (TMA) and acetic acid/acetate ($AcOH/AcO^-$), and the enzymatic markers Xanthine oxidase (XO), and Myeloperoxidase (MPO), with possible methods for incorporation on a test strip.

Investigation based on the search criteria found a range of potential biomarkers, but the selected markers were included based on their apparent usefulness and compatibility with strip detection.

Trimethylamine (TMA, $N(CH_3)_3$):

Bacterial formation of TMA is associated with several marine genera of bacteria, such as *Alteromonas*, *Photobacterium* and *Vibrio*, as well as some genera of *Enterobacteriaceae* [182]. Trimethylamine forming species of *Enterobacteriaceae* includes *E. coli*, *Salmonella enterica*, *Proteus vulgaris* and *Serratia marcescens*, of which *E. coli*, *P. vulgaris* and *S. enterica* are known to use Trimethylamine-N-oxide (TMAO) as a terminal electron acceptor during anaerobic respiration with the bacterial enzyme TMAO reductase (EC

1.7.2.3) reducing TMAO to TMA, while *S. marcescens* produce TMA while oxidizing DL-carnitine under aerobic conditions [183-187]. A Rieske-type oxygenase/reductase capable of transforming L-carnitine to TMA has been observed in human microbiota, such as certain strains of *Klebsiella pneumoniae*, *Acinetobacter baumannii*, and *Citrobacter freundii* (and *E. coli*) [188]. Of the TMA-producing bacteria, *E. coli* is the most frequently occurring and relevant for in UTI. This infers a potential for TMA as a selective *E. coli* biomarker. However, vaginal fluid is a potential TMA contamination source [189].

Detection of TMA has seen some interest in food industry due to the applicability as an objective measuresement of freshness in some types of fish. McCarrick et al. [190] developed a colorimetric chemical sensor based on calix[4]arene with nitrophenylazophenol chromogenic moieties, immobilized on filter paper that changes color from yellow to red when exposed to TMA concentrations between 0.02 ppm and 30 ppm.

Acetic acid/Acetate ($AcOH/AcO^-$):

Acetate production have been observed in many pathogens commonly and uncommonly associated with UTI. Acetate is a common product from heterofermentative fermentation, such as in the mixed-acid fermentation carried out by *Enterobacteriaceae.* Apart from the more general glucose metabolism pathways of acetate, there are various other pathways depending on pathogen and available substrates. The most common pathway is as a product of metabolism of glucose/citrate as a carbon source through the pyruvate formate-lyase pathway and the phosphotransacetylase-acetate kinase (Pta-ackA), see Table 2 in [191]. On one hand, a wide range of bacteria appear to produce acetate, including gram-positive bacteria (hence broader than NIT). On the other hand, unless fresh samples are used, it can also be contaminated by a wider range of sources.

There are many chemical sensors for acetate (see Table 6 in [191]). The primary important parameters of the chemical sensors are the solvent, range, detection limit and interfering chemicals. Secondary parameters are cost, health/environment hazard, and how simple it is to obtain. The most promising chemical sensor was found to be

Bromopyrogallol red as reported by Tavallali et al. [192]. It operates in a 50/50 DMSO/ H_2O solvent, with a linear range from 19-42 µM, a 2.5 µM detection limit, without any reported interfering chemicals.

Xanthine oxidase XO:

Xanthine Oxidase (XO) is an enzyme involved in purine catabolism, and production of reactive oxygen species and reactive nitrogen species, which can be utilized by white blood cells as a tool to fight infecting pathogens [193-195]. XO is elevated during certain conditions,and has been observed in urine during UTI, with the highest activity for *E. coli* and *P. aeruginosa* [196, 197]. The research had not concluded the source of XO in infected urine, but e.g. Xi et al. [198] proposed a purine salvage path in *E.* coli involving Xanthine dehydrogenase (convertible to XO), and similar behaviour have been shown in other bacteria [191].

XO can catabolize purines (e.g. hypoxanthine, xanthine) to uric acid while producing reactive oxygen species, and the catabolism to uric acid in the presence of H_2O and O_2 produces hydrogen peroxide, which can be used together with Horse radish peroxidase and an appropriate chromogen to produce a colored dye.

Myeloperoxidase MPO:

MPO is a glycosylated peroxidase enzyme stored in large amounts in azurophilic granules of polymorphonuclear leukocytes (5% of cell content) and in monocytes (1% of cell content) [199]. Neutrophil granulocytes are the most abundant type of white blood cell with the primary function of phagocytosis and microbial killing [200]. In the presence of hydrogen peroxide, MPO can catalyse the formation of hypochlorous acid (HOCl) from a chloride substrate, which is strongly microbicidal [201]. The activity of urinary MPO in response to UTI might be controlled by characteristics of the invading microorganisms that allow modulation of the immune response. Billips et al. [202] infected mice with uropathogenic *E. coli* strains NU14 and MG1655, and observed significantly increased levels of MPO of the MG1655 strain in both bladder tissue and urine compared to control

mice. NU14 strain on the other hand produced a far lower increase of MPO. The NU14 strain and other clinical *E. coli* strains modulate the immune response by suppressing cytokine secretion from urothelium and hindering the MPO expression [202]. Furthermore, there can be MPO activity inhibition through spontaneously forming urine constituents without direct involvement of bacteria, such as cyanate (CNO^-) formed by urea which is able to inhibit MPO in intact neutrophils [203]. A possible example of the immune response modulation is given by Fraser et al. [204] who measured MPO in men with urethritis due to *N. gonorrhoeae* and *C. trachomatis*, without observing any significant difference between MPO levels of infected men and controls. Steinhoff et al. [205] 140 suggested freezing at -20 ^oC as a possible cause to why the infection did not elevate MPO. However, the reported evasive abilities of the infecting pathogens to modulate the immune response can also be a reason. There are reports of virulence factors that grant *N. gonorrhoeae* resistance towards the immune system by modulating PMNs' ability to perform phagocytosis, as well as modulating the release of antimicrobial components [206]. *C. trachomatis* has an observed resistance towards PMNs through selective inhibition of the respiratory burst by inhibiting the superoxide generation of the NADPH oxidase [207]. MPO might have a role in UTI diagnosis (in combination with other markers) as a distinguishing marker of infection related to immune modulating microorganisms.

Bromide and Thiocyanate substrates are favoured over chloride, but are in low conentrations in urine and therefore chloride is considered the preferred MPO substrate in urine. Thus, the detection of MPO can be done using available chemical sensors for hypochlorite dissociated from hypochloric acid, (see Table 8 in [191]).

6.2.1.5 Future work:

In the thesis work, the candidate started working with developing a paper-based colorimetric test for acetate in urine as a broad spectrum marker for UTI based on the indicator Bromopyrogallol red. The work had to be postponed due to a lack of time and reorganized priorities. However, the initial review and experiments revealed that the work is promising and the candidate will continue the research in the near future.

BPR is a pyrogallolsulfogallein derivative that appears to be appropriate for use in human urine independently of pH. The normal human pH has a range of 5.5-7.0 with a median of 6.2 [208]. Dissociation stages of BPR in Table 8 show that the wavelength maxima are constant between pKa_{a2} and pKa_{a4}, hence abnormal urinary pH should not affect the color of the indicator. Furthermore, Tavallali et al. demonstrated that BzO^-, F^-, Cl^-, Br^-, I^-, NO_3^-, HSO_4^-, OH^-, CN^- and CO_3^{2-} did not produce visible color change in 50:50 BPR:DMSO, but did produce a color change in a 1:1 ratio for acetate.

Table 8 Acid dissociation constants and wavelength maxima for BPR

pKa_{a1}	H_3A^- (λ)	pKa_{a2}	H_2A^{2-}(λ)	pKa_{a3}	HA^{3-}(λ)	pKa_{a4}	A^{4-}(λ)
	433,530	4.4	556	9.0	556	11.3	598
0.16		4.39		9.13		11.29	

The indicator needs to be designed to change color in the relevant range of acetate concentrations produced by bacteria in human urine as reported in the literature. An equation was derived to calculate the necessary indicator concentration for a mixture of acetic acid (weak acid), BPR indicator (4-protic acid), and a strong base (e.g. NaOH), the concentrations can be derived based on charge and mass balance:

AcOH: [*HA*], index *A*. BPR: [H^4I], index *I*. Base: [*BOH*], index *B*. Volume *V*, initial concentration C, diluted concentration $\overline{C}$ and dissociation constant *K.*

Weak acid:

$$[HA] \overset{K_A}{\rightarrow} [A^-] + [H^+]$$

$$x = [H^+]$$

$$K_A = \frac{[A^-]x}{[HA]}$$

$$\overline{C_A} = \frac{C_A V_A}{V_A + V_I + V_B} = [A^-] + [AH]$$

$$[A^-] = \overline{C_A}\left[\frac{K_A}{K_A + x}\right]$$

4-protic Indicator:

$$\left[H_{p-i}I^{i-}\right] \xrightarrow{K_{I(i+1)}} \left[H_{p-(i+1)}I^{(i+1)-}\right] + x, for\ p = 4\ and\ i \in [0,3]$$

$$\overline{C_I} = \frac{C_I V_I}{V_A + V_I + V_B} = [H_4I] + [H_3I^-] + [H_2I^{2-}] + [HI^{3-}] + [I^{4-}]$$

$$K_{I1j} = \prod_{n=1}^{j} K_{In}$$

$$[H_4I] = \frac{[H_3I^-]x}{K_{I1}} = \frac{[H_2I^{2-}]x^2}{K_{I12}} = \frac{[HI^{3-}]x^3}{K_{I13}} = \frac{[I^{4-}]x^4}{K_{I14}}$$

$$= \overline{C_I}\left[\frac{x^4}{x^4 + K_{I1}x^3 + K_{I12}x^2 + K_{I13}x + K_{I14}}\right]$$

Base:

$$[BOH] \xrightarrow{K_B} [B^+] + [OH^-], [H_2O] \xrightarrow{K_w} x + [OH^-]$$

$$K_B = \frac{[B^+]K_w}{x[BOH]}$$

$$\overline{C_B} = \frac{C_B V_B}{V_A + V_I + V_B} = [BOH] + [B^+]$$

$$[B^+] = \overline{C_B}\left[\frac{K_B x}{K_B x + K_w}\right]$$

Charge balance:

$$[A^-] + [H_3I^-] + 2[H_2I^{2-}] + 3[HI^{3-}] + 4[I^{4-}] + [OH^-] = [H^+] + [B^+]$$

$$\overline{C_A}\left[\frac{K_A}{K_A + x}\right] + \overline{C_I}\left[\frac{K_{I1}x^3 + 2K_{I12}x^2 + 3K_{I13}x + 4K_{I14}}{x^4 + K_{I1}x^3 + K_{I12}x^2 + K_{I13}x + K_{I14}}\right] + \frac{K_w}{x} = x + \overline{C_B}\left[\frac{K_B x}{K_B x + K_w}\right]$$

$$\overline{C_A}\alpha_A(x) + \overline{C_I}\alpha_I(x) - \overline{C_B}\alpha_B(x) - \left(x - \frac{K_w}{x}\right) = 0$$

This equation can be solved implicitly for x. However, it is more useful to explicitly calculate the required volume of added acid/indicator/base as a function of a pH-range.

An example: For a known volume and concentration of weak acid and indicator, and a known concentration for strong base, what is the concentration of acetate?

$$V_B(x) = \frac{V_A\left(C_A\alpha_A(x) - \left(x - \frac{K_w}{x}\right)\right) + V_I\left(C_I\alpha_I(x) - \left(x - \frac{K_w}{x}\right)\right)}{\left(C_B\alpha_B(x) + \left(x - \frac{K_w}{x}\right)\right)}$$

$$V_B(x) \geq 0$$

This allows simple calculation of any anion concentration, by inserting in the mass balance equations, such as for acetate

$$[A^-] = \frac{C_A V_A \alpha_A(x)}{V_A + V_I + V_B(x)}.$$

In this way, the reaction can be tuned to change color in the desired concentration range.

Figur 28 Preliminary BPR and acetic acid experiments. Left glass: BPR, right glass: BPR+Acetate

6.2.2 A compact device for urine collection and transport in porous media

6.2.2.1 Background

For development of a paper-based device it required some degree of predictive modelling to ensure that the time dependence can be accounted for in the design. This work investigates the use of capillary flow in filter paper in compact point of care microfluidic devices as a method of transporting body fluid samples to a set of chemical sensor pads.

6.2.2.2 Objective

- Model the flow in porous media.
- Investigating the inherent resistance to transport of contaminating liquid.

6.2.2.3 Challenges

- Utilizing capillary flow in porous media in a packaged device, with a controlled/predictable flow speed and time to reach a desired position.
- Particular challenges were the effects of gravity, unintended additional capillaries, contamination and evaporation, and the purpose of the work is to investigate solutions to achieve a robust device.

6.2.2.4 Results

On the condition that the liquid sample has sufficient time to saturate the filter paper, the transport of miscible liquid contaminants are mainly left to the mechanisms of diffusion, which was found to provide an inherent resistance to contamination. However, unintended capillaries between the filter paper and a surface provided an increase in the transport rate for both sample and contamination. This was avoided by sealing possible gaps on the sides of the filter paper with adhesive tape, and by applying a force perpendicular to the paper surface to force the paper to be flat and thereby prevent formation of air pockets between the filter paper surface and contacting surfaces

180 µm thick Whatman grade 1 filter paper cut into 2 cm x 10 cm strips were used as porous medium, and slides of 4mm thick PMMA was used to form channel walls around

the filter paper. Five experimental cases were set up. (1) Two PMMA slides were glued onto a PMMA plate 2cm apart so that a paper strip could be placed between and be covered by a PMMA slide as a cover. This PMMA cover slide was cut approximately 2 filter paper thicknesses narrower than the filter paper width so as to create a narrow channel on each side of the PMMA cover slide. (2) Filter paper placed between two PMMA slides with open sides. (3) Filter paper strips placed between two PMMA slides, where sides were sealed with tape (adhesive that does not dissolve in water) under controlled compression. (4) Filter paper strips were laminated with one end left open. (5) Uncovered filter paper. For (1)-(4) see Figure 29.

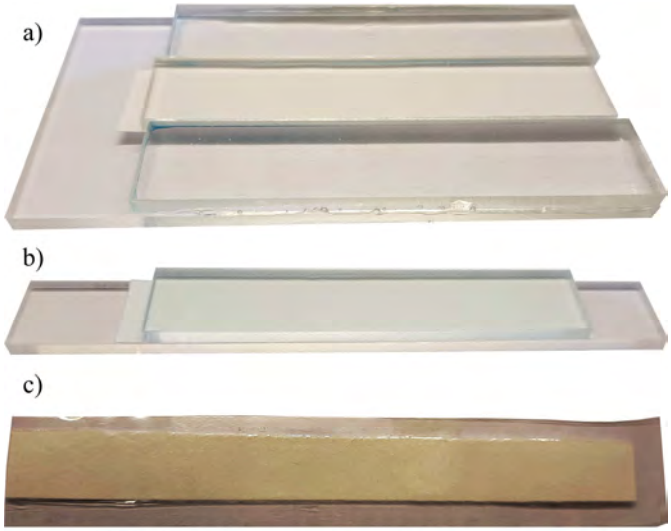

Figure 29 simple wicking experimental setup, inlet on the left side. a) PMMA slides as a cover and walls for the capillary flow with capillaries on the sides, b) similar to a) but without side capillaries, c) laminated filter paper

The capillary flow situation is considered to be similar to capillary rise between two plates as in Figure 30.

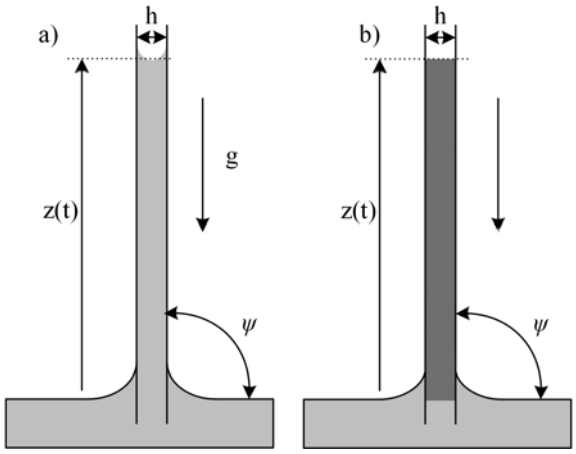

Figure 30 Capillary rise between two plates of width w (into the paper plane) separated by a distance h. a) air between plates, b) porous media sandwiched by plates.

By assuming that the width of the plates is much greater than the separation between the plates, the curvature along the width of the plates can be ignored, and the Laplace pressure can be expressed as

$$\Delta p = \frac{2\sigma \cos\theta}{h}$$

Where σ is surface tension, θ is the contact angle and h is separation between slides [209]. Alternatively if there is capillary rise between two different materials, the capillary rise is expected to occur as long as the meniscus does not exhibit an inflection point [210]. The pressure difference can be described as:

$$\Delta p = \frac{\sigma(\cos\theta_0 + \cos\theta_1)}{h}$$

The force balance takes into account the Inertia (LHS), and surface tension (F_σ), viscous forces (F_μ) and weight (F_g):

$$\frac{d(m\dot{z})}{dt} = F_\sigma - F_\mu - F_g$$

where $F_\mu = 12\mu z\dot{z}A/h^2$, from average velocity Poiseuille-flow in a rectangular channel with *w>>h*, $F_g = \rho g \sin\psi \; zA$, and $F_\sigma = 2\sigma\cos\theta\, A/h$. Equations can be derived for different cases.

(1) Neglect inertia (Washburn equation and modified Washburn equation):

$$F_\sigma = F_\mu + F_g$$

Results in differential equation [209, 211, 212]

$$\dot{z} = \frac{a}{z} - b, \text{where} = \frac{\sigma h cos\theta}{6\mu}, b = \frac{\rho g h^2}{12\mu}\sin\psi$$

For boundary condition z(0)=0, solutions are

$$z(t) = \begin{cases} \sqrt{2at} & for\ b = 0 \\ \frac{a}{b}\left[1 + W\left(-e^{-1-\frac{b^2}{a}t}\right)\right] & for\ b > 0 \end{cases}$$

where W is the upper branch Lambert W function for flow against gravity and lower branch for flow along gravity. The time-derivative for both of these solutions diverge at t=0, but the time-derivative for the gravity dependent solution

$$\dot{z} = -b\frac{W\left(-e^{-1-\frac{b^2}{a}t}\right)}{1 + W\left(-e^{-1-\frac{b^2}{a}t}\right)}$$

Converges to zero for the upper branch W-function $(\lim_{t\to\infty}(z) = a/b)$, while the lower branch derivative converges to a constant rate $(\lim_{t\to\infty}(\dot{z}) = -b)$ [213].

(2) Neglect viscosity and gravity:

A convergent solution for t=0 and z(0)=0 can be found by assuming that viscosity and weight is negligible initially compared to capillary force and inertial forces, which gives a second order nonlinear ordinary differential equation

$$\frac{d(\dot{z}z)}{dt} - c^2 = 0, \text{where } c^2 = \frac{2\sigma\, cos\,\theta}{\rho h}$$

With the solution:

$$z(t) = ct$$

(3) Neglect gravity:

Gives the differential equation:

$$\frac{d(z\dot{z})}{dt} + A(z\dot{z}) - B = 0$$

where $= \frac{12\mu}{\rho h^2}$, $B = \frac{2\sigma \cos\theta}{\rho h}$

With the solution [214]:

$$z(t) = \sqrt{\frac{2B}{A^2}[At - (1 - e^{-At})]}$$

(4) Darcy's law for variable cross-section, neglecting gravity [215]

The flow distance as a function of time can be implicitly expressed through darcy's law with instantly uniform flowrate $Q = v(x)A(x)$ and an initial flow resistance R_0:

$$\frac{kR_0}{\mu}\int_0^z A(z')dz' + \int_0^z \left[A(z)\int_0^{z'} \frac{1}{A(x)}dx\right]dz' = Dt$$

Which for a linearly increasing cross-section gives the 1D implicit solution

$$\frac{(1+az)^2}{2}\left[ln(1+az) - \frac{1}{2}\right] + \frac{1}{4} = a^2Dt$$

This can easily be converted to an explicit function for z in terms of the Lambert W function:

$$z(t) = \frac{1}{a}\left[e^{\frac{1}{2}\left(W\left(e^{-1}(a^2Dt-1)\right)+1\right)} - 1\right] = \frac{1}{a}\left[\sqrt{\frac{a^2Dt-1}{W\left(e^{-1}(a^2Dt-1)\right)}} - 1\right]$$

By substituting $a = 1/r_0$, and $z = r - r_0$, the equation is converted into radial form for outward flow in a sector segment, or inward radial flow with lower branch lambert function

$$\frac{r(t)}{r_0} = \sqrt{\frac{r_0^{-2}Dt - 1}{W\left(e^{-1}(r_0^{-2}Dt - 1)\right)}}$$

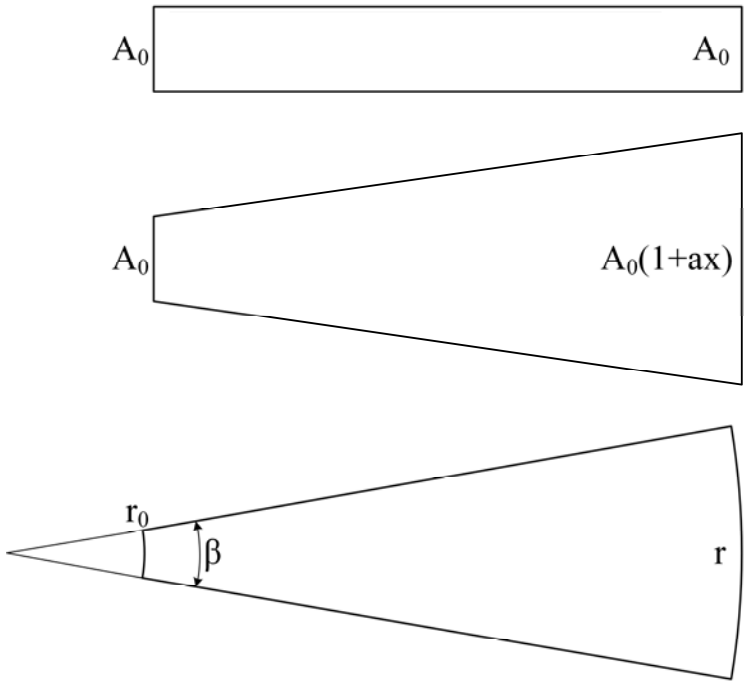

Figure 31 Relevant material geometry

The three plane flow sections are the most relevant shapes that may be encountered or required to describe capillary flow in the device. Transport with or without gravity in strips of constant crossection, or varying crossection.

6.2.2.5 Results

The experimental test devices shown in Figure 29 were intended to imitate the conditions that may be encountered for the real device as a concept shown in Figure 32. Wicking experiments were carried out by recording video of the capillary flow and determining distance and time data from the video file. Nonlinear regression based on the Washburne equation and modified Washburne equation was used on the data.

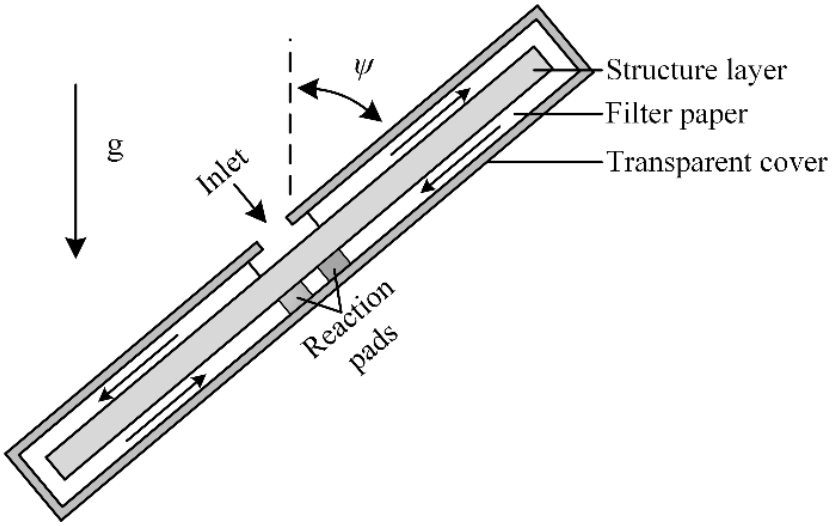

Figure 32 Device concept (layer dimensions not to scale)

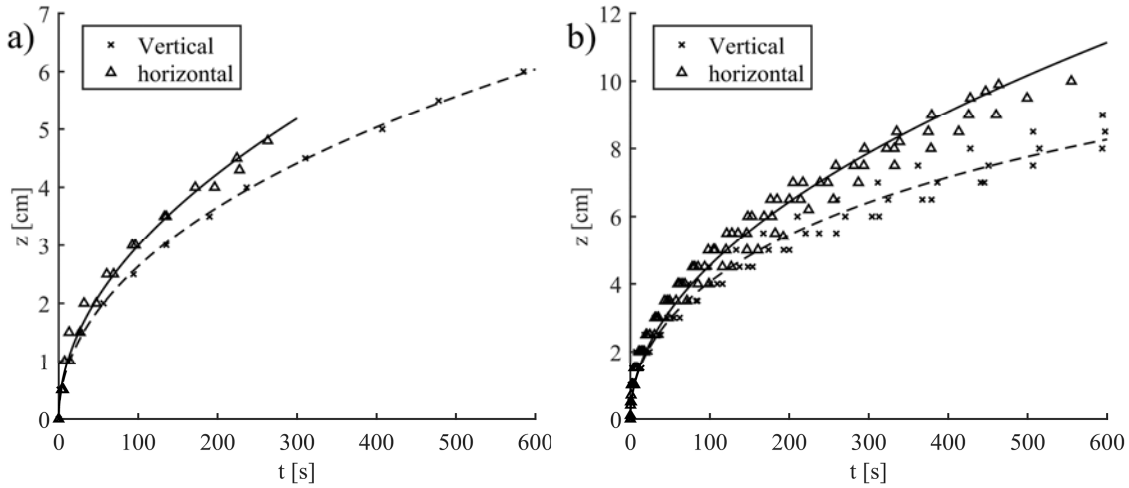

Figure 33 horizontal and vertical measurements with Washburne and modified Washburn equation nonlinear fit: a) Wicking of uncovered filter paper strips b) Wicking of paper strips compressed between PMMA slides

Table 9 Nonlinear regression parameters

	Orientation	a (95% CI)	b (95% CI)
Uncovered	Horizontal	0.0448 (0.0425-0.0472)	
	Vertical	0.0379 (0.0338-0.0422)	0.001836 (0.0006-0.0031)
Covered	Horizontal	0.1034 (0.1002-0.1066)	
	Vertical	0.1046 (0.0912-0.1180)	0.00797 (0.0053-0.0106)

Z tests of the *a*-parameter could not reject the null hypothesis of the covered case that they are equal at 5% significance (p=0.569), indicating that the nonlinear regression have fit the same parameter in both the standard Washburn and modified washburn equation. The uncovered case rejected the null hypothesis at 5% significance (p=0.001), hence the uncovered vertical and horizontal case are not operating with the same parameters. The two estimates for horizontal flow (a_1t_1=a_2t_2) show that the uncovered case needed approximately 2.3 times the time of the covered case to reach a given distance. Evaporation was prevented in the covered case, and there is a difference in distance between horizontal and vertical for a given time, the difference in the *a* parameter between the two nonlinear fittings may be caused by the area available for evaporation in the horizontal case being larger.

Capillary flow in folded laminated paper was used to imitate the conditions in Fig. 2 in the extreme case where ψ=90°. Upon inspection, the Washburne equation is greater than or equal to the modified Washburne equation (except for very small values of *b* where it is no longer a valid solution), therefore capillary flow time is expected to be the slowest in the extreme case, which gives the largest possible *b* parameter. As predicted, the water flowed at different velocities towards the fold, but reached the final length (twice the distance from inlet to fold) in the same time.

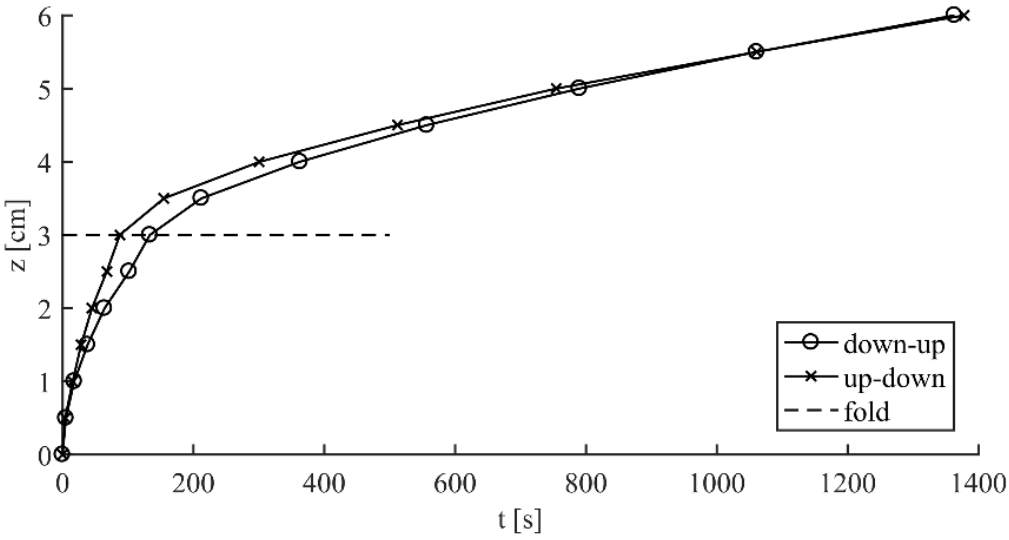

Figure 34 Wicking of laminated filter paper strips of total length 6 cm

Scenario (1)-(3) were tested, see Figure 35, as expected the unintentional capillaries caused a large increase in capillary flow velocity, demonstrating the importance of avoiding unintended capillaries to retain control of the capillary flow. These capillary flow scenarios were also tested for contamination resistance by dispensing a secondary liquid after the filter paper was saturated. The results showed that the time taken by the contamination to reach 8 cm was on the order of minutes for the unintentional capillaries case (1), while it was on the order of hours for the variable height and fixed height cases (2)-(3).

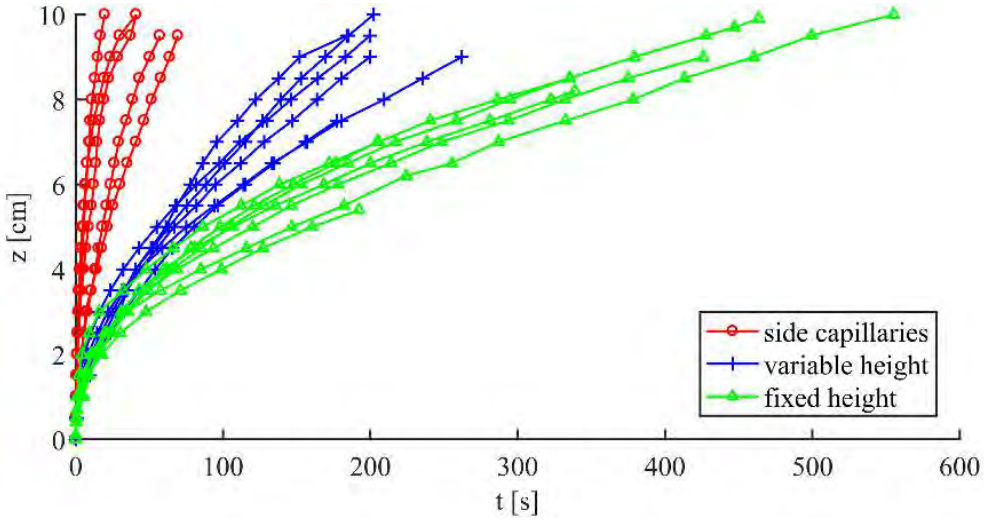

Figure 35 Horizontal capillary flow

6.2.2.6 Future work:

Accurate measurement of capillary flow distance while the capillary flow develops was challenging as it happenened very rapidly and there was often not a clear liquid front. Both the Washburne and modified Washburne equation has an infinite flow velocity at t=0, which is unphysical. A possible solution is to repeat the experiments in paper strips with the same material and same thickness, but smaller width and a microscope. For flow in a rectangular porous strip ($w>>h$) the flow distance is ideally independent of width, and it should therefore be possible to make more accurate measurements as the start-up length for flow development depends on the width of the channel. Although if the width is reduced so that it is on the order of the thickness, assumptions for the capillary

pressure are no longer valid. Velocity between parallel plates due to a pressure gradient with transient term can be expressed as [216]

$$u_z(y,t) = -\frac{1}{2\mu}\frac{\partial p}{\partial z}h^2\left\{1-\left(\frac{y}{h}\right)^2 - \frac{32}{\pi^3}\sum_{k=1}^{\infty}\frac{(-1)^{k+1}}{(2k-1)^3}cos\left[\frac{(2k-1)\pi}{2}\frac{y}{h}\right]exp\left[-\frac{(2k-1)^2\pi^2}{4h^2}\nu t\right]\right\}$$

Where development can be described in terms of the nondimensional parameter $\nu t/h^2$. By changing the width of the channel, the time required to reach a sufficient level of development can be reduced and measurements in the developing stages of the capillary flow can be improved. With more accurate measurements in the transient stages it may be possible to run smooth piecewise nonlinear regression, to avoid the problem of infinite flow speed in the initial stage of the model. However, the initial stage of the capillary flow is not very important for the purpose of modelling.

6.2.3 A diaper pad for diaper-based urine collection and colorimetric screening of urinary biomarkers

6.2.3.1 Background

The review of biomarkers, the investigation into capillary flow in compact devices, and the requirements for compatibility with smartphone based colorimetric analysis, formed the foundation for constructing a prototype of a diaper inlay with absorbent materials for liquid transport, a polymer-based swelling valve mechanism and chemical reaction pads for rapid screening of urinary tract infection of incontinent diaper-wearing elderly.

6.2.3.2 Objective

- Fabricate and test a prototype that is capable of achieving the desired functions for the application
- Make the results valid for as long as possible
- Model the capillary flow and diffusion mechanics of the design in a way that can be used to optimize the design.
- Define a set of tests that can be used to:
    - Test the function of the device under optimization
    - Characterize a device generation so that it can be compared to other generations

6.2.3.3 Challenges

Common colorimetric reaction pads made from polymers such as the pads on urine dipsticks, are normally dipped in a sample, taken out, and read within minutes by naked-eye or a dipstick reader. The desired application requires an extended validity window on the order of hours to offer any significant value, within the context of the intended application.

Optimize and obtain a satisfactory degree of control over the flow time within the device to balance the saturation of the reaction pads and superabsorbent polymer valve.

6.2.3.4 Modelling of capillary filling

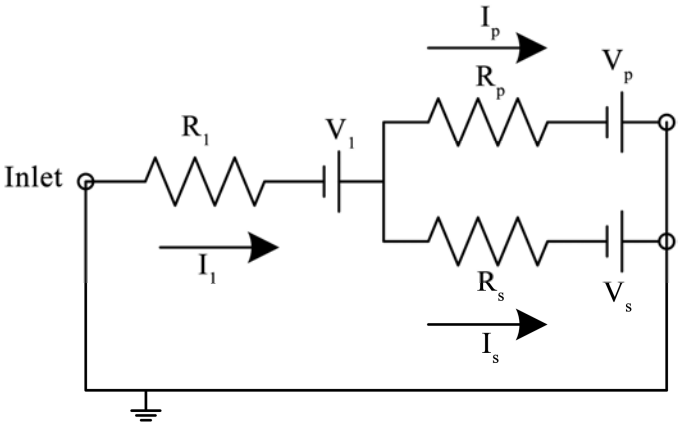

Figure 36 Capillary device filling equivalent circuit

Capillary filling can be modelled as a resistor and voltage source (transport medium) in series with two resistors and voltage sources in parallel (reaction pads and superabsorbent polymer)

The currents can be described based on Kirchhoffs voltage law.

$$\begin{bmatrix} R_1 & R_s & 0 \\ R_1 & 0 & R_p \\ 1 & -1 & -1 \end{bmatrix} \begin{bmatrix} I_1 \\ I_s \\ I_p \end{bmatrix} = \begin{bmatrix} V_s + V_1 \\ V_p + V_1 \\ 0 \end{bmatrix}$$

$$\begin{bmatrix} I_1 \\ I_s \\ I_p \end{bmatrix} = \begin{bmatrix} \frac{V_1(R_p + R_s) + V_s R_p + V_p R_s}{R_1 R_p + R_1 R_s + R_p R_s} \\ \frac{V_1 R_p + V_s(R_1 + R_p) - V_p R_1}{R_1 R_p + R_1 R_s + R_p R_s} \\ \frac{V_1 R_s - V_s R_1 + V_p(R_1 + R_s)}{R_1 R_p + R_1 R_s + R_p R_s} \end{bmatrix}$$

Neither I_p nor I_s can be allowed to be zero as this constitutes unsuccessful pad saturation or polymer swelling, respectively.

The process optimization was performed in iterations by measuring the time necessary to saturate reaction pads and close the valve, then modifying the design based on the equivalent circuit, and repeating until desired behavior was achieved. The optimization parameters were chosen to prevent major changes to the design, while still having a

significant impact on the result. Material and dimensions of pad conduction strips were chosen as parameters to optimize pad resistance (Rp), and the amount of SAP was chosen as parameter to optimize the SAP resistance (Rs):

6.2.3.5 Modelling of interpad diffusion

The network of reaction pads are connected as a K_6 complete graph with one interior vertex connected to a boundary vertex and the remaining five interior vertices connected to another boundary vertex (see Figure 37). This is supposed to represent a chemical concentration in one pad as a source, and the absence of this concentration in the remaining pads as a sink [217, 218]

$$K_{ij} = \begin{cases} \sum_j g_{ij} & for\ i = j \\ -g_{ij} & for\ (i,j) \in E \\ 0 & Otherwise \end{cases}$$

Where g is the edge weight representing conductance in the Kirchhoff matrix K where Column 1 and 2 corresponds to *a* (source) and *b* (sink) boundary vertices respectively. Column 3 to 8 corresponds to internal vertices 1-6 respectively.

$$K = \begin{bmatrix} g_{aa} & -g_{ab} & -g_{a1} & -g_{a2} & -g_{a3} & -g_{a4} & -g_{a5} & -g_{a6} \\ -g_{ab} & g_{bb} & -g_{b1} & -g_{b2} & -g_{b3} & -g_{b4} & -g_{b5} & -g_{b6} \\ -g_{a1} & -g_{23} & g_{11} & -g_{12} & -g_{13} & -g_{14} & -g_{15} & -g_{16} \\ -g_{a2} & -g_{24} & -g_{12} & g_{22} & -g_{23} & -g_{24} & -g_{25} & -g_{26} \\ -g_{a3} & -g_{25} & -g_{13} & -g_{23} & g_{33} & -g_{34} & -g_{35} & -g_{36} \\ -g_{a4} & -g_{26} & -g_{14} & -g_{24} & -g_{34} & g_{44} & -g_{45} & -g_{46} \\ -g_{a5} & -g_{27} & -g_{15} & -g_{25} & -g_{35} & -g_{45} & g_{55} & -g_{56} \\ -g_{a6} & -g_{28} & -g_{16} & -g_{26} & -g_{36} & -g_{46} & -g_{56} & g_{66} \end{bmatrix}$$

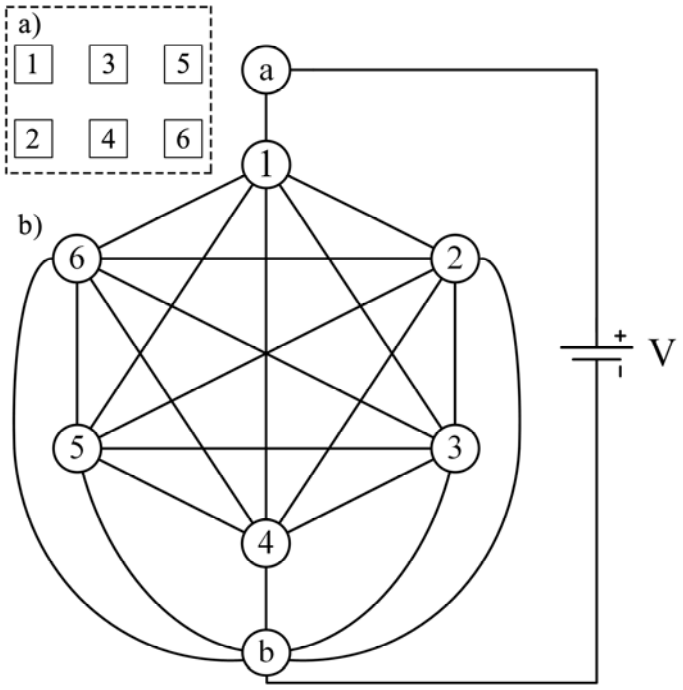

Figure 37 a) Layout of reaction pads, b) Diffusion equivalent circuit

If pads are simplified as a line source with width equal to pad width (i.e. neglect the orientation) and neglecting fringes, the resistances can be expressed as:

$$R_{12} = R_{13} = R_{24} = R_{34} = R_{35} = R_{46} = R_{56} = R$$
$$R_{14} = R_{23} = R_{36} = R_{45} = \sqrt{2}R$$
$$R_{15} = R_{26} = 2R$$
$$R_{16} = R_{25} = \sqrt{5}R$$
$$R_{ij} = R_{ji} = \frac{1}{g_{ij}}$$

Where R is the minimum interpad resistance. In this configuration under the given assumptions, the conductances are split into pad conductance and medium conductance, and the constants c_1 and c_2 are defined as the sum of inverse distance from a pad to all others.

$$c_1 = \frac{5}{2} + \frac{1}{\sqrt{2}} + \frac{1}{\sqrt{5}}, c_2 = 3 + \sqrt{2}$$

c_1 correspond to Pad 1,2,5 and 6, and c_2 correspond to pad 3 and 4.

$$K = \begin{bmatrix} g_p & 0 & -g_p & 0 & 0 & 0 & 0 & 0 \\ 0 & 5g_p & 0 & -g_p & -g_p & -g_p & -g_p & -g_p \\ -g_p & 0 & g_p + c_1 g_m & -g_m & -g_m & -g_m/\sqrt{2} & -g_m/2 & -g_m/\sqrt{5} \\ 0 & -g_p & -g_m & g_p + c_1 g_m & -g_m/\sqrt{2} & -g_m & -g_m/\sqrt{5} & -g_m/2 \\ 0 & -g_p & -g_m & -g_m/\sqrt{2} & g_p + c_2 g_m & -g_m & -g_m & -g_m/\sqrt{2} \\ 0 & -g_p & -g_m/\sqrt{2} & -g_m & -g_m & g_p + c_2 g_m & -g_m/\sqrt{2} & -g_m \\ 0 & -g_p & -g_m/2 & -g_m/\sqrt{5} & -g_m & -g_m/\sqrt{2} & g_p + c_1 g_m & -g_m \\ 0 & -g_p & -g_m/\sqrt{5} & -g_m/2 & -g_m/\sqrt{2} & -g_m & -g_m & g_p + c_1 g_m \end{bmatrix}$$

The Kirchhoff matrix can be used to solve for the interior voltage potentials and the net current for fixed boundary potentials:

$$Kv = i$$

$$\begin{bmatrix} A & B \\ B^T & D \end{bmatrix} \begin{bmatrix} V_b \\ V_i \end{bmatrix} = \begin{bmatrix} I \\ 0 \end{bmatrix}$$

Where *K* is partitioned corresponding to exterior and interior vertices

$$A = K_{1:2,1:2}, \qquad B = K_{1:2,3:8}, \qquad D = K_{3:8,3:8}$$

In the graph, there are two boundary vertices and six interior vertices. The interior vertex voltages V_i and net current *I* for a given applied boundary voltage V_b can be calculated by through the partitioned matrices (net current is calculated with the Schur complement):

$$V_i = -D^{-1}B^T V_b$$

$$I = (A - BD^{-1}B^T)V_b = (K/D)V_b$$

If the parameter r is defined as the ratio of g_p over g_m, the interior vertex potentials can be expressed as a function of boundary vertex potentials and the parameter r, through the normalized *K**, while the current can be expressed as a function of boundary vertex potentials, the parameter r and the minimum interpad resistance R

$$K^* = \frac{K}{R} = \begin{bmatrix} r & 0 & -r & 0 & 0 & 0 & 0 & 0 \\ 0 & 5r & 0 & -r & -r & -r & -r & -r \\ -r & 0 & r+c_1 & -1 & -1 & -1/\sqrt{2} & -1/2 & -1/\sqrt{5} \\ 0 & -r & -1 & r+c_1 & -1/\sqrt{2} & -1 & -1/\sqrt{5} & -1/2 \\ 0 & -r & -1 & -1/\sqrt{2} & r+c_2 & -1 & -1 & -1/\sqrt{2} \\ 0 & -r & -1/\sqrt{2} & -1 & -1 & r+c_2 & -1/\sqrt{2} & -1 \\ 0 & -r & -1/2 & -1/\sqrt{5} & -1 & -1/\sqrt{2} & r+c_1 & -1 \\ 0 & -r & -1/\sqrt{5} & -1/2 & -1/\sqrt{2} & -1 & -1 & r+c_1 \end{bmatrix}$$

$$V_i = -D^{*-1}B^{*T}V_b$$

$$I = \frac{1}{R}\left(A^* - B^*D^{*-1}B^{*T}\right)V_b$$

For r<<1 (*Rp*>>*Rm*) the pad entrance resistances dominate the interpad resistance network and essentially becomes a pad resistance in series with 5 pad resistances in parallel which causes one fifth of the current to go to each sink pad. For larger r, the current will prioritize the path of least resistance and the current will differ between different pads. However for a source in the center pads (3 and 4), the difference is smaller because the total distance from source pad to the other pads are shorter.

The process optimization was carried out by measuring the time between pad saturation and the first observable color interference between pads or observable fading of color resulting from diffusion out of pads, then modifying the design parameters, and repeating until desired behavior is achieved. The design parameters to optimize were intertwined with the optimization of capillary flow, through the dimensions and connection of the pad conduction strips compared to the distance of the material connecting the pads.

6.2.3.6 Design, fabrication and assembly

Home care service providers are the focus of the problem and a technical solution requires a design compatible with their everyday work routines. The diaper pad was designed with the intention to be mounted in a diaper with the inlet hole in the support layer (Figure 38 and 39) towards the patient. As urine enters the inlet hole, it comes into contact with the non-woven fabric (NWF) and the cellophane side of a conduction unit (CU), see Figure 39. The sample is transported past the cellophane side of the CU through

the protection pad and buffer layer within the superabsorbent polymer (SAP) frame, to the superabsorbent polymer.

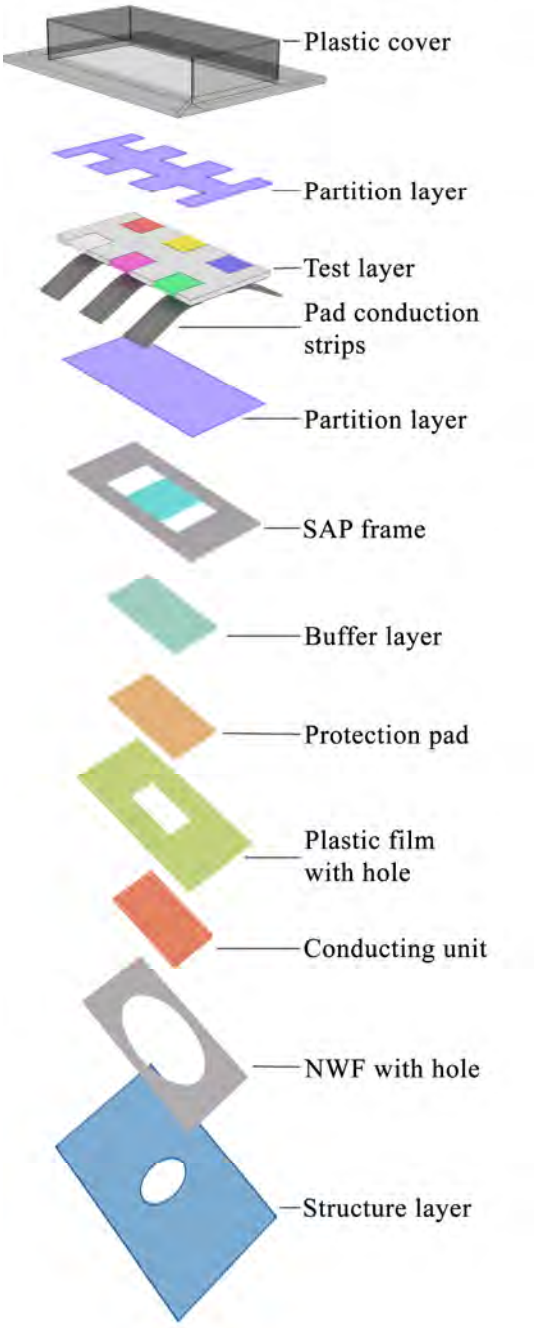

Figure 38 Device design

The sample is also transported in parallel along the pad conduction strips outside the SAP frame to the reaction pads. Reaction pads in the test layer are separated from the SAP by a partition layer of double-sided adhesive tape (DFAT), and the test layer is adhered to the plastic cover with another DFAT partition layer to prevent interference along the plastic cover. As the SAP swells, the cellophane side of the CU expands towards the open inlet hole and prevents additional liquid from outside the device to reach the test layer.

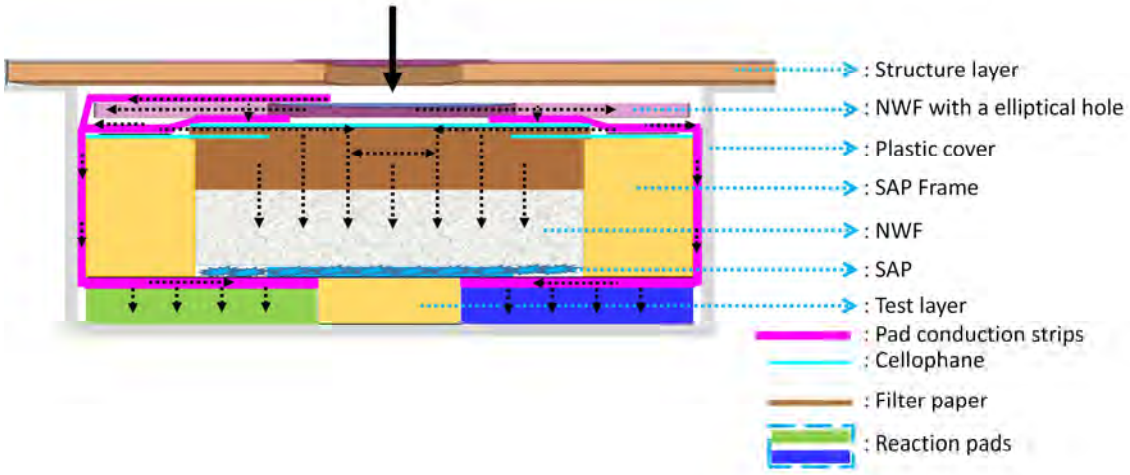

Figure 39 Device cross-section

In the attempt to satisfy the Affordability (of the ASSURED criteria) only affordable materials and processes have been used in the design. The main processes are shown in Figure 40, which mainly consists of various cutting tools for the various types of materials. The design is made layer-wise to facilitate assembly. Every step is displayed in Figure 41, and consists of stacking layers of materials as shown in Figure 38.

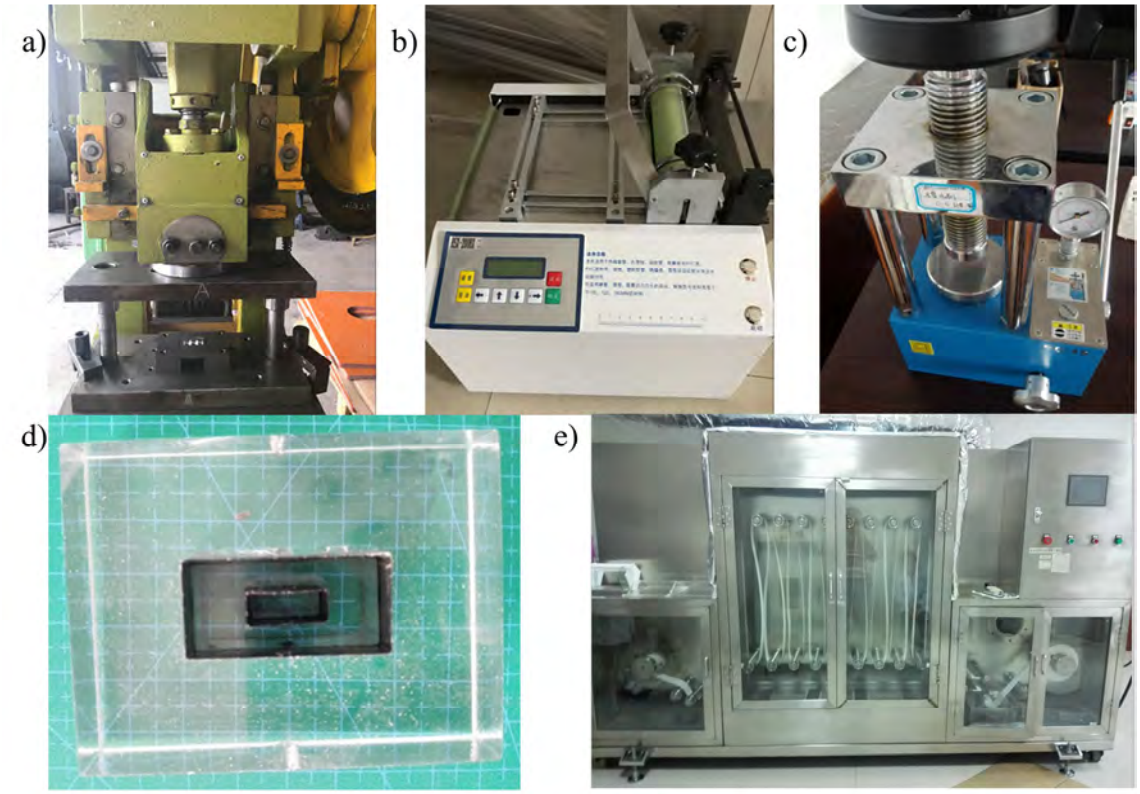

Figure 40 Machines used for manufacturing: a) Customized punching machine for hard materials, b) Size-adjustable cutting machine for medium-hard materials, c) Tablet machine for cutting soft materials, d) Customized steel knife for soft materials, e) paper impregnation dryer for reaction pads.

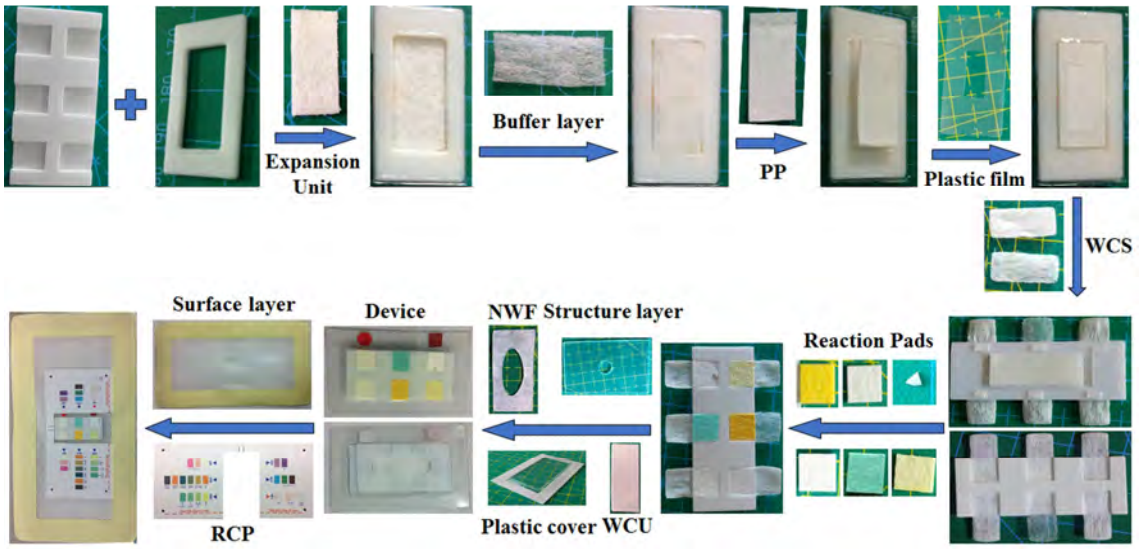

Figure 41 Assembly procedure

6.2.3.7 Proposed experiments for design optimization and generation comparison

For the purpose of control in the design, development and optimization phases of development a set of experiments was proposed to provide a basis for comparison so that variation in performance resulting from updating the design could be quantified

6.2.3.7.1 Valve closing time and performance test

Experimental determination of the required time for the valve to close and batch success rate over time.

6.2.3.7.1.1 Experimental procedure

(1) Dispense sample onto a packaged device.
(2) Monitor the inlet and record the time necessary for the valve to close.
(3) Dispense a strongly colored liquid after the valve is closed.
(4) Monitor the device in regular or irregular time intervals to see if the colored liquid can penetrate into the device.
(5) After a predefined time period, record whether the device is a success or failure
(6) Repeat steps (1)-(5).

6.2.3.7.1.2 Method of analysis

- Calculate a Clopper-Pearson exact confidence interval (CPCI) or Continuity corrected Wilson score interval on the proportion of successes [219].
- Investigate the distribution of recorded time points for valve closing, to select a method for finding a confidence interval [220].
    - One/two-sample Kolmogorov-Smirnov (KS) test for univariate normality.
    - Calculate a Student's t test CI for the mean if the sample can be assumed to be normally distributed.
    - Calculate a Wilcoxon signed rank CI (WCI) if an assumption of normality is unreasonable, but the data is symmetric around the median.
    - Calculate a binomial sign test CI if the data is neither normally distributed nor symmetric around the median.

6.2.3.7.2 Flow speed/saturation test

Experimental determination of the necessary time to saturate the reaction pads in a full device. All latent design and assembly parameters may contribute to variance of recorded time, hence it cannot be inferred from the distribution of recorded time whether variance is significantly affected by specific contributions. However, it is useful in determining the robustness and consistency of the design.

6.2.3.7.2.1 Experimental procedure

(1) Dispense sample in the inlet of a packaged device.

(2) Record the time from the sample was dispensed until a sufficient degree of saturation has been achieved.

6.2.3.7.2.2 Method of analysis

Calculate central tendency and a confidence interval.

6.2.3.7.3 Superabsorbent polymer swelling and reaction pad saturation optimization

Paired valve and saturation time data.

6.2.3.7.3.1 Experimental protocol:

Run the abovementioned two experiments (6.2.3.7.1 and 6.2.3.7.2) in parallel on the same devices.

6.2.3.7.3.2 Method of analysis:

Parametric or non-parametric paired statistical tests.

6.2.3.7.4 Interpad interference (diffusion)

Experimental determination of either time for visible interference or proportion of devices without interference within a predefined time.

6.2.3.7.4.1 Experimental protocol:

(1) Dispense sample and saturate a pad.

(2) Monitor either:

a. The time necessary to diffuse from the saturated pad to any of the unsaturated pads.
b. If there is no clearly defined point in time where the diffusion is obvious, instead record whether the test is a success or failure after a predefined time period.

6.2.3.7.5 Color retention

Determination of reaction color and behaviour over time.

6.2.3.7.5.1 Experimental protocol:

(1) Dispense a sample on a packaged device.
    a. Ensure that the sample with reaction chemical does not evaporate.
(2) Record the colors of the device in predefined regular or irregular time intervals.
    a. A scanner can be used to provide relatively stable conditions.
(3) Extract color data.

6.2.3.7.5.2 Method of analysis:

Discriminant analysis for a relevant time interval. If the colors can be successfully discriminated and classified over the relevant time interval, there is a sufficient degree of information provided by the colorimetric reaction despite the extended time. Use successful discrimination as a basis of definition for reference colors.

6.2.3.7.6 Maximum or Effective absorption volume

Determine necessary volume to successfully saturate the device as well as the effective volume that would be required if poured onto the device (i.e. imitate more real conditions)

6.2.3.7.6.1 Experimental protocol

(1) Dispense sample on packaged device.
    a. In the inlet for maximum absorbed volume.
    b. From a distance (possibly at an angle) at a higher pouring rate than the device absorption rate.

(2) Measure the necessary volume to achieve the desired level of saturation.

6.2.3.7.7 Diagnostic tests

Performance compared to a standard solution with known analyte concentrations.

6.2.3.7.7.1 Experimental protocol:

(1) Dispense standard artificial urine samples on packaged devices.

(2) Record time True/False Positives/Negatives.

6.2.3.7.7.2 Method of analysis:

- Odds ratio estimation and confidence interval.
- Pearson's χ^2 test.

6.2.3.7.8 Agreement between methods

Performance compared to alternative method, either with known analyte concentrations or arbitrary urine samples.

6.2.3.7.8.1 Experimental protocol:

(1) Dispense arbitrary urine samples on packaged devices and alternative method (e.g. urine dipstick).

(2) Record whether the methods agree or disagree for each sample (paired).

6.2.3.7.8.2 Method of analysis:

- Odds ratio estimation and confidence interval.
- Pearson's χ^2 test or McNemar's test.
- Cochran–Mantel–Haenszel test.

6.2.3.8 Demonstration of the set of characterization experiments:

6.2.3.8.1 Valve-closing and saturation

In 27 tested devices, each with 6 reaction pads, 4 devices failed to completely saturate all 6 pads (1 was left unsaturated), which gave a success proportion of $\hat{p} = 0.852$ (95% CPCI 0.663-0.958). Improvements to fabrication and assembling processes reduced the failures to zero in a batch of 212 tests $\hat{p} = 1$ (95% CPCI 0.982-1) A median of 12 urine

drops (100 µL/drop) dispensed on the inlet of the device was necessary to successfully saturate the device.

KS test for normality of time was rejected at 5% significance level ($p<0.001$).Two-sample KS-test could not reject that Saturation time and valve were from the same distribution at the 5% significance level ($p=0.076$). A paired Wilcoxon signed rank test for zero median between the two data sets could not be rejected at the 5% significance level ($p=0.062$). the pseudo-median (Hodges-Lehmann estimator) recorded time necessary to observe saturation and valve-closing was 7.025 (95% WCI 6.8-7.3) and 7.375 (95% WCI 6.95-7.65) minutes respectively (see Boxplot in Figure 42).

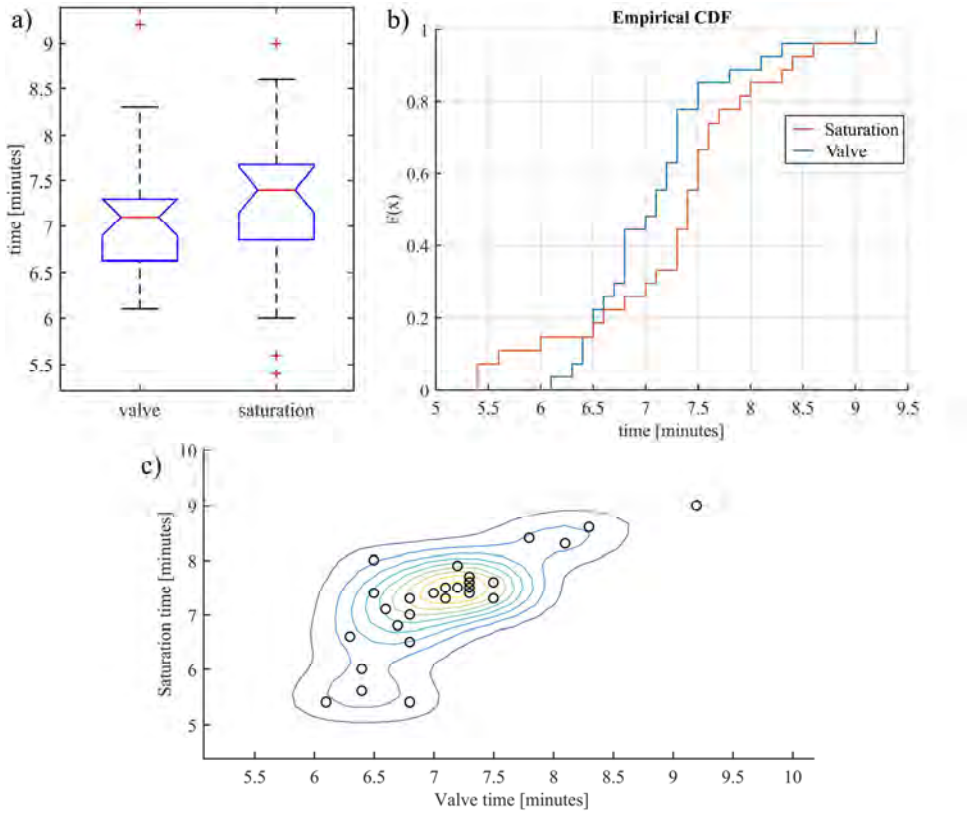

Figur 42 Valve and saturation time data, a) boxplot, b) empirical cumulative density function, c) scatter plot with KS density contours

6.2.3.8.2 Interference

For 27 tests with optimized design for interference prevention there were no observable interference within the desired time interval defined as 8 hours, or after the extended duration of 22 hours (the last observation). However, after a period of time (between 8

and 22 hours) the chemicals in the reaction pads diffuse into the transport medium to such an extent that it causes a slight color gradient.

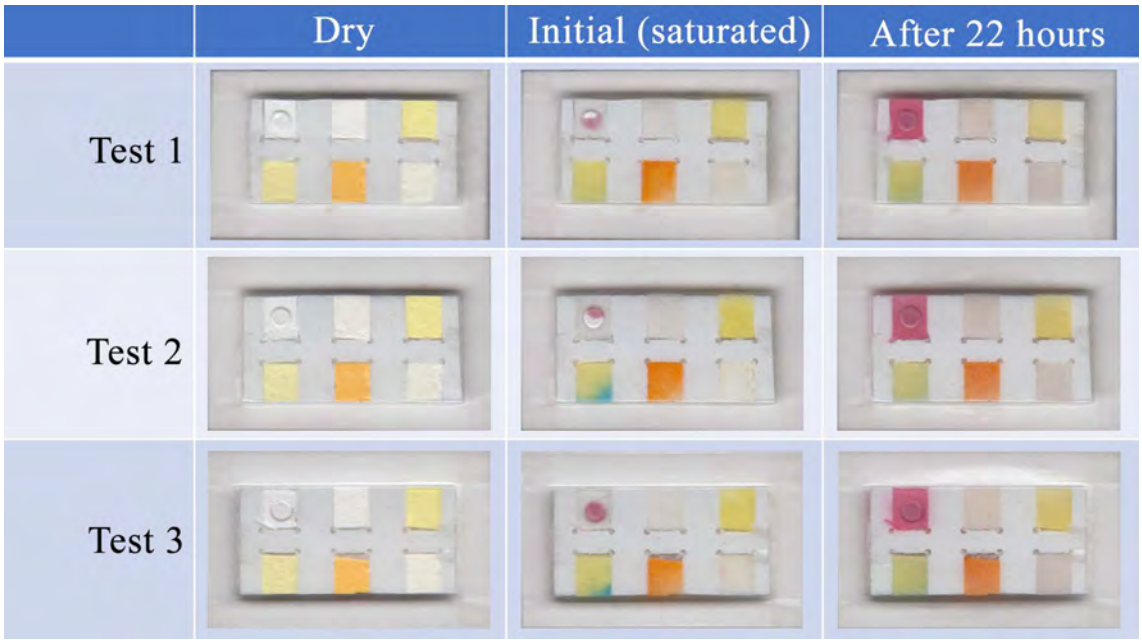

Figure 43 Interference experiments

6.2.3.8.3 Color retention

Reaction pads saturated with artificial urine was scanned periodically for approximately 20 hours, and the average pixel value was extracted from 15 devices in parallel for each time step and for 3 concentration levels. Nonlinear fisher discriminant analysis [221] was performed on the datasets, see Figure 44. The datasets exhibited a low amount of overlapping samples for all time steps except for the Glucose and Leukocyte esterase reaction. By separating the data into an initial set and a final set based on minimization of resubstitution error, the collected Glucose and Leukocyte Esterase data could be classified reasonably well, but put in place a necessary minimum time of 30 minutes before the test could be read to obtain consistent results.

6.2.3.9 Conclusion

A disposable absorbent pad developed for urine collection and screening in diapers was able to absorb a small volume of urine to saturate a set of six chemical reaction pads and a superabsorbent polymer-based swelling valve. The valve sealed the inlet in

approximately 7 minutes. There were no observable chemical interference between the pads, and the reaction colors were sufficiently stable to distinguish three concentration levels for each biomarker within the desired time interval defined from 30 minutes to 8 hours. The device therefore satisfies the requirement initially set for the application. Saturation and valve-closing time were consistent, the reaction colors were distinguishable, interference and external contamination was preventable. With these features, the device can collect and screen urine within a home care service environment without requiring much effort or time from a nurse.

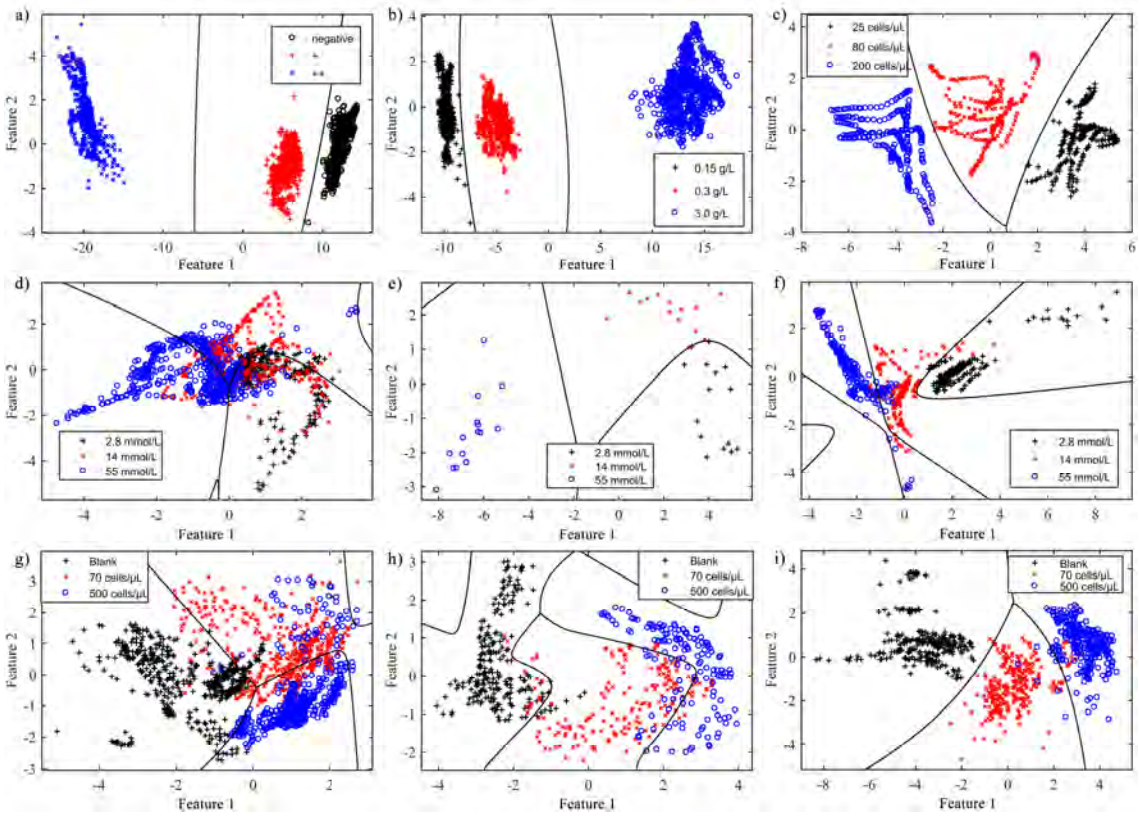

Figure 44 Nonlinear fisher mapped plots [222] of relevant biomarker reactions in sealed environment. Quadratic classifier rules for all plots except for h) which is mixed gaussian. a) Nitrite 0-22.5 hours, 0% resubstitution error, b) Proteins 0-22.5 hours, 0% error, c) blood 0-8 hours, 0.12% error, d) Glucose 0-19.5 hours, 31% error, e) Glucose initial color, 4.4% error, f) Glucose 30 min-19.5 hours, 8% error, g) Leukocytes 0-19.5 hours, 20% error, h) Leukocytes 0-30 min, 11% error, i) Leukocytes 30min-19.5 hours, 3.3% error.

7 Main Conclusions and perspectives

This doctoral thesis covers a research and development of a paper-based microfluidic solution for challenges surrounding incontinent diaper-wearing elderly within an application oriented and user-driven project. The solution consists of:

- *Screening module:* A capillary flow driven device intended to be mounted in a diaper, and perform automatic urine sampling, isolation and colorimetric analysis.
- *Read-out/analysis module:* A smartphone app capable of extracting color data from an image of the screening module to provide objective, illumination/device independent qualitative or semi-quantitative classification of biomarkers in urine, based on the comparison of colorimetric reactions with a set of reference colors.

The research and development has focused on the use of affordable materials and affordable fabrication methods, to facilitate fabrication in a commercialization context in the case that the results of this doctoral study are taken further. Due to the application oriented and user-driven nature of the study, the success of the work requires a degree of maturity that would allow a subsequent path from lab to market, otherwise there is no actual possibility to solve the problem at hand. Within the project, the idea has gone from initial idea stage to a stage where it is ready for validation/demonstration in relevant environment, which is equivalent to Technology Readiness Level 5 or 6 [223].

This doctoral study shows what was considered the most promising solution to a problem presented by the users (municipal nurses) that attempts to satisfy all requirements pertaining to the problem, such as:

- Portable
- User-friendly
- Affordable
- Non-invasive
- Automatic sampling
- Analysis system

- Dipstick equivalent functionality
- Compatible with standard commercially available adult diapers.

However, the candidate makes no claim that this is the only solution, but it appears to be the most promising under the given constraints. If the problem constraints were loosened, it may have resulted in a completely different path of research. Alternative solutions that were under consideration in initial stages includes such solutions as capacitance measurements using smartphone screen, electrochemical sensor etc. As these methods were not compatible with the problem constraints, the application-oriented nature of the problem took precedence in the choice of solution.

The results obtained demonstrate that the device functions as intended albeit further improvements are still desired.

References

1. Foxman, B., The epidemiology of urinary tract infection. Nature Reviews Urology, 2010. 7(12): p. 653-660.
2. Ahmed, N.H., T. Hussain, and I. Biswal, Comparison of Etiological Agents and Resistance Patterns of the Pathogens Causing Community Acquired and Hospital Acquired Urinary Tract Infections. Journal of Global Infectious Diseases, 2014. 6(3): p. 135-136.
3. Peleg, A.Y. and D.C. Hooper, Hospital-Acquired Infections Due to Gram-Negative Bacteria. The New England journal of medicine, 2010. 362(19): p. 1804-1813.
4. Lo, D.S., et al., Community-acquired urinary tract infection: age and gender-dependent etiology. Journal Brasileiro de Nefrologia, 2013. 35(2): p. 93-98.
5. McLaws, M.L., et al., The prevalence of nosocomial and community-acquired infections in Australian hospitals. The Medical Journal of Australia, 1988. 149(11-12): p. 582-590.
6. Ott, E., et al., The Prevalence of Nosocomial and Community Acquired Infections in a University Hospital: An Observational Study. Deutsches Ärzteblatt International, 2013. 110(31-32): p. 533-540.
7. Weinstein, J.W., et al., A decade of prevalence surveys in a tertiary-care center: trends in nosocomial infection rates, device utilization, and patient acuity. Infection Control and Hospital Epidemiology, 1999. 20(8): p. 543-548.
8. Kalsi, J., et al., Hospital-acquired urinary tract infection. International Journal of Clinical Practice, 2003. 57(5): p. 388-391.
9. Dias Neto, J.A., et al., Community acquired urinary tract infection: etiology and bacterial susceptibility. Acta Cirurgica Brasileira, 2003. 18: p. 33-36.
10. Hidron, A.I., et al., NHSN annual update: antimicrobial-resistant pathogens associated with healthcare-associated infections: annual summary of data reported to the National Healthcare Safety Network at the Centers for Disease Control and Prevention, 2006-2007. Infection Control and Hospital Epidemiology, 2008. 29(11): p. 996-1011.

11. Sievert, D.M., et al., Antimicrobial-Resistant Pathogens Associated with Healthcare-Associated Infections: Summary of Data Reported to the National Healthcare Safety Network at the Centers for Disease Control and Prevention, 2009-2010. Infection Control and Hospital Epidemiology, 2013. 34(1): p. 1-14.
12. Weiner, L.M., et al., Antimicrobial-Resistant Pathogens Associated With Healthcare-Associated Infections: Summary of Data Reported to the National Healthcare Safety Network at the Centers for Disease Control and Prevention, 2011-2014. Infection Control and Hospital Epidemiology, 2016. 37(11): p. 1288-1301.
13. Fluit, A.C., J. Verhoef, and F.J. Schmitz, Frequency of isolation and antimicrobial resistance of gram-negative and gram-positive bacteria from patients in intensive care units of 25 European university hospitals participating in the European arm of the SENTRY Antimicrobial Surveillance Program 1997-1998. European Journal of Clinical Microbiology & Infectious Diseases, 2001. 20(9): p. 617-625.
14. Ronald, A., The etiology of urinary tract infection: traditional and emerging pathogens. Disease-a-Month, 2003. 49(2): p. 71-82.
15. Gorczynska, E., et al., Incidence, clinical outcome, and management of virus-induced hemorrhagic cystitis in children and adolescents after allogeneic hematopoietic cell transplantation. Biology of Blood and Marrow Transplantation, 2005. 11(10): p. 797-804.
16. Paduch, D.A., Viral lower urinary tract infections. Current Urology Reports, 2007. 8(4): p. 324-335.
17. Colodner, R., et al., Community-acquired and hospital-acquired candiduria: comparison of prevalence and clinical characteristics. European Journal of Clinical Microbiology & Infectious Diseases, 2008. 27(4): p. 301-305.
18. Bukhary, Z.A., Candiduria: a review of clinical significance and management. Saudi Journal of Kidney Diseases and Transplantation, 2008. 19(3): p. 350-360.

19. Nguyen-Van-Tam, S., et al., Risk factors for hospital-acquired urinary tract infection in a large English teaching hospital: a case-control study. Infection, 1999. 27(3): p. 192-197.
20. Fisher, J.F., et al., Candida urinary tract infections--treatment. Clinical Infectious Diseases, 2011. 52 Suppl 6: p. S457-466.
21. Platt, R., et al., Risk factors for nosocomial urinary tract infection. American Journal of Epidemiology, 1986. 124(6): p. 977-985.
22. Center for Disease Control, Urinary Tract Infection (Catheter-Associated Urinary Tract Infection [CAUTI] and Non-Catheter-Associated Urinary Tract Infection [UTI]) and Other Urinary System Infection [USI]) Events in Device-associated Module UTI. 2017.
23. Kauffman, C.A., et al., Candida urinary tract infections--diagnosis. Clinical Infectious Diseases, 2011. 52 Suppl 6: p. S452-456.
24. Rivett, A.G., J.A. Perry, and J. Cohen, Urinary candidiasis: a prospective study in hospital patients. Urological Research, 1986. 14(4): p. 183-186.
25. Bichler, K.-H., et al., EAU Guidelines for the Management of Urogenital Schistosomiasis. European Urology. 49(6): p. 998-1003.
26. Vester, U., et al., Urinary tract morbidity due to Schistosoma haematobium infection in Mali. Kidney International, 1997. 52(2): p. 478-481.
27. Ossai, O.P., et al., Bacteriuria and urinary schistosomiasis in primary school children in rural communities in Enugu State, Nigeria, 2012. The Pan African Medical Journal, 2014. 18(Suppl 1): p. 15.
28. Shaikh, N., et al., Prevalence of urinary tract infection in childhood: a meta-analysis. The Pediatric Infectious Disease Journal, 2008. 27(4): p. 302-308.
29. Foxman, B., Epidemiology of urinary tract infections: incidence, morbidity, and economic costs. The American Journal of Medicine, 2002. 113(1): p. 5-13.
30. Giesen, L.G., et al., Predicting acute uncomplicated urinary tract infection in women: a systematic review of the diagnostic accuracy of symptoms and signs. BMC Family Practice, 2010. 11(1): p. 78.

31. Lipsky, B.A., Urinary tract infections in men. Epidemiology, pathophysiology, diagnosis, and treatment. Annals of Internal Medicine, 1989. 110(2): p. 138-150.
32. Ryder, N.B., Notes on Stationary Populations. Population Index, 1975. 41(1): p. 3-28.
33. U.S. Department of Commerce, Current population reports. Series P-23. Special studies. Current population reports. Series P-23, Special studies, 1969
34. Hamilton-Miller, J.M.T., Issues in urinary tract infections in the elderly. World Journal of Urology, 1999. 17(6): p. 396-401.
35. Yoshikawa, T.T., Unique aspects of urinary tract infection in the geriatric population. Gerontology, 1984. 30(5): p. 339-344.
36. Abrams, P., et al., The standardisation of terminology of lower urinary tract function: report from the Standardisation Sub-committee of the International Continence Society. Neurourology and Urodynamics, 2002. 21(2): p. 167-178.
37. Irwin, D.E., et al., Population-based survey of urinary incontinence, overactive bladder, and other lower urinary tract symptoms in five countries: results of the EPIC study. European Urology, 2006. 50(6): p. 1306-1315.
38. Malmsten, U.G., et al., Urinary incontinence and lower urinary tract symptoms: an epidemiological study of men aged 45 to 99 years. The Journal of Urology, 1997. 158(5): p. 1733-1737.
39. Thomas, T.M., et al., Prevalence of urinary incontinence. The British Medical Journal, 1980. 281(6250): p. 1243-1245.
40. Aggazzotti, G., et al., Prevalence of urinary incontinence among institutionalized patients: a cross-sectional epidemiologic study in a midsized city in northern Italy. Urology, 2000. 56(2): p. 245-249.
41. Ouslander, J.G., R.L. Kane, and I.B. Abrass, Urinary incontinence in elderly nursing home patients. Jama, 1982. 248(10): p. 1194-1198.
42. Shamliyan, T.A., et al., Male urinary incontinence: prevalence, risk factors, and preventive interventions. Reviews in Urology, 2009. 11(3): p. 145-165.

43. Woodford, H.J. and J. George, Diagnosis and management of urinary tract infection in hospitalized older people. Journal of the American Geriatrics Society, 2009. 57(1): p. 107-114.
44. Marques, L.P., et al., Epidemiological and clinical aspects of urinary tract infection in community-dwelling elderly women. Brazilian Journal of Infectious Diseases, 2012. 16(5): p. 436-441.
45. Raz, R., Urinary Tract Infection in Postmenopausal Women. Korean Journal of Urology, 2011. 52(12): p. 801-808.
46. Starer, P. and L.S. Libow, Obscuring urinary incontinence. Diapering of the elderly. Journal of the American Geriatrics Society, 1985. 33(12): p. 842-846.
47. Omli, R., et al., Pad per day usage, urinary incontinence and urinary tract infections in nursing home residents. Age and Ageing, 2010. 39(5): p. 549-554.
48. Skotnes, L.H., et al., Urinary incontinence in Norwegian nursing home residents. Open Journal of Nursing, 2012. 2(02): p. 116-122
49. Bailey, K.L., et al., PRN1: Overactive bladder cost of illness: Analysis of Medi-Cal claims. Value in Health, 2012. 3(2): p. 139-140.
50. Brown, J.S., W.F. McGhan, and S. Chokroverty, Comorbidities associated with overactive bladder. The American Journal of Managed Care, 2000. 6(11 Suppl): p. S574-579.
51. Nitz, N.M., et al., Medical costs after initiation of drug treatment for overactive bladder: effects of selection bias on cost estimates. The American Journal of Managed Care, 2005. 11(4 Suppl): p. S130-139.
52. Darkow, T., C.L. Fontes, and T.E. Williamson, Costs associated with the management of overactive bladder and related comorbidities. Pharmacotherapy, 2005. 25(4): p. 511-519.
53. Warren, J.W., Catheter-associated urinary tract infections. Infectious disease clinics of North America, 1997. 11(3): p. 609-622.
54. Maki, D.G. and P.A. Tambyah, Engineering out the risk for infection with urinary catheters. Emerging Infectious Diseases, 2001. 7(2): p. 342-347.

55. Hooton, T.M., et al., Diagnosis, Prevention, and Treatment of Catheter-Associated Urinary Tract Infection in Adults: 2009 International Clinical Practice Guidelines from the Infectious Diseases Society of America. Clinical Infectious Diseases, 2010. 50(5): p. 625-663.
56. Trautner, B.W. and R.O. Darouiche, Role of biofilm in catheter-associated urinary tract infection. American Journal of Infection Control, 2004. 32(3): p. 177-183.
57. Stark , R.P. and D.G. Maki Bacteriuria in the Catheterized Patient. New England Journal of Medicine, 1984. 311(9): p. 560-564.
58. Saint, S. and C.E. Chenoweth, Biofilms and catheter-associated urinary tract infections. Infectious Disease Clinics of North America, 2003. 17(2): p. 411-432.
59. Kelly, C.E., Evaluation of Voiding Dysfunction and Measurement of Bladder Volume. Reviews in Urology, 2004. 6(Suppl 1): p. S32-S37.
60. Truzzi, J.C., et al., Residual urinary volume and urinary tract infection--when are they linked? The Journal of Urology, 2008. 180(1): p. 182-185.
61. Omli, R., et al., Residual urine as a risk factor for lower urinary tract infection: a 1-year follow-up study in nursing homes. Journal of the American Geriatric Society, 2008. 56(5): p. 871-874.
62. Hershkovitz, A., et al., Is routine screening for urinary tract infection in rehabilitation day-hospital elderly patients necessary? Archives of Gerontology and Geriatrics, 2002. 34(1): p. 29-36.
63. May, M., et al., Post-void residual urine as a predictor of urinary tract infection--is there a cutoff value in asymptomatic men? The Journal of Urology, 2009. 181(6): p. 2540-2544.
64. Huang, A.J., et al., Clinical Significance of Postvoid Residual Volume in Older Ambulatory Women. Journal of the American Geriatrics Society, 2011. 59(8): p. 1452-1458
65. Gehrich, A., et al., Establishing a mean postvoid residual volume in asymptomatic perimenopausal and postmenopausal women. Obstetrics & Gynecology, 2007. 110(4): p. 827-832.

66. Haylen, B.T., et al., Immediate postvoid residual volumes in women with symptoms of pelvic floor dysfunction. Obstetrics & Gynecology, 2008. 111(6): p. 1305-1312.
67. Ruud Bosch, J.L., Postvoid residual urine in the evaluation of men with benign prostatic hyperplasia. World Journal of Urology, 1995. 13(1): p. 17-20.
68. Milleman, M., P. Langenstroer, and M.L. Guralnick, Post-void residual urine volume in women with overactive bladder symptoms. The Journal of Urology, 2004. 172(5): p. 1911-1914.
69. Kolman, C., et al., Distribution of post-void residual urine volume in randomly selected men. The Journal of Urology, 1999. 161(1): p. 122-127.
70. Zhang, S.-J., et al., Relationship between age and prostate size. Asian Journal of Andrology, 2013. 15(1): p. 116-120.
71. Berges, R. and M. Oelke, Age-stratified normal values for prostate volume, PSA, maximum urinary flow rate, IPSS, and other LUTS/BPH indicators in the German male community-dwelling population aged 50 years or older. World Journal of Urology, 2011. 29(2): p. 171-178.
72. Rovner, B.W., et al., The prevalence and management of dementia and other psychiatric disorders in nursing homes. International Psychogeriatrics, 1990. 2(1): p. 13-24.
73. Agata, E.D., M.B. Loeb, and S.L. Mitchell, Challenges in assessing nursing home residents with advanced dementia for suspected urinary tract infections. Journal of the American Geriatrics Society, 2013. 61(1): p. 62-66.
74. Schüssler, S. and C. Lohrmann, Dementia in Nursing Homes. 2017, Springer.
75. Mitchell, S.L., et al., Infection management and multidrug-resistant organisms in nursing home residents with advanced dementia. JAMA Internal Medicine, 2014. 174(10): p. 1660-1667.
76. D'Agata, E. and S.L. Mitchell, Patterns of antimicrobial use among nursing home residents with advanced dementia. Archives of International Medicine, 2008. 168(4): p. 357-362.

77. Pop-Vicas, A., et al., Multidrug-resistant gram-negative bacteria in a long-term care facility: prevalence and risk factors. Journal of the American Geriatrics Society, 2008. 56(7): p. 1276-1280.
78. Dorr, D.A., S.D. Horn, and R.J. Smout, Cost analysis of nursing home registered nurse staffing times. Journal of the American Geriatrics Society, 2005. 53(5): p. 840-845.
79. Garrett, C., The Effect of Nurse Staffing Patterns on Medical Errors and Nurse Burnout. AORN Journal. 87(6): p. 1202-1204.
80. Poghosyan, L., et al., Nurse Burnout and Quality of Care: Cross-National Investigation in Six Countries. Research in nursing & health, 2010. 33(4): p. 288-298.
81. Kennedy, B.R., Stress and burnout of nursing staff working with geriatric clients in long-term care. Journal of Nursing Scholarship, 2005. 37(4): p. 381-382.
82. Aiken, L.H., et al., Hospital nurse staffing and patient mortality, nurse burnout, and job dissatisfaction. JAMA, 2002. 288(16): p. 1987-1993.
83. Cimiotti, J.P., et al., Nurse staffing, burnout, and health care–associated infection. American journal of infection control, 2012. 40(6): p. 486-490.
84. Jennings, B.M., Advances in Patient Safety: Work Stress and Burnout Among Nurses: Role of the Work Environment and Working Conditions, in Patient Safety and Quality: An Evidence-Based Handbook for Nurses, R.G. Hughes, Editor. 2008, Agency for Healthcare Research and Quality (US): Rockville (MD).
85. Barnett, B.J. and D.S. Stephens, Urinary tract infection: an overview. The American Journal of the Medical Sciences, 1997. 314(4): p. 245-249.
86. Baldassarre, J.S. and D. Kaye, Special problems of urinary tract infection in the elderly. Medical Clinics of North America, 1991. 75(2): p. 375-390.
87. Ackermann, R.J. and P.W. Monroe, Bacteremic urinary tract infection in older people. Journal of the American Geriatric Society, 1996. 44(8): p. 927-933.
88. Singer, M., et al., The third international consensus definitions for sepsis and septic shock (sepsis-3). JAMA, 2016. 315(8): p. 801-810.

89. McCue, J.D., Gram-negative bacillary bacteremia in the elderly: incidence, ecology, etiology, and mortality. Journal of the American Geriatric Society, 1987. 35(3): p. 213-218.
90. Meyers, B.R., et al., Bloodstream infections in the elderly. The American Journal of Medicine, 1989. 86(4): p. 379-384.
91. Esposito, A.L., et al., Community-acquired bacteremia in the elderly: analysis of one hundred consecutive episodes. Journal of the American Geriatric Society, 1980. 28(7): p. 315-319.
92. Tal, S., et al., Profile and prognosis of febrile elderly patients with bacteremic urinary tract infection. Journal of Infection, 2005. 50(4): p. 296-305.
93. Wester, A.L., et al., Age-related differences in symptoms, diagnosis and prognosis of bacteremia. BMC Infectious Diseases, 2013. 13: p. 346.
94. Stearns-Kurosawa, D.J., et al., The Pathogenesis of Sepsis. Annual review of pathology, 2011. 6: p. 19-48.
95. Girard, T.D. and E.W. Ely, Bacteremia and sepsis in older adults. Clinics in Geriatric Medicine, 2007. 23(3): p. 633-647.
96. Centers for Disease Control Prevention, Urinary tract infection (UTI) event for long-term care facilities, in NHSN Long-term Care Facility Component - Urinary Tract Infection. 2015, Center for Disease Control Prevention.
97. McGeer, A., et al., Definitions of infection for surveillance in long-term care facilities. American journal of infection control, 1991. 19(1): p. 1-7.
98. Loeb, M., et al., Development of minimum criteria for the initiation of antibiotics in residents of long-term-care facilities: results of a consensus conference. Infection Control and Hospital Epidemiology, 2001. 22(2): p. 120-124.
99. Bayer Healthcare, Multistix® 10 SG · Multistix® 9 · Multistix® 9 SG · Multistix® 8 SG · Multistix® 7 · N-Multistix® SG · N-Multistix® · Multistix® SG · Multistix® · Bili-Labstix® Reagent Strips. 2005.
100. Powell, H.R., D.A. McCredie, and M.A. Ritchie, Urinary nitrite in symptomatic and asymptomatic urinary infection. Archives of Disease in Childhood, 1987. 62: p. 138-140.

101. Khasriya, R., et al., The inadequacy of urinary dipstick and microscopy as surrogate markers of urinary tract infection in urological outpatients with lower urinary tract symptoms without acute frequency and dysuria. The Journal of Urology, 2010. 183(5): p. 1843-1847.
102. Scheifele, D.W. and A.L. Smith, Home-testing for recurrent bacteriuria, using nitrite strips. American Journal of Diseases of Children, 1978. 132(1): p. 46-48.
103. Devillé, W., et al., The urine dipstick test useful to rule out infections. A meta-analysis of the accuracy. BMC Urology, 2004. 4(1): p. 1-14.
104. Gorina, Y., et al., Prevalence of incontinence among older americans. Vital & health statistics. Series 3, Analytical and epidemiological studies, 2014(36): p. 1-33.
105. Belmin, J., et al., Reliability of sampling urine from disposable diapers in elderly incontinent women. Journal of the American Geriatrics Society, 1993. 41(11): p. 1182-1186.
106. Pezzlo, M., Detection of urinary tract infections by rapid methods. Clinical Microbiological Reviews, 1988. 1(3): p. 268-280.
107. Boonen, K.J.M., et al., Urine flow cytometry as a primary screening method to exclude urinary tract infections. World Journal of Urology, 2013. 31(3): p. 547-551.
108. Cabuz, C., et al., Portable flow cytometer. 2002, Google Patents. WO 2002010713 A2
109. Hintsche, R., et al., Chemical microsensor systems for medical applications in catheters. Sensors and Actuators B: Chemical, 1995. 27(1): p. 471-473.
110. Bing-Jonsson, P.C. and S. Tønnessen, Urinary tract infection among older patients in the home care services. Journal of clinical nursing, 2017.
111. Davy, J., On a Gaseous Compound of Carbonic Oxide and Chlorine. Philosophical Transactions of the Royal Society of London, 1812. 102: p. 144-151.
112. Xia, F., S. Tadigadapa, and Q.M. Zhang, Electroactive polymer based microfluidic pump. Sensors and Actuators A: Physical, 2006. 125(2): p. 346-352.

113. Cate, D.M., et al., Recent Developments in Paper-Based Microfluidic Devices. Analytical Chemistry, 2015. 87(1): p. 19-41.
114. Blow, N., Microfluidics: the great divide. Nature Methods, 2009. 6(9): p. 683-686.
115. Yamada, K., et al., Toward practical application of paper-based microfluidics for medical diagnostics: state-of-the-art and challenges. Lab on a Chip, 2017. 17(7): p. 1206-1249.
116. Toley, B.J., et al., Tunable-delay shunts for paper microfluidic devices. Analytical Chemistry, 2013. 85(23): p. 11545-11552.
117. Houghtaling, J., et al., Dissolvable Bridges for Manipulating Fluid Volumes in Paper Networks. Analytical Chemistry, 2013. 85(23): p. 11201-11204.
118. Li, X., et al., Fabrication of paper-based microfluidic sensors by printing. Colloids and Surfaces B: Biointerfaces, 2010. 76(2): p. 564-570.
119. Evans, E., et al., Rational Selection of Substrates to Improve Color Intensity and Uniformity on Microfluidic Paper-Based Analytical Devices. The Analyst, 2014. 139(9): p. 2127-2132.
120. Li, X., J. Tian, and W. Shen, Quantitative biomarker assay with microfluidic paper-based analytical devices. Analytical and Bioanalytical Chemistry, 2010. 396(1): p. 495-501.
121. Martinez, A.W., S.T. Phillips, and G.M. Whitesides, Three-dimensional microfluidic devices fabricated in layered paper and tape. Proceedings of the National Academy of Sciences, 2008. 105(50): p. 19606-19611.
122. Ge, L., et al., 3D origami-based multifunction-integrated immunodevice: low-cost and multiplexed sandwich chemiluminescence immunoassay on microfluidic paper-based analytical device. Lab on a Chip, 2012. 12(17): p. 3150-3158.
123. Lei, K.F., et al., Paper-based microfluidic sensing device for label-free immunoassay demonstrated by biotin–avidin binding interaction. Talanta, 2015. 134(Supplement C): p. 264-270.

124. Mu, X., et al., Multiplex Microfluidic Paper-based Immunoassay for the Diagnosis of Hepatitis C Virus Infection. Analytical Chemistry, 2014. 86(11): p. 5338-5344.
125. Lei, K.F., et al., Paper-based enzyme-free immunoassay for rapid detection and subtyping of influenza A H1N1 and H3N2 viruses. Analytica Chimica Acta, 2015. 883(Supplement C): p. 37-44.
126. Grant, B.D., et al., A paper-based immunoassay to determine HPV vaccination status at the point-of-care. Vaccine, 2016. 34(46): p. 5656-5663. doi: 10.1016/j.vaccine.2016.09.021. http://creativecommons.org/licenses/by-nc-nd/4.0/
127. Ahuja, S., Monitoring water quality: Pollution assessment, analysis, and remediation. 2013: Newnes.
128. Zhang, M., et al., Three-dimensional paper-based electrochemiluminescence device for simultaneous detection of Pb2+ and Hg2+ based on potential-control technique. Biosensors and Bioelectronics, 2013. 41: p. 544-550.
129. Qi, J., et al., Three-dimensional paper-based microfluidic chip device for multiplexed fluorescence detection of Cu2+ and Hg2+ ions based on ion imprinting technology. Sensors and Actuators B: Chemical, 2017. 251(Supplement C): p. 224-233.
130. Lin, Y., et al., Detection of heavy metal by paper-based microfluidics. Biosensors and Bioelectronics, 2016. 83(Supplement C): p. 256-266.
131. Meredith, N.A., et al., Paper-based analytical devices for environmental analysis. Analyst, 2016. 141(6): p. 1874-1887.
132. Lia, B. and P. Nesser, Terror mot drikkevann–en oversikt over terrorgruppers interesse for å ramme offentlig vannforsyning. FFI/Rapport-2003/01919,(Kjeller: Forsvarets forskningsinstitutt), http://rapporter.ffi.no/rapporter/2003/01919.pdf, 2003.
133. Pardasani, D., et al., µ-PADs for detection of chemical warfare agents. Analyst, 2012. 137(23): p. 5648-5653.

134. Pesenti, A., et al., Coupling paper-based microfluidics and lab on a chip technologies for confirmatory analysis of trinitro aromatic explosives. Analytical Chemistry, 2014. 86(10): p. 4707-4714.
135. Marriott, N.G. and R.B. Gravani, Food Contamination Sources, in Principles of Food Sanitation. 2006, Springer US: Boston, MA. p. 76-82.
136. Jokerst, J.C., et al., Development of a Paper-Based Analytical Device for Colorimetric Detection of Select Foodborne Pathogens. Analytical Chemistry, 2012. 84(6): p. 2900-2907.
137. Dou, M., et al., Low-cost bioanalysis on paper-based and its hybrid microfluidic platforms. Talanta, 2015. 145: p. 43-54.
138. Zhang, Y., P. Zuo, and B.-C. Ye, A low-cost and simple paper-based microfluidic device for simultaneous multiplex determination of different types of chemical contaminants in food. Biosensors and Bioelectronics, 2015. 68(Supplement C): p. 14-19.
139. Kettler, H., K. White, and S.J. Hawkes, Mapping the landscape of diagnostics for sexually transmitted infections: key findings and recommendations. 2004.
140. Evaluate, EvaluateMedTech® World Preview 2017, Outlook to 2022. 2017.
141. De La Maisonneuve, C. and J.O. Martins, Public Spending on Health and Long-term Care. 2013.
142. Syse, A. and D.Q. Pham, Befolkningsframskrivinger 2014-2100: Dødelighet og levealder. Økonomiske analyser Statistisk Sentralbyrå, 2014. 4: p. 44-50.
143. Roser, M. Our World in Data. Available from: https://ourworldindata.org/life-expectancy/.
144. United Nations. World Population Prospects 2017. 2017; Available from: https://esa.un.org/unpd/wpp/.
145. Stuckler, D., et al. The political economy of universal health coverage. in Background paper for the global symposium on health systems research. Geneva: World Health Organization. 2010.
146. European Union, Regulation (EU) 2017/746 of the European Parliament and of the Council of 5 April 2017 on in vitro diagnostic medical devices and repealing

Directive 98/79/EC and Commission Decision 2010/227/EU, in Official Journal of the European Union. 2017.

147. Boumans, R., Understanding Europe's New In Vitro Diagnostic Medical Devices Regulation. Emergo, 2016.
148. Maloney, L.T. and B.A. Wandell, Color constancy: a method for recovering surface spectral reflectance. Journal of the Optical Society of America A, 1986. 3(1): p. 29-33.
149. Foster, D.H., Color constancy. Vision Research, 2011. 51(7): p. 674-700.
150. Barnard, K., V. Cardei, and B. Funt, A comparison of computational color constancy algorithms. I: Methodology and experiments with synthesized data. IEEE Transactions on Image Processing, 2002. 11(9): p. 972-984.
151. Barnard, K., et al., A comparison of computational color constancy Algorithms. II. Experiments with image data. IEEE Transactions on Image Processing, 2002. 11(9): p. 985-996.
152. McGeough, C.M. and S. O'Driscoll, Camera phone-based quantitative analysis of C-reactive protein ELISA. IEEE Transactions on Biomedical Circuits and Systems, 2013. 7(5): p. 655-659.
153. Sumriddetchkajorn, S., K. Chaitavon, and Y. Intaravanne, Mobile device-based self-referencing colorimeter for monitoring chlorine concentration in water. Sensors and Actuators B: Chemical, 2013. 182(0): p. 592-597.
154. Yetisen, A.K., et al., A smartphone algorithm with inter-phone repeatability for the analysis of colorimetric tests. Sensors and Actuators B: Chemical, 2014. 196(0): p. 156-160.
155. Verhoeven, G.J.J., It's all about the format – unleashing the power of RAW aerial photography. International Journal of Remote Sensing, 2010. 31(8): p. 2009-2042.
156. Luo, M.R., G. Cui, and B. Rigg, The development of the CIE 2000 colour-difference formula: CIEDE2000. Color Research & Application, 2001. 26(5): p. 340-350.

157. García, A., et al., Mobile phone platform as portable chemical analyzer. Sensors and Actuators B: Chemical, 2011. 156(1): p. 350-359.
158. Intaravanne, Y., S. Sumriddetchkajorn, and J. Nukeaw, Cell phone-based two-dimensional spectral analysis for banana ripeness estimation. Sensors and Actuators B: Chemical, 2012. 168: p. 390-394.
159. Sumriddetchkajorn, S., K. Chaitavon, and Y. Intaravanne, Mobile-platform based colorimeter for monitoring chlorine concentration in water. Sensors and Actuators B: Chemical, 2014. 191: p. 561-566.
160. Lopez-Ruiz, N., et al., Smartphone-based simultaneous pH and nitrite colorimetric determination for paper microfluidic devices. Analytical chemistry, 2014. 86(19): p. 9554-9562.
161. Hong, J.I. and B.Y. Chang, Development of the smartphone-based colorimetry for multi-analyte sensing arrays. Lab on a Chip, 2014. 14(10): p. 1725-1732.
162. Wong, J.X., F.S. Liu, and H.-Z. Yu, Mobile app-based quantitative scanometric analysis. Analytical chemistry, 2014. 86(24): p. 11966-11971.
163. Sicard, C., et al., Tools for water quality monitoring and mapping using paper-based sensors and cell phones. Water Research, 2015. 70: p. 360-369.
164. Bagherinia, H. and R. Manduchi, Robust real-time detection of multi-color markers on a cell phone. Journal of real-time image processing, 2013. 8(2): p. 207-223.
165. Shen, L., J.A. Hagen, and I. Papautsky, Point-of-care colorimetric detection with a smartphone. Lab on a Chip, 2012. 12(21): p. 4240-3.
166. Tyburski, E.A., et al., Disposable platform provides visual and color-based point-of-care anemia self-testing. The Journal of Clinical Investigation, 2014. 124(10): p. 4387-4394.
167. Fangi, G., G. Gagliardini, and E.S. Malinverni, Photointerpretation and small scale stereoplotting with digitally rectified photographs with geometrical constraints. International Archives Of Photogrammetry Remote Sensing And Spatial Information Sciences, 2002. 34(5): p. 160-167.

168. Agarwal, A., C. Jawahar, and P. Narayanan, A survey of planar homography estimation techniques. Centre for Visual Information Technology, Tech. Rep. IIIT/TR/2005/12, 2005.
169. Ikeuchi, K., Computer vision: A reference guide. 2014: Springer Publishing Company.
170. Weinberger, K.Q., and L.K. Saul. Distance metric learning for large margin nearest neighbor classification. Journal of Machine Learning Research, 10(Feb), 207-244.
171. Loog, M. and R.P. Duin, Linear dimensionality reduction via a heteroscedastic extension of LDA: the Chernoff criterion. IEEE Transactions on Pattern Analysis and Machine Intelligence, 2004. 26(6): p. 732-739.
172. Leong, P. and S. Carlile, Methods for spherical data analysis and visualization. Journal of neuroscience methods, 1998. 80(2): p. 191-200.
173. Johnson, R.A. and D.W. Wichern, Applied multivariate statistical analysis. Vol. 4. 1992: Prentice hall Englewood Cliffs, NJ.
174. Wilks, S.S., Multivariate statistical outliers. Sankhyā: The Indian Journal of Statistics, Series A, 1963: p. 407-426.
175. Lecca, M., A full linear 3 × 3 color correction between images. Journal of Real-Time Image Processing, 2013: p. 1-19.
176. Finlayson, G.D., M.S. Drew, and B.V. Funt, Color constancy: generalized diagonal transforms suffice. JOSA A, 1994. 11(11): p. 3011-3019.
177. Csink, L., et al., Color normalization and object localization. Rehrmann [42], 1998: p. 49-55.
178. Finlayson, G.D., B. Schiele, and J.L. Crowley, Comprehensive colour image normalization, in Computer Vision. European conference on computer vision, 1998. Springer. p. 475-490.
179. Iqbal, Z. and M. Eriksson, Classification and quantitative optical analysis of liquid and solid samples using a mobile phone as illumination source and detector. Sensors and Actuators B: Chemical, 2013. 185(0): p. 354-362.

180. Fisher, R.A., The use of multiple measurements in taxonomic problems. Annals of Eugenics, 1936. 7(2): p. 179-188.
181. Del Castillo, E., Process optimization: a statistical approach. Vol. 105. 2007: Springer Science & Business Media.
182. Barrett, E.L. and H.S. Kwan, Bacterial reduction of trimethylamine oxide. Annual Review Microbiology, 1985. 39: p. 131-149.
183. Ishimoto, M. and O. Shimokawa, Reduction of trimethylamine N-oxide by Escherichia coli as anaerobic respiration. Journal of Basic Microbiology, 1978. 18(3): p. 173-181.
184. Styrvold, O.B. and A.R. Strom, Dimethylsulphoxide and trimethylamine oxide respiration of Proteus vulgaris. Evidence for a common terminal reductase system. Archives of Microbiology, 1984. 140(1): p. 74-78.
185. Kwan, H.S. and E.L. Barrett, Purification and properties of trimethylamine oxide reductase from Salmonella typhimurium. Journal of Bacteriology, 1983. 155(3): p. 1455-1458.
186. Jourlin, C., et al., Conservation of cis-acting elements within the tor regulatory region among different Enterobacteriaceae. Gene, 1995. 152(1): p. 53-57.
187. Unemoto, T., et al., Formation of trimethylamine from DL-carnitine by Serratia marcescens. Biochimica et Biophysica Acta, 1966. 121(1): p. 220-222.
188. Zhu, Y., et al., Carnitine metabolism to trimethylamine by an unusual Rieske-type oxygenase from human microbiota. Proceedings of the National Academy of Sciences, 2014. 111(11): p. 4268-4273.
189. Wolrath, H., et al., Trimethylamine and trimethylamine oxide levels in normal women and women with bacterial vaginosis reflect a local metabolism in vaginal secretion as compared to urine. Apmis, 2005. 113(7-8): p. 513-516.
190. McCarrick, M., S.J. Harris, and D. Diamond, Assessment of a chromogenic calix[4]arene for the rapid colorimetric detection of trimethylamine. Journal of Materials Chemistry, 1994. 4(2): p. 217-221.

191. Karlsen, H. and T. Dong, Biomarkers of urinary tract infections: state of the art, and promising applications for rapid strip-based chemical sensors. Analytical Methods, 2015. 7(19): p. 7961-7975.
192. Tavallali, H., et al., A new application of bromopyrogallol red as a selective and sensitive competition assay for recognition and determination of acetate anion in DMSO/water media. Dyes and Pigments, 2012. 94(3): p. 541-547.
193. Meneshian, A. and G.B. Bulkley, The physiology of endothelial xanthine oxidase: from urate catabolism to reperfusion injury to inflammatory signal transduction. Microcirculation, 2002. 9(3): p. 161-75.
194. Cantu-Medellin, N. and E.E. Kelley, Xanthine oxidoreductase-catalyzed reactive species generation: A process in critical need of reevaluation. Redox Biology, 2013. 1: p. 353-358.
195. Radi, R., Peroxynitrite, a stealthy biological oxidant. The Journal of Biological Chemistry, 2013. 288(37): p. 26464-26472.
196. Giler, S., et al., Urine xanthine oxidase activity in urinary tract infection. Journal of Clinical Pathology, 1978. 31(5): p. 444-446.
197. Ciragil, P., E.B. Kurutas, and M. Miraloglu, New markers: urine xanthine oxidase and myeloperoxidase in the early detection of urinary tract infection. Disease Markers, 2014: p. 269362.
198. Xi, H., B.L. Schneider, and L. Reitzer, Purine catabolism in Escherichia coli and function of xanthine dehydrogenase in purine salvage. Journal of Bacteriology, 2000. 182(19): p. 5332-5341.
199. Klebanoff, S.J., Myeloperoxidase: friend and foe. Journal of Leukocyte Biology, 2005. 77(5): p. 598-625.
200. Hampton, M.B., A.J. Kettle, and C.C. Winterbourn, Inside the neutrophil phagosome: oxidants, myeloperoxidase, and bacterial killing. Blood, 1998. 92(9): p. 3007-3017.
201. Wright, H.L., et al., Neutrophil function in inflammation and inflammatory diseases. Rheumatology, 2010. 49(9): p. 1618-1631.

202. Billips, B.K., et al., Modulation of Host Innate Immune Response in the Bladder by Uropathogenic Escherichia coli. Infection and Immunity, 2007. 75(11): p. 5353-5360.
203. Qian, M., J.W. Eaton, and S.P. Wolff, Cyanate-mediated inhibition of neutrophil myeloperoxidase activity. Biochemical Journal, 1997. 326(Pt 1): p. 159-166.
204. Fraser, P.A., et al., Neutrophil enzymes in urine for the detection of urethral infection in men. Genitourinary Medicine, 1995. 71(3): p. 176-179.
205. Steinhoff, J., et al., Renal graft rejection or urinary tract infection? The value of myeloperoxidase, C-reactive protein, and alpha2-macroglobulin in the urine. Transplantation, 1997. 64(3): p. 443-447.
206. Johnson, M.B. and A.K. Criss, Resistance of Neisseria gonorrhoeae to neutrophils. Frontiers in Microbiology, 2011. 2: p. 77.
207. Tauber, A.I., et al., Inhibition of human neutrophil NADPH oxidase by Chlamydia serovars E, K, and L2. Infection and Immunity, 1989. 57(4): p. 1108-1112.
208. Rose, C., et al., The Characterization of Feces and Urine: A Review of the Literature to Inform Advanced Treatment Technology. Critical Reviews in Environmental Science and Technology, 2015. 45(17): p. 1827-1879.
209. De Gennes, P.-G., F. Brochard-Wyart, and D. Quéré, Capillarity and wetting phenomena: drops, bubbles, pearls, waves. 2013: Springer Science & Business Media.
210. Bullard, J.W. and E.J. Garboczi, Capillary rise between planar surfaces. Physical Review E, 2009. 79(1): p. 011604.
211. Fries, N. and M. Dreyer, An analytic solution of capillary rise restrained by gravity. Journal of Colloid and Interface Science, 2008. 320(1): p. 259-263.
212. Schwiebert, M.K. and W.H. Leong, Underfill flow as viscous flow between parallel plates driven by capillary action. IEEE Transactions on Components, Packaging, and Manufacturing Technology: Part C, 1996. 19(2): p. 133-137.
213. Miller, B., Critical evaluation of upward wicking tests. International Nonwovens Journal, 2000. 9: p. 35-40.

214. Bosanquet, C.H., LV. On the flow of liquids into capillary tubes. The London, Edinburgh, and Dublin Philosophical Magazine and Journal of Science, 1923. 45(267): p. 525-531.
215. Elizalde, E., R. Urteaga, and C.L.A. Berli, Rational design of capillary-driven flows for paper-based microfluidics. Lab on a Chip, 2015. 15(10): p. 2173-2180.
216. Papanastasiou, T., G. Georgiou, and A.N. Alexandrou, Viscous fluid flow. 1999: CRC Press.
217. Curtis, E.B. and J.A. Morrow, Inverse problems for electrical networks. Vol. 13. 2000: World Scientific.
218. Ellens, W., et al., Effective graph resistance. Linear algebra and its applications, 2011. 435(10): p. 2491-2506.
219. Vollset, S.E., Confidence intervals for a binomial proportion. Statistics in Medicine, 1993. 12(9): p. 809-824.
220. Scherer, R., PropCIs: Various confidence interval methods for proportions. R package version 0.2–5. 2014.
221. Loog, M., R.P.W. Duin, and R. Haeb-Umbach, Multiclass linear dimension reduction by weighted pairwise Fisher criteria. IEEE Transactions on Pattern Analysis and Machine Intelligence, 2001. 23(7): p. 762-766.
222. Duin, R.P.W., et al., PRTools 4.1. A Matlab Toolbox for Pattern Recognition, Software and Documentation downloaded May, 2010.
223. European Commission, Horizon 2020 – Work programme 2014-2015 General Annexes. 2014.